Calhoun: The NPS Institutional Archive

DSpace Repository

Theses and Dissertations | 1. Thesis and Dissertation Collection, all items

1969-10

An investigation of a transonic turbine test rig.

Esdaile, Stewart Gary

Monterey, California. U.S. Naval Postgraduate School

http://hdl.handle.net/10945/12496

Copyright is reserved by the copyright owner

Downloaded from NPS Archive: Calhoun

Calhoun is the Naval Postgraduate School's public access digital repository for research materials and institutional publications created by the NPS community. Calhoun is named for Professor of Mathematics Guy K. Calhoun, NPS's first appointed -- and published -- scholarly author.

Dudley Knox Library / Naval Postgraduate School
411 Dyer Road / 1 University Circle
Monterey, California USA 93943

http://www.nps.edu/library

NPS ARCHIVE
1969
ESDAILE, S.

AN INVESTIGATION OF A TRANSONIC TURBINE TEST RIG

Stewart Gary Esdaile

DUDLEY KNOX LIBRARY
NAVAL POSTGRADUATE SCHOOL
MONTEREY, CA 93943-5101

United States
Naval Postgraduate School

THESIS

An Investigation of a Transonic
Turbine Test Rig

by

Stewart Gary Esdaile

October 1969

This document has been approved for public release and sale; its distribution is unlimited.

T133763

An Investigation of a Transonic
Turbine Test Rig

by

Stewart Gary Esdaile
Captain, Canadian Armed Forces
B.Eng., Royal Military College, 1964

Submitted in partial fulfillment of the
requirements for the degree of

MASTER OF SCIENCE IN AERONAUTICAL ENGINEERING

from the

NAVAL POSTGRADUATE SCHOOL
October 1969

NPS ARCHIVE
1969
ESDAILE, S.

ABSTRACT

The Transonic Turbine Test Rig installed in the Turbo-Propulsion Laboratory at the Naval Postgraduate School was designed such that losses in nozzles and rotor blading and overall performance characteristics can be determined for operation at several combinations of blade configurations, pressure ratios and speeds. This study relates the empirical data for stator loss coefficients to those determined for the converging-nozzle stator presently installed, and discusses reasons for some of the discrepancies. Also discussed are results of the flow nozzle calibration, locked rotor data, and temperature and inlet swirl effects. A method is proposed to reduce these effects for future work on the Turbine Test Rig.

LIBRARY
NAVAL POSTGRADUATE SCHOOL
MONTEREY, CALIF. 93940

DUDLEY KNOX LIBRARY
NAVAL POSTGRADUATE SCHOOL
MONTEREY, CA 93943-5101

TABLE OF CONTENTS

I. INTRODUCTION ---------- 13

II. EQUIPMENT MODIFICATIONS ---------- 15

III. FLOW RATE DETERMINATION ---------- 17

A. Nozzle Calibration ---------- 17

B. Turbine Flow Rate ---------- 18

IV. ANALYSIS AND DATA REDUCTION ---------- 19

A. General ---------- 19

B. Description of Method 1 ---------- 22

C. Description of Method 2 ---------- 24

V. NATURE OF PROBLEM ---------- 27

VI. DESCRIPTION OF TESTS ---------- 30

VII. RESULTS AND ANALYSIS OF TESTS ---------- 34

VIII. CONCLUSIONS AND RECOMMENDATIONS ---------- 44

APPENDIX A Prediction of Stator Discharge Angle and Stator Loss Coefficient ---------- 79

APPENDIX B Prediction of Torque on Closure Plate and Shroud ---------- 88

APPENDIX C Prediction of Stator Discharge Pressure Distribution ---------- 90

APPENDIX D Computer Output (Run 15) ---------- 95

Computer Program FLOCAL ---------- 106

Computer Program TTTR ---------- 109

LIST OF TABLES

I. PREDICTED AND EXPERIMENTAL VALUES OF STATOR LOSS COEFFICIENT -- 27

II. SUMMARY OF RUNS -- 31

III. PREDICTION OF STATOR DISCHARGE ANGLE ------------------- 82

IV. LOSS COEFFICIENT BY METHOD OF AINLEY ------------------- 83

V. LOSS COEFFICIENT BY METHOD OF TRAUPEL ------------------ 85

VI. LOSS COEFFICIENT BY METHOD OF SODERBERG ---------------- 87

LIST OF FIGURES

Figure Page

1. Piping Installation, Transonic Turbine Test Rig --------- 48

2. Transonic Turbine Test Rig ------------------------------ 49

3. Turbine Blading Arrangement ----------------------------- 50

4. Floating Stator Assembly -------------------------------- 51

5. Stator Torque Capsule Support Assembly ----------------- 52

6. Turbine and Shroud Details ------------------------------ 53

7. Mean Radius Blade Profile, Converging Nozzles ---------- 54

8. Mean Radius Blade Profile, Circular Arc, Sharp Leading Edge Rotor -- 55

9. Honeycomb Flow Straightener ----------------------------- 56

10. Stator Roller Bearing Supports ------------------------- 57

11. Nozzle Calibration Coefficient ------------------------- 58

12. Thermodynamic Process for an Axial Turbomachine --------- 59

13. Velocity Diagram of a Turbine Stage -------------------- 60

14. Total-Static Turbine Efficiency ------------------------ 61

15. Referred Stator Axial Force versus Referred RPM --------- 62

16. Referred Stator Torque versus Referred RPM ------------- 63

17. Referred Stator Torque versus Stator Pressure Ratio ----- 64

18. Flow Function versus Stator Pressure Ratio ------------- 65

19. Referred Velocities versus Stator Pressure Ratio -------- 66

20. Stator Loss Coefficient versus Stator Pressure Ratio ---- 67

21. Referred Axial Force versus Stator Pressure Ratio with Locked Rotor --- 68

22. Referred Stator Torque versus Stator Pressure Ratio with Locked Rotor --- 69

23. Referred Flow Rate versus Stator Pressure Ratio with Locked Rotor --- 70

24. Flow Function versus Stator Pressure Ratio with Locked Rotor -- 71

25. Stator Pressure Ratio versus Overall Pressure Ratio with Locked Rotor -- 72

26. Referred Velocities versus Stator Pressure Ratio with Locked Rotor -- 73

27. Stator Loss Coefficient versus Stator Pressure Ratio with Locked Rotor -- 74

28. Temperature Increase of Capsule Support versus Referred Flow Rate with Honeycomb Installed --------------------- 75

29. Predicted Error in Stator Torque due to Temperature Effect on Capsule Support -------------------------------- 76

30. Referred Stator Torque versus Stator Pressure Ratio with Honeycomb Installed -------------------------------- 77

31. Flow Exit Angle From Honeycomb versus Referred Flow Rate --- 78

32. Predicted Velocity Profiles at Stator Discharge --------- 93

TABLE OF SYMBOLS

Latin

A	Cross-sectional area (in^2)
a	Speed of sound (ft/sec)
b	Blade width (in)
C	Conversion factor, $2g_c\ J\ C_p$ ($ft^2/sec^{2\,o}R$)
C_n	Nozzle discharge coefficient
C_p	Specific heat at constant pressure ($Btu/lbm.^oR$)
d	Throat diameter (in)
F	Force (lbf)
g_c	Gravitational constant ($32.174\ lbm\text{-}ft/lbf\text{-}sec^2$)
h	Blade height (in)
h_w	Differential pressure across flow nozzle (in H_2O)
J	Joules constant (778.16 ft-lbf/Btu)
K_t	Area reduction factor
K_{is}	Isentropic head coefficient (dimensionless)
M	Mach number (dimensionless)
M	Moment (ft-lbf)
N	Rotational speed (rpm)
P_T	Total pressure (psia)
P	Static pressure (psia)
R_g	Gas constant ($ft\text{-}lbf/lbm\text{-}^oR$)
Re	Reynolds Number (dimensionless)
R_m	Mean radius (in)
r	Radius (in)
s	Distance between blades (in)

T_T	Total temperature $(^{\circ}R)$
T	Static temperature $(^{\circ}R)$
t	Trailing edge thickness of blade (in)
U	Peripheral velocity (ft/sec)
V	Absolute velocity (ft/sec)
W	Relative velocity (ft/sec)
$\dot{w}$	Flow rate (lbm/sec)
Z	Number of blades

Greek

α	Absolute flow angle (degrees)
β	Relative flow angle (degrees)
γ	Ratio of specific heats (dimensionless)
ε	Correction factor for pressure distribution
ζ	Loss coefficient (dimensionless)
η	Efficiency (dimensionless)
ξ	Area restriction factor (dimensionless)
Φ	Flow function (dimensionless)
ω	Angular velocity (radians/sec)

Subscripts

a	Axial direction
av	Average
ax	Annulus exit area
C	Continuity analysis
h	Hub
is	Isentropic
m	Mean streamline

M	Momentum analysis
n	Flow nozzle properties
ref	Referred value
s	Stator
t	Tip
T	Turbine
th	Throat
u	Peripheral or tangential direction
o	Stator entrance properties
1	Stator discharge properties
2	Rotor discharge properties

I. INTRODUCTION

Much of the design and analysis of modern turbines is based on the experience of the designer and his use of empirical data available in the literature. As a result, many investigations of test turbines are being carried out in an effort to more fully explain and mathematically model the flow phenomena in stationary and rotating channels. Present methods for design of axial flow machines base calculations on a reference diameter, usually taken as the mean of the hub and tip. A major simplification is then made by assuming that at any point in a cross-section, such parameters as total pressure and temperature and axial velocity have the same values as at the reference diameter. The overall characteristics of a stage are then determined, but depend on how accurately flow discharge angles and loss coefficients are known. Thus, it is extremely important to be able to predict these values as functions of blade geometry, Mach number and certain other flow parameters. Such a method as just described is conventionally known as a "One-Dimensional Analysis".

The Transonic Turbine Test Rig (TTTR) located at the Turbopropulsion Laboratory is a particularly desirable test machine because it permits evaluation of performance at many combinations of operating conditions and configurations. One of the most important features of the TTTR is that it enables one to evaluate flow angles and loss coefficients using momentum and moment of momentum equations, without making extensive flow surveys which cause an upset of the true flow conditions. The empirical methods available for prediction of flow angles and loss coefficients yield results varying from unreasonably low values to one so conservative it would be unlikely the machine would operate. Results from previous runs on the TTTR showed the latter trend in loss coefficients, although the TTTR had a reasonable overall performance.

This thesis investigates the methods by which the loss coefficients are determined for the TTTR and relates these coefficients to those predicted by the literature. It then describes the investigation carried out to explain the apparent discrepancies, and examines the effect of some of the more important parameters used to evaluate the loss coefficient.

The author would like to express his appreciation for the competent assistance provided by Mr. Jim Hammer and members of the Turbopropulsion Laboratory. Special thanks are extended to Dr. M. H. Vavra for his guidance and advice during the investigation.

II. EQUIPMENT MODIFICATIONS

The TTTR instrumentation has been described extensively by Commons [Ref. 4] and Lenzini [Ref. 6]. Discussion here will be limited to recent modifications made to the TTTR.

Fig. 1 shows the piping and valve location in the Turbine test cell. Fig. 2 shows a cross-section of the floating stator and support assembly, while Fig. 3 shows a more detailed cross-section of the stator plenum and hub area. The closure plate assembly shown in Fig. 3 was instrumented with additional strain gauges on the flexures, and the back face towards the rotor had three static pressure taps installed at known radii. Results of these pressure readings and closure plate torque calibration are discussed later.

Fig. 4 shows the floating stator assembly with the locations of the axial force and torque capsule supports and Fig. 5 shows a more detailed view of the torque capsule support assembly. The capsule support assembly was moved from the previous location between the overhead support and plenum casing to its position at the upstream end of the stator in an attempt to reduce both the temperature effect on the capsule and the errors induced by differential thermal expansion.

Fig. 6 shows the stator exit and shroud area. Two additional pressure taps, P13 and P14 were installed, with the hope of correlating the stator discharge tip pressure to the shroud pressure at the same plane. In addition, the machine was completely dismantled and cleaned, and new pressure lines were installed in many cases. The pressure lines were connected to a mercury manometer board in a logical sequence, extending from the nozzle to the plenum assembly and along the shroud to the rotor discharge, so that the pressure distribution through the machine could be readily observed.

Fig. 7 shows the converging nozzles presently installed in the TTTR and Fig. 8 shows the circular-arc, sharp leading-edge rotor used.

III. FLOW RATE DETERMINATION

A. NOZZLE CALIBRATION

Previous nozzle calibration techniques have been described by Naviaux [1] and Lenzini [Ref. 6]. It was shown that the nozzle coefficient was a function of nozzle Reynolds number. However, former results for nozzle coefficients were determined as a function of the Reynolds number based on the conditions of the ASME standard calibrating orifice, rather than on the flow nozzle. As a result, it was decided to repeat the nozzle calibration to obtain a new relationship, and to determine if any deterioration of the nozzle had taken place.

The program for the data reduction is given in Appendix D, program FLOCAL. The method used is similar to that given by Williams [2], which was found to be more suitable for computer computations. The basic equation is given in the ASME Power Test Code [3] and values of the constants are taken from Stearns.[4] Tests were carried out at nozzle supply pressures of 26, 29, 34 and 39 psia over a range of Reynolds numbers from 2×10^5 to 12×10^5. Fig. 11 shows the results of these tests, with nozzle coefficient plotted as a function of Reynolds number. The curve differs from that given by Lenzini [Ref. 6], being higher by 2 to 3 percent. The curve also shows a maximum coefficient occuring at a Reynolds number of 6×10^5 and then decreasing as Reynolds number is increased. It is suspected that this increasing trend of nozzle coefficient each time a calibration is performed indicates some deterioration of the nozzle.

---

[1] Naviaux, J. C., "Transonic Turbine Test Rig Exhauster System Tests and Tests of a Reaction Turbine, "Naval Postgraduate School Thesis, December, 1966.

[2] Williams, D. D., "Determination of Performance Parameters of a Dual-Discharge Radial Turbine, "Naval Postgraduate School Thesis, December, 1968.

[3] Flow Measurement, Chapt. 4, Part 5, Supplement to ASME Power Test Codes, ASME, New York, N. Y., 1959, p. 57ff.

[4] Stearns, R. F., et al., Flow Measurement With Orifice Meters. New York: D. van Norstrand Company, 1951. pg. 65-212.

An analytical curve for the nozzle coefficient was obtained by using a least-squares polynomial curve fit. A fourth-order polynomial was chosen as the best fit to the data, namely:

$$C_n = 9.5208828 \times 10^{-1} + 4.4891640 \times 10^{-7}\ Re - 7.5810743 \times 10^{-13}\ Re^2 + 5.5023778 \times 10^{-19}\ Re^3 - 1.4571314 \times 10^{-25}\ Re^4$$

The maximum error between the analytical curve and the actual data points for a range of Reynolds numbers between 4×10^5 and 12×10^5 is 0.2 percent.

B. TURBINE FLOW RATE

The program to obtain the turbine flow rate is given in subroutine FLORAT of program TTTR, and employs a procedure similar to that described in section A. The labyrinth leak rate uses a formula determined by Lenzini [Ref. 6] which is a function of plenum pressure ratio and temperature. The labyrinth leak rate was found to be only 2 percent of the total flow rate. The recalibration of the nozzle and improved flow rate determination resulted in referred turbine flow rates which were 3 percent higher than those previously used.

IV. ANALYSIS AND DATA REDUCTION

A. GENERAL

The basic equations for a one-dimensional flow analysis of the TTTR are well known and have been described in detail by Commons [Ref. 4], Lenzini [Ref. 6] and Messegee [Ref. 7]. The reference diameter referred to previously is twice the mean radius:

$$R_m = \frac{R_{hub} + R_{tip}}{2}$$

The data for the TTTR are reduced by program TTTR given in Appendix D, which also gives the results of Run 15. Fig. 12 shows the thermodynamic process for an axial turbomachine and the stator loss coefficient is designated ζ_s. Fig. 13 shows the associated velocity diagram for a turbine stage.

It is of interest here to summarize the assumptions made in using the one-dimensional analysis, as they will have a large bearing on the accuracy of the results. These assumptions are:

1. Adiabatic, steady flow, so that the absolute and relative enthalpies are constant respectively along any streamline.

2. Cylindrical stream surfaces, so there is no bending of the stream surface, or radial component of velocity.

3. Uniform conditions ahead of the stator so there is no total pressure or total temperature gradient in the radial direction.

4. Completely radial flow into the plenum, and axial flow into the stator with no tangential velocity component.

5. Shear stresses are negligible on the annulus and shroud, and symmetrical wakes occur at the trailing edges of the blades.

The validity of these assumptions will be discussed later and where invalid assumptions were found to exist their influence on the loss coefficient will be discussed.

When analysing the reduced data, nearly all variables were plotted as functions of the stator discharge pressure ratio P_{TO}/P_1. The following discussion will show why P_{TO}/P_1 is an important parameter. From the equation of momentum

$$M = \frac{\dot{w}_T}{g_c} RV_u$$

and using

$$\Phi = \frac{\dot{w}_T \sqrt{R_g/g_c \; T_{TO}}}{P_{TO} \; A_{ths}} = \left(\frac{P_1}{P_{TO}}\right)^{\frac{1}{n}} \sqrt{\frac{2\gamma}{\gamma - 1} \left[1 - \left(\frac{P_1}{P_{TO}}\right)^{\frac{n-1}{n}}\right]}$$

where

$$n = \frac{\gamma}{1 + \zeta_\rho \; (\gamma - 1)}$$

and

$$\zeta_\rho = \frac{P_{TO} - P_{T1}}{P_{TO} - P_1}$$

hence

$$\Phi = f_1 \left(\frac{P_{TO}}{P_1} \; , n, \gamma \right)$$

Thus

$$M = \frac{P_{TO} \; A_{ths} \; \Phi}{g_c \sqrt{R_g/g_c \; T_{TO}}} \; RV_u$$

or

$$\frac{M}{P_{TO}} = M_{ref} = \frac{V_u}{\sqrt{T_{TO}}} \quad f_1 \left(\frac{P_{TO}}{P_1} \; , n, \gamma \right)$$

Now

$$V_u^2 = V^2 \sin^2 \alpha = C\left(T_{T0} - T_1\right) \sin^2 \alpha$$

or

$$V_u^2 = C\, T_{T0} \left[1 - \left(\frac{P_1}{P_{T0}}\right)^{\frac{n-1}{n}}\right] \sin^2 \alpha$$

and

$$\frac{V_u}{\sqrt{T_{T0}}} = \sqrt{C} \left[1 - \left(\frac{P_1}{P_{T0}}\right)^{\frac{n-1}{n}}\right]^{\frac{1}{2}} \sin \alpha = f_2\left(\frac{P_{T0}}{P_1}, n, \gamma\right)$$

Hence

$$M_{ref} = f_3\left(\frac{P_{T0}}{P_1}, n, \gamma, \alpha\right)$$

For an ideal gas γ is constant, and for small pressure ratios n is nearly a constant. Thus, if it is assumed that the stator discharge angle is constant:

$$M_{ref} = f_4\left(\frac{P_{T0}}{P_1}\right)$$

and

$$\phi = f_1\left(\frac{P_{T0}}{P_1}\right)$$

and

$$\frac{V_u}{\sqrt{T_{T0}}} = f_2\left(\frac{P_{T0}}{P_1}\right)$$

Using the loss coefficient as defined by Vavra [Ref. 8]:

$$\zeta_s = 1 - \phi^2 = 1 - \left(\frac{V_1}{V_{1is}}\right)^2 = \frac{T_1 - T_{1is}}{T_{T0} - T_{1is}} = \frac{T_1/T_{T0} - T_{1is}/T_{T0}}{1 - T_{1is}/T_{T0}}$$

$$= \frac{\left(P_1/P_{T0}\right)^{\frac{n-1}{n}} - \left(P_1/P_{T0}\right)^{\frac{\gamma-1}{\gamma}}}{1 - \left(P_1/P_{T0}\right)^{\frac{\gamma-1}{\gamma}}} = f_s\left(\frac{P_{T0}}{P_1}, n, \gamma\right)$$

And, consistent with the above assumptions for n and γ,

$$\zeta_s = f_5 \left(\frac{P_{T0}}{P_1} \right)$$

B. DESCRIPTION OF METHOD 1

It is possible to solve for the stator discharge properties by satisfying continuity at the throat plane and the exit plane, provided certain parameters are accurately known and some assumptions are made. At the exit plane, from continuity:

$$\dot{w}_T = \rho_1 V_{a1} A_1$$

From the perfect gas relationship

$$\rho_1 = \frac{P_1}{R_g T_1}$$

Thus

$$V_{a1} = \frac{\dot{w}_T R_g T_1}{P_1 A_1} \qquad (1)$$

However T_1 is not known until V_1 is determined. If one assumes that the same pressure and temperature acting at the exit also exist across the throat plane, then continuity may be applied at the throat:

$$\dot{w}_T = \rho_1 V_1 A_{ths}$$

Then using

$$\rho_1 = \frac{P_1}{R_g T_1} \quad \text{and} \quad T_1 = T_{T0} - \frac{V_1^2}{C}$$

$$V_1 = \frac{\dot{w}_T}{P_1 A_{ths}} = \frac{\dot{w}_T R_g T_1}{P_1 A_{ths}} = \frac{\dot{w}_T R_g}{P_1 A_{ths}} \left(T_{T0} - \frac{V_1^2}{C} \right)$$

or

$$V_1^2 + \frac{C P_1 A_{ths}}{\dot{w}_T R_g} V_1 = \frac{\dot{w}_T R_g}{P_1 A_{ths}} T_{T0}$$

Let

$$C_2 = \frac{C\ P_1\ A_{ths}}{\dot{w}_T\ R_g}$$

Thus

$$V_1^2 + C_2\ V_1 = C\ T_{TO}$$

And completing the square:

$$V_1^2 + C_2\ V_1 + \left(\frac{C_2}{2}\right)^2 = \left(V_1 + \frac{C_2}{2}\right)^2 = C\ T_{TO} + \left(\frac{C_2}{2}\right)^2$$

Hence

$$V_1 = \sqrt{CT_{TO} + \left(\frac{C_2}{2}\right)^2} - \left(\frac{C_2}{2}\right) \qquad (2)$$

and

$$T_1 = T_{TO} - \frac{V_1^2}{C} \qquad (3)$$

Once V_{a1} is determined from (1),

$$\alpha_1 = \cos^{-1}\left(\frac{V_{a1}}{V_1}\right) = \cos^{-1}\left(\frac{A_{ths}}{A_1}\right) \quad \text{and } V_{u1} = V_1 \sin \alpha_1$$

and all quantities are available to determine ζ_s.

It is important to examine in detail the assumptions made in arriving at ζ_s by continuity only, which are:

1. The same pressure P_1 and temperature T_1 exist at the throat and exit plane.
2. There is no change of V_1 from the throat to the exit plane.
3. The correct pressure distribution for P_1 is accurately known.
4. The areas A_{ths} and A_1 are known exactly.
5. There is one-dimensional or uniform flow at both the throat and exit plane, which implies no boundary layer restriction.

In the data reduction, P_1 was taken as the mean of the measured hub and tip pressures, and A_1 was the annulus exit area reduced by a factor K_t to account for the trailing edge thickness.

C. DESCRIPTION OF METHOD 2.

In this method both continuity and momentum are applied, where the tangential velocity is determined from the momentum equation, while the axial velocity is determined from knowledge of the axial forces acting on the stator and by applying continuity at the stator exit. From angular momentum:

$$V_{u1} = \frac{M\, g_c}{\dot{w}_T\, R_{m1}} \tag{4}$$

At the stator exit plane, a parabolic pressure distribution is assumed to exist, which is expressed by equation 12 of Lenzini [Ref. 6] and is repeated here:

$$P_{1av} = \frac{P_{hub}}{3}\left[\frac{(1+\varepsilon)\,R_{tip}^2 + R_{tip}\,R_{hub} - (2+\varepsilon)\,R_{hub}^2}{(R_{tip}^2 - R_{hub}^2)}\right]$$

$$+ \frac{P_{tip}}{3}\left[\frac{(2+\varepsilon)\,R_{tip}^2 - R_{tip}\,R_{hub} - (1+\varepsilon)\,R_{hub}^2}{(R_{tip}^2 - R_{hub}^2)}\right] \tag{5}$$

The value of ε determines the shape of the parabola. A value for ε is first assumed and with this first approximation for P_{1av}, the force balance equation may be solved for V_{a1},

$$V_{a1M} = \frac{g_c}{\dot{w}_T}\left(R - P_{1av}\,A_{axs}\right) \tag{6}$$

where R = the algebraic sum of the measured forces and the pressure forces acting on the stator. Thus V_{a1M} is a direct function of the value of ε, or the shape of the pressure distribution. Continuity is then written for the exit plane as in Method 1, employing the perfect gas relations, to obtain:

$$V_{alC} = \frac{\dot{w}_T R_g}{P_1 A_1}\left(T_{TO} - \frac{V_1^2}{C}\right) = \frac{\dot{w}_T R_g}{P_1 A_1}\left[T_{TO} - \frac{1}{C}\left(V_{alC}^2 + V_{ul}^2\right)\right]$$

Let

$$C_1 = \frac{\dot{w}_T R_g}{P_1 A_1}$$

Then

$$V_{alC} = C_1 T_{TO} - \frac{C_1}{C} V_{alC}^2 - \frac{C_1}{C} V_{ul}^2$$

or

$$V_{alc}^2 + \frac{C}{C_1} V_{alc} = CT_{TO} - V_{ul}^2$$

and completing the square:

$$V_{alc}^2 + \frac{C}{C_1} V_{alC} + \left(\frac{C}{2C_1}\right)^2 = \left(V_{alC} + \frac{C}{2C_1}\right)^2 = CT_{TO} - V_{ul}^2 + \left(\frac{C}{2C_1}\right)^2$$

or

$$V_{alc} = \sqrt{CT_{TO} - V_{ul}^2 + \left(\frac{C}{2C_1}\right)^2} - \left(\frac{C}{2C_1}\right) \tag{7}$$

Equations (6) and (7) are compared and the value of ε is changed appropriately until the two methods produce the same value of V_{al}. In summary then, the steps are:

1. Assume an initial value of ε and determine P_{lav} from equation (5).
2. Solve for V_{ul} from equation (4).
3. Solve for V_{alM} from equation (6).
4. Solve for V_{alC} from equation (7).
5. Compare the two values of V_{al} and vary ε until the two values of V_{al} become equal.
6. Compute ζ_s.

The assumptions made using this method are as follows:

1. The stator torque can be measured accurately, yielding a correct value of V_{u1}.

2. The correct pressure distribution for P_1 is known accurately, or conversely the iterated value of ε will yield the correct pressure distribution.

3. The correct axial force is being recorded.

4. The area A_1 is known exactly.

5. There is one-dimensional or uniform flow in the nozzles, so no boundary layer correction factor is required.

As in Method 1, the area A_1 was reduced by the same factor K_t to account for the effect of trailing edge thickness.

If the assumptions for both methods are met, then either method should result in essentially the same values for V_{a1}, V_{u1}, α, and ζ_s, respectively.

V. NATURE OF PROBLEM

A survey of previous results has shown that ζ_s has ranged from negative values to as high as 0.30. The result of this has produced stator or rotor efficiencies of over one-hundred percent, but the overall machine had a total-static efficiency in the order of eighty percent at the design point. The conclusion reached was that the determination of overall performance was correct, but that some error existed, either in the theory of calculating stator loss coefficients or in measuring the properties necessary to arrive at the loss coefficient.

Appendix A presents several methods by which the stator discharge angle and stator loss coefficients may be predicted. In addition, a curve fit of data is given by Vavra [Ref. 8]. A summary of these values and some representative ones from previous work by Lenzini [Ref. 6] are presented in Table I below.

TABLE I

Predicted and Experimental Values of ζ_s

	Source	ζ_s
Predicted Values	Ainley	0.0756
	Traupel	0.1545
	Soderberg	0.1022
	Vavra	0.1400
Experimental	Lenzini	-0.0100 to 0.3000

Since previous work by Lenzini [Ref. 6] indicated that the overall total-static turbine efficiency was about eighty percent, it was concluded that many of the above values were too high, and that an average value for the loss coefficient ζ_s of 0.08 would be more in order. The problem then became one of determining where the error in computing the loss coefficient was occuring and to reduce the error as much as possible.

In order to determine the error, it was assumed that the theory to calculate ζ_s was correct and that the error arose from invalid assumptions and incorrect measurements of some variables. If a value for ζ_s is assumed, certain parameters can be calculated and plotted as a function of P_{TO}/P_1, and then actual measurements could be compared against these predicted values. Thus, based on the definition of ζ_s, several important relationships could be developed:

$$\zeta_s = \frac{T_1 - T_{1is}}{T_{TO} - T_{1is}} = \frac{\left(T_{TO} - V_1^2/C\right) - T_{TO}\left(P_1/P_{TO}\right)^{\frac{\gamma - 1}{\gamma}}}{T_{TO} - T_{TO}\left(P_1/P_{TO}\right)^{\frac{\gamma - 1}{\gamma}}}$$

Let $X = \left(P_1/P_{TO}\right)^{\frac{\gamma - 1}{\gamma}}$

Hence

$$\zeta_s = \frac{\left(1 - V_1^2/CT_{TO}\right) - X}{1 - X} = 1 - \frac{V_1^2/CT_{TO}}{\left(1 - X\right)}$$

and using $C_\rho = \frac{\gamma}{\gamma - 1}\frac{R_g}{J}$

$$\frac{V_1}{a_{TO}} = \sqrt{\frac{2}{\gamma - 1}\left(1 - \zeta_s\right)\left(1 - X\right)} \qquad (8)$$

With the chosen value of $\zeta_s = 0.08$ and $\gamma = 1.4$,

$$\frac{V_1}{a_{T0}} = 2.1450\ (1 - X)^{\frac{1}{2}} \tag{9}$$

and

$$\frac{T_1}{T_{T0}} = 1 - \frac{\gamma - 1}{2}\left(\frac{V_1}{a_{T0}}\right)^2 \tag{10}$$

From

$$\dot{w}_T = \rho_1\ V_1\ A_{ths} = p_{T0}\left(\frac{P_1}{P_{T0}}\right)\left(\frac{T_{T0}}{T_1}\right)\ \frac{A_{ths}}{R_g\ T_{T0}}\ \frac{V_1}{\sqrt{\gamma g_c\ R_g\ T_{T0}}}\sqrt{\gamma g_c\ R_g\ T_{T0}}$$

$$\frac{\dot{w}_T\ R_g\ T_{T0}}{P_{T0}\ A_{ths}\ \sqrt{\gamma g_c\ R_g\ T_{T0}}} = \frac{\dot{w}_T\sqrt{R_g/g_c\ T_{T0}}}{\sqrt{\gamma}\ \ P_{T0}\ A_{ths}} = \left(\frac{P_1}{P_{T0}}\right)\left(\frac{1}{T_1/T_{T0}}\right)\left(\frac{V_1}{a_{T0}}\right)$$

or

$$\Phi = \sqrt{\gamma}\ \left(\frac{P_1}{P_{T0}}\right)\left(\frac{1}{T_1/T_{T0}}\right),\left(\frac{V_1}{a_{T0}}\right) \tag{11}$$

Then $M = \frac{\dot{w}_T}{g_c}\ R_{ml}\ V_{ul} = \frac{\Phi A_{ths}\ P_{T0}\ R_{ml}\ V_{ul}}{g_c\ \sqrt{R_g/g_c\ T_{T0}}}$

or

$$\frac{M}{P_{T0}} = M_{ref} = \sqrt{\gamma}\ A_{ths}\ R_{ml}\ \Phi\left(\frac{V_{ul}}{a_{T0}}\right) \tag{12}$$

VI. DESCRIPTION OF TESTS

A new electrical read-out system was employed for the strain-gauges on the closure plate. It was decided to calibrate both the closure-plate axial force and torque with the closure-plate mounted on the stator, rather than using the previous method of calibrating away from the TTTR and then possibly destroying the calibration during the installation in the stator casing.

A summary of the operating runs is listed in Table II. The first series of runs was carried out at pressure ratios of 1.5 and 2.0 over the full range of RPM allowable by the torque capacity of the air dynamometer. The configuration was unhooded with rotor axial clearances of 0.250 in. and 0.500 in. Several pressure leaks developed on nearly every run, and only Run 8 was considered sufficiently trouble-free to be used for analysis.

Once the high loss coefficients were confirmed to exist from the data of Run 8 and reduction by Method 1 and Method 2, it was decided to attempt some locked rotor tests at axial clearances of 0.250 in. and 0.500 in. and 2.000 in. to determine the conditions at zero RPM and a pressure ratio of 1.5. Few problems were incurred during this series of tests, and data points could be repeated to within 1 percent or better. During the last run however, several pressure lines were torn loose, which required extensive repairs before any further runs could be made.

During the runs up to and including Run 14, the standard method of operation had been to leave the inlet valve of Tank 1 full open and gradually open the turbine inlet valve to increase the pressure ratio.

TABLE II

Summary of Runs

Run	Configuration	Purpose
1 - 4	ASME Standard Pipe and Orifice Installed P_{noz} varied	To determine nozzle calibration coefficient.
5 6	Rotor removed Rotor removed	Closure plate axial and torque calibration
7 8 9 10 11	Operating, PR = 2.0, AX = 0.250" Operating, PR = 1.5, AX = 0.250" Operating, PR = 1.5, AX = 0.500" Operating, PR = 2.0, AX = 0.500" Operating, PR = 2.0, AX = 0.500"	To check the system after modifications and determine operating data
12 13 14	Locked Rotor, AX = 0.500" Locked Rotor, AX = 2.000" Locked Rotor, AX = 0.250"	To examine the system operation at zero RPM and various clearances.
15	Operating, PR = 1.5, AX = 0.250"	To confirm previous results
16 17 18 19	Honeycomb, flexures installed Honeycomb, flexures removed Honeycomb, flexures installed Honeycomb, flexures removed	To determine the effects of the torque flexures and various turbine inlet valve openings.
20 21	Nozzles installed, rotor removed, flexures removed Nozzles installed, rotor removed, flexures installed	To determine the effects of torque flexures and inlet valve openings with no rotor influence.

As a result, a pressure drop in the order of 50 in. of mercury was occuring across the turbine inlet valve. Also, it was noticed that after shutting off the flow to the stator, there were residual values of stator axial force and torque in the order of 1.0 and 5.0 percent respectively, which gradually dropped to zero after some time.

In an effort to examine the validity of the assumption of no inlet tangential velocity ahead of the stator, the stator was removed and the honeycomb flow straightener shown in Fig. 9 was installed. Also, during the next series of tests, the method of operation was changed and a further modification was employed. For Run 16, the honeycomb was installed and the turbine valve operated as before. Because a residual torque reading was again observed, it was decided to remove the stator torque flexures which take up some of the torque and transmit the axial force to the cradle assembly. A system of roller bearings was installed between the cradle assembly and stator plenum casing in place of the torque flexures, as shown in Fig. 10. Also, a thrust collar was fastened on the stator support shaft and allowed to press against the support bearing, as a means of transmitting the stator axial force to the cradle assembly. The next series of runs was performed by either gradually opening the turbine valve to obtain the desired pressure ratio, or fully opening the valve and adjusting the pressure ratio by slowly closing a dump valve in the delivery line near the Allis-Chalmers compressor. It was possible to obtain similar flow rates as used during all previous tests, but because of the much less restricted flow, considerably smaller pressure ratios were required.

Prior to Run 16, a thermocouple was installed on the torque capsule support assembly, and during the next series of tests the temperature of the assembly was monitored. Also, the discharge temperature from the Allis-Chalmers compressor was varied from 90° to 130° F to provide a sufficient temperature gradient at the stator in order to examine the effects of differential thermal expansion. During Run 17, the flow exit angle from the honeycomb was measured using a 5-hole probe, to find out whether the flow leaving the honeycomb straightener was truly axial as desired.

Once an improved method of operation was determined, a final series of tests was performed with stator nozzles reinstalled, but the rotor removed to eliminate any influence it might have. The same procedure was adopted as above, with the flexures installed and the turbine valve operated either fully open or partly open, and then the flexures were removed and the roller bearing supports installed, and the valve operated either fully open or partly open.

VII. RESULTS AND ANALYSIS OF TESTS

Fig. 14 shows the total-static turbine efficiency as a function of isentropic head coefficient. It is seen that a maximum efficiency of 79.6 percent occurs at a k_{is} of 4.2. Previous results for these operating conditions quoted a maximum efficiency of 83 percent at the same k_{is}. However, the efficiency is directly proportional to the dynamometer torque M_d and inversely proportional to the flow rate $\dot{w}_T$ for given inlet conditions and speed N. Since the calculated flow rate is now considered to be in the order of 3.0 percent higher because of the corrected nozzle coefficient, this would account for the difference, and it was therefore concluded that the correct results were being obtained.

Fig. 15 shows the referred stator axial force as a function or referred RPM. It can be seen that there is some non-linearity when the curve is continued to the locked rotor condition, which can be accounted for by the changing pressure distribution around the shroud with the rotor locked.

Fig. 16 shows the referred stator torque as a function of referred speed. There is good linearity to the locked rotor condition, indicating the locked rotor torque is in the range of its expected value. When the referred torque is plotted as a function of stator pressure ratio, as shown in Fig. 17, there is a difference between the results of Method 1 and Method 2 and a considerable difference between the actual and the predicted value for the assumed $\zeta_s = 0.08$. The difference between the methods is due to the resulting higher pressure of P_1 by Method 2. It can be concluded however, that the torque measurements at a pressure ratio of 1.45 are about 8 percent too high. It will be discussed later how this can occur.

Fig. 18 shows the flow function Φ plotted against the stator pressure ratio. The curve extends well to the locked rotor condition. The reference curve shows that the actual Φ is more in error at the lower than at the higher pressure ratios when using Method 1. The difference between the curves of Method 1 and Method 2, as discussed previously, is due to the higher P_1 by Method 2. Although Φ is a function of both $\dot{w}_T$ and A_{ths} for fixed inlet conditions, it was concluded that A_{ths} was in error. Build-up of dirt deposits on the blades and the presence of an increasingly thick boundary layer at higher pressure ratios would result in a lower effective throat area than was used.

Fig. 19 shows the dimensionless velocity ratios V_{a1}/a_{T0} and V_{u1}/a_{T0} as functions of the stator pressure ratio. In both cases the curves extend smoothly to the locked rotor condition, and there is generally good agreement between the two data reduction methods. It can be seen that both V_{a1}/a_{T0} and V_{u1}/a_{T0} are lower than the calculated values for an assumed $\zeta_s = 0.08$. When using Method 1, V_{a1} is determined from equation (1), and a low value of V_{a1} could be due to a high value of pressure P_1 or the reduction factor K_t. When using Method 2, V_{a1} is determined by varying ε until equations (6) and (7) agree, which means in effect that P_1 is varied. Method 2 implicitly assumes that V_{u1} is correct. Examination of the behaviour of equations (6) and (7) when reducing the data revealed that equation (7) generally produced a lower V_{a1} than equation (6), and its value changed very little during the iteration. The strongest variables in equation (7) are P_1 and K_t, and a low value of V_{a1} would be due to high values of P_1 and K_t, which is in agreement with the previous conclusion for Method 1. The magnitude of V_{u1} has little effect on V_{a1} in equation (7). Since V_{a1} by equation (6) is generally higher than by equation (7), and because changing P_{1av} causes equation (6) to change more rapidly than equation (7), the iteration scheme forces P_1 higher in order to reduce the net stator force and thus reduce V_{a1} in equation (6). The increase in P_1 causes only a slight reduction in V_{a1} by equation (7). If the initial value for P_1 with $\varepsilon = 0$ were too high then the above undesirable situation would occur, and the net result would be too high a value of P_1 and too low a value of V_{a1}. A desirable condition would occur if the initial value of V_{a1} by equation (7) were higher than that by equation (6), since the iteration scheme would then reduce P_1 causing a higher resultant V_{a1}. Previous work by Commons [Ref. 4] indicated that the stator hub pressure and the stator tip pressure measured with the arrangement of Fig. 6 were 5 percent higher and 5 percent lower, respectively, than the pressured obtained by flow surveys after the stator. The overall effect of these errors would produce a higher initial P_1 than the correct value, which is consistent with the previous conclusion for the low value of V_{a1}. Examination of the results from Run 15 given in Appendix D shows that the hub pressure acting on the hub area produces the largest effect on the net force in equation (6). As a consequence, a slightly low value of P_{hub} would result in the undesirable condition of a higher value of V_{a1} by equation (6) than by equation (7).

When using Method 1, the low value of V_{u1}/a_{T0} in relation to the calculated curve for an assumed $\zeta_s = 0.08$ would be due to the low values of V_{a1} and V_1 caused by an erroneously high pressure P_1. This supports the previous argument where it was stated that high values of P_1 could be causing the errors. Using Method 2, equation (4) shows that the low value of V_{u1} could be caused by a low stator torque reading. However, that condition would conflict with the conclusion from Fig. 17 which shows the torque to be reading about 8.0 percent high. A reduction in the stator torque would result in a further deviation of V_{u1} from the calculated curve for $\zeta_s = 0.08$, and an increase in the mean loss coefficient. This situation can be resolved only by concluding that the angle of 75.9^o chosen to calculate the velocity components from equation (9) was too high. A reduction in the chosen flow angle would result in a higher V_{a1} and lower V_{u1} for a given V_1.

Fig. 20 shows the stator loss coefficients calculated by the two methods as a function of stator pressure ratio. It can be seen that the losses obtained by either method are at least 50 percent higher than the predicted value. The higher loss coefficient by Method 2 is due to the higher pressures resulting from Method 2 and the fact that constant pressure lines diverge. Fig. 20 also shows that the loss coefficients determined by both methods decrease slightly as the stator pressure ratio and the flow rate increases. Such a condition is opposite to that expected, since at higher pressure ratios an increased possibility of separation exists, and a thicker boundary layer with greater secondary losses should occur. The apparent reduction of the loss coefficient as the stator pressure ratio increases is likely due to an unexpected flow condition at higher flow rates. It will be shown later that at higher flow rates a changing inlet flow condition does occur.

Fig. 21 shows the referred stator axial force as a function of stator pressure ratio for three axial clearances of 0.250 in. 0.500 in. and 2.000 in. It can be seen that at a clearance of 0.500 in. a more negative axial force occurs than at 0.250 in. or 2.000 in. It is suspected that the presence of the locked rotor at various axial clearances causes a changing pressure distribution on the shroud, and thus the rotor axial clearance has a large effect on the stator axial force and the shroud pressure distribution.

Fig. 22 shows the referred stator torque as a function of the stator pressure ratio. The same reversal of trend occurs when the axial clearance is increased, confirming the fact that the presence of the rotor influences conditions upstream. The locked rotor results shown in Fig. 22 at the three different axial clearances further supports the previous conclusion from Fig. 17, namely that the stator torque is reading high.

Fig. 23 shows the referred flow rate as a function of stator pressure ratio for the three axial clearances at the locked rotor configuration. It can be seen that there is good agreement at each of the three axial clearances, so the changing torque with clearance is not due to a different flow rate. Fig. 23 also shows that the flow rate approaches a maximum as the pressure ratio nears the critical value, but that choking does not occur.

Fig. 24 shows the flow function Φ with changing stator pressure ratio for the locked rotor condition. As in Fig. 23 there is no effect of clearance on flow rate. However, the same trend of a lower flow function than desirable is occuring, which confirms the results of Fig. 18.

Fig. 25 shows the stator discharge pressure ratio as a function of the overall pressure ratio P_{TO}/P_2. It can be seen there is a linear relationship between stator pressure ratio and overall pressure ratio. Fig. 25 also shows the increasing difference between Method 1 and Method 2 as the overall pressure ratio is increased.

Fig. 26 shows the referred velocities as a function of stator pressure ratio for the locked rotor configuration. The same trend in V_{a1} occurs with the locked rotor results as was noticed in Fig. 19 when the rotor was unlocked, confirming the conclusion that some error exists in the pressure P_1 and the reduction factor K_t. However, Method 2 results in a tangential velocity component which is greater than the calculated value for the assumed $\zeta_s = 0.08$. It can therefore be concluded that the increased value of V_{u1}/a_{TO} is directly due to an error in the stator torque measurement and that the high torque reading is caused by some combination of temperature effect on the assembly and an inlet swirl at the stator plenum.

Fig. 27 shows the stator loss coefficient as a function of stator pressure ratio for the locked rotor condition. Equation (8) gives the relationship between the pressure ratio, exit velocity and stator loss coefficient, and it can be seen that for a given pressure ratio a low velocity will result in a high loss coefficient, and conversely, if the velocity were too high, the loss coefficient could become negative. When using Method 1 the loss coefficient is a unique function of the throat pressure and area where the throat pressure was assumed to be the same as that existing at the exit plane. Behaviour of equation (2) shows that a low velocity will result if a combination of the pressure and throat area is too large. It has been previously shown that the throat area appears to be too large and Figures 20 and 27 show that at low pressure ratios the throat pressure must be high also. Appendix C gives a predicted pressure distribution at the exit plane, and it can be seen that a parabolic, rather than a linear variation would be more in order, resulting in a slightly higher P_1 than the linear variation from hub to tip would predict. From this it may be concluded that assumption 1 of Section 4.B, namely that equal pressures exist at the throat and exit plane would be in error. As the stator discharge pressure ratio increases the loss coefficient decreases somewhat, indicating that the pressure at the throat and exit plane are more nearly equal. When using Method 2, an erroneously high stator torque reading will produce a high tangential velocity component resulting in a higher net velocity than should exist for a given pressure ratio. It should be noticed that the loss coefficient by Method 2 increases with increasing pressure ratio even though the stator torque is high. This indicates that the error in hub pressure P_{hub} and exit pressure P_1 have a stronger effect than does the stator moment and it was concluded earlier from the analysis of Fig. 19 that P_1 was indeed too high.

Fig. 28 shows the measured temperature of the torque capsule support assembly as the flow rate is increased, and Fig. 29 shows the results of the temperature analysis on the cradle assembly. It can be seen that as the cradle assembly heats up, a positive error occurs in the stator torque reading, indicating that the reading becomes too high as the inlet temperature increases. The reason for the increasing torque error is the unequal expansion of the capsule support assembly and the connectors between the point of action of the torque arm and the upper end of capsule support. The stator torque flexures prevent free rotation of the stator as the capsule assembly grows due to thermal expansion. The two steel rods and the Invar ring of the torque capsule do not expand by an equal amount in the opposite direction to cancel the thermal expansion of the capsule support. The differential thermal expansion causes an additional tensile force on the capsule and a higher apparent torque reading. Additional analysis showed that it would be impractical to compensate for this thermal expansion by making the support assembly of the same type of material as the capsule ring and steel attachments, since the compensation would be possible only for a fixed temperature. In addition it would be impractical to thermally shield or cool the assembly as was done with the dynamometer capsule, since this set-up would present severe complications if the turbine were operated inside the closed hood. Thus the only practical way to eliminate the thermal effect on the capsule support assembly was to give the stator freedom to rotate so that no additional tension could be applied to the capsule. A solution was accomplished by removing the torque flexures and installing roller bearing supports to maintain the stator alignment, and a thrust collar was fastened to the stator support shaft and allowed to press against the support bearing as a means of transmitting the stator axial force to the cradle assembly.

Fig. 30 shows the referred stator torques obtained with the honeycomb flow straightener replacing the guide vanes. Test data are shown at different openings of the turbine inlet valve and the tests were carried out with the torque flexures installed or removed. If the flow after the honeycomb were axial, and if the flow entered the stator assembly with no whirl components, the stator torque would be zero for any pressure ratio. Fig. 30 shows that the stator torque was only zero at zero flow rate, and increased with increasing pressure ratio. From the results of Fig. 30 it can be concluded that temperature effects caused by the presence of the torque flexures and throttling the flow by partly closing the turbine inlet valve influence the stator torque readings. With the turbine valve full open less torque occurs when the flexures are removed, indicating that the temperature effect due to the flexures has been reduced. When the pressure ratio is set with the turbine valve partly closed a considerably larger torque occurs and it is again higher if the torque flexures are installed. Since an increasing torque with increasing pressure ratio still occurs when the turbine valve is full open and the torque flexures are removed, it can be concluded that either the honeycomb is not truly axial or the flow still enters the stator plenum with a small whirl component.

Fig. 31 shows the flow angles measured after the honeycomb straightener. It can be seen that the velocity after the honeycomb has a tangential component which increases with increasing flow rate. From Figures 30 and 31 it can be concluded that the partly opened turbine valve causes whirl components in the delivery pipe, and the flow enters the stator assembly with a tangential velocity. Hence, assumption 4 of Section 4.a, namely, that the flow into the plenum is radial and no whirl component exists ahead of the stator is not satisfied with the present installation. Because the honeycomb has openings of about 1/8 inch it is apparently not capable of completely turning the flow into the axial direction. It was found also that the stator blockage factor ξ through the honeycomb is about 0.72, where ξ represents the ratio of the actual flow area and that necessary to pass the flow if the expansion were isentropic. Because of the low valves of ξ it can be concluded there must exist large whirl components ahead of the honeycomb causing flow separation at the inlet and large losses.

VIII. CONCLUSIONS AND RECOMMENDATIONS

From the preceding analysis, it can be concluded that the stator torque reading is about 8 percent too high, and that this error is due to a combination of the temperature effect on the capsule support assembly and an inlet swirl caused by the turbine inlet valve and piping. It is recommended that the turbine be operated with the turbine inlet valve full open at all times, and that the pressure ratio be set by closing a dump valve near the air supply.

During the last series of runs with the stator nozzles installed and the rotor removed, inconsistent and residual values of stator axial force occured when the torque flexures were removed and the roller bearings installed. This was due to the mechanical friction inherent in the present system. It is felt that a better system should be designed which would allow the stator to rotate and move axially without restraints. This would make the stator a truly free-floating assembly and eliminate the influence of temperature on the measurement of the stator torque. Such a system would require the use of ball-bearings mounted in such a way that they would allow both rotation and axial movement of the stator and thermal expansion or contraction of the casing, but maintain the stator axial alignment.

The analysis of the cradle assembly showed also that thermal effects occur in the horizontal direction which affect the capsule measuring the stator axial force. This problem could be eliminated by constructing a cradle support assembly similar to that used for the torque measurement but made of aluminum. Proper installation of this cradle would allow its growth or contraction to be in the same direction as the horizontal members of the stator cradle, thus compensating for thermal effects on these members.

It is suggested that a honeycomb flow straightener and series of screens be installed in the delivery pipe just ahead of the inlet to the stator plenum chamber, and that the conical screen presently installed in the plenum chamber be removed. This should produce a more uniform flow into the plenum and eliminate the tangential component, while removal of the conical screen should eliminate some of the existing total pressure gradient at the entrance to the stator nozzles.

From the analysis of the pressure effects on the loss coefficient it can be concluded that extensive flow surveys should be done at different operating conditions to accurately determine the pressure distribution at the stator discharge. Means must then be found to ensure that accurate hub and tip pressures can be recorded since they have a large effect on the loss coefficient. It was shown that the assumption of stator exit pressure also acting at the throat plane was erroneous and the assumption could be eliminated if the throat hub and tip pressure taps were accurately located at the throat plane. At present there is up to a 5 percent error between the four sets of taps. The flow surveys must be carried out with probes which properly compensate for Mach number effect, depth of immersion and pitch angle. Very useful information could be gained by using a hot wire anemometer probe to accurately determine velocity profiles and magnitudes in the stator area at different operating conditions.

Results of the prediction of closure plate torque and shroud torque given in Appendix B show these values never exceed 0.1 percent of the stator torque reading. This amount is considered negligible and thus the closure plate torque webs, strain gauges and wires could be removed. This would eliminate the congestion in the hub area and allow the closure plate greater freedom of movement, since some friction might be caused by the presently installed equipment. The predicted torque as a function of pressure ratio and speed agreed very well with the strain gauge readings and so it is concluded the closure plate and shroud torques could be accounted for during the data reduction by using an empirical formula. Results of the forces on the closure plate due to the pressure distribution on the face agreed to within 1.0 percent of the strain gauge reading. Considerable effort was required to numerically integrate the pressure over the face area, and since measurement of the closure plate axial force by the strain gauges was much quicker and produced comparable results, it is recommended the closure plate pressure lines be removed.

It can be concluded that several of the assumptions utilized to solve the equations for a one-dimensional analysis were not valid, and that ignoring their effects can produce very poor results. Appendix C shows that cylindrical stream surfaces cannot exist, and a radial component of velocity must be taken into account. Flow surveys made by Commons [Ref. 4] show that there is a variation of the total pressure at the stator entrance and thus a radial entropy gradient exists. The results of this investigation have shown that the flow is not completely radial into the plenum or axial into the stator and that a tangential component of velocity does exist. However, these unsatisfactory conditions can be reduced by incorporating the equipment modifications suggested.

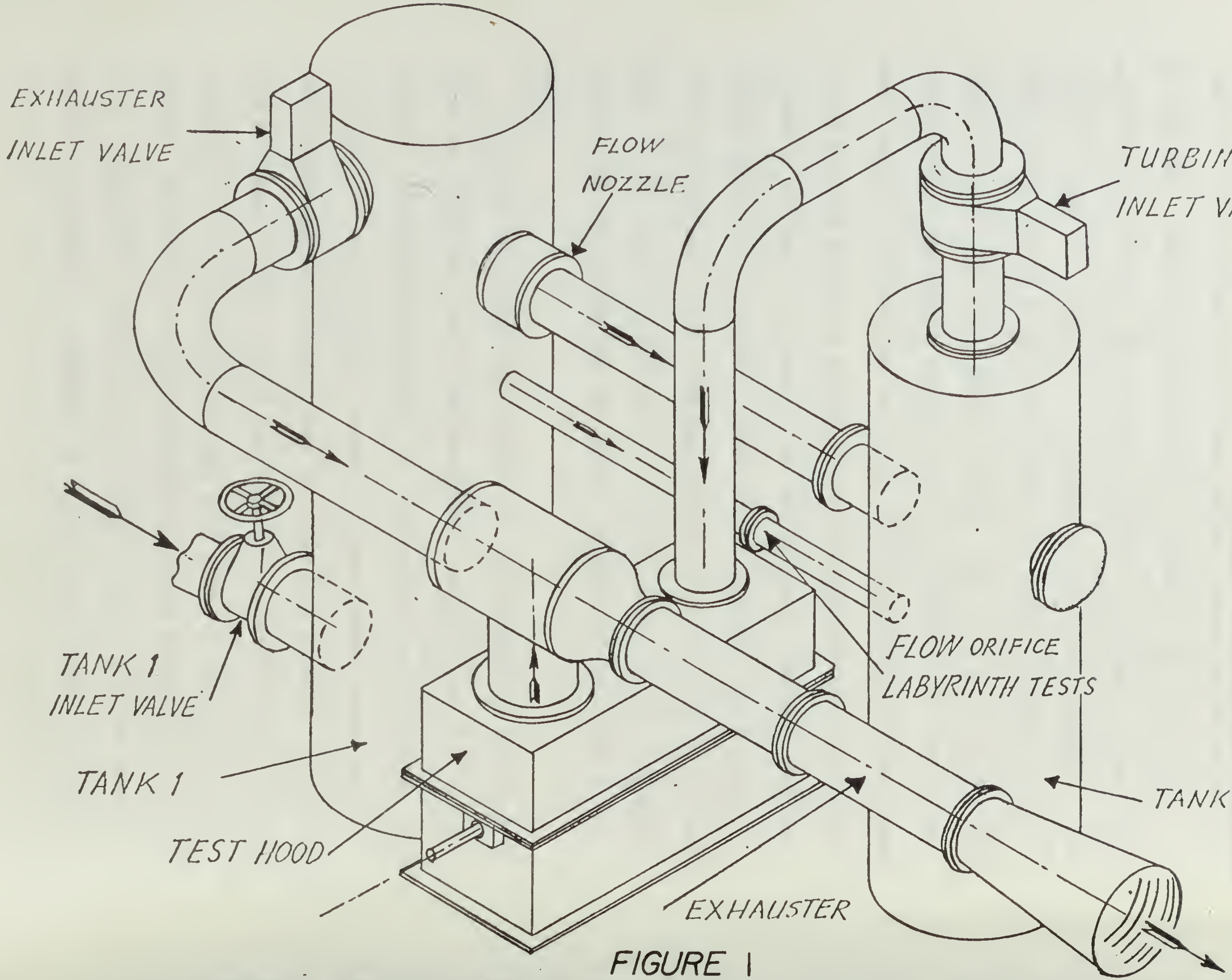

FIGURE 1
PIPING INSTALLATION, TRANSONIC TURBINE TEST RIG

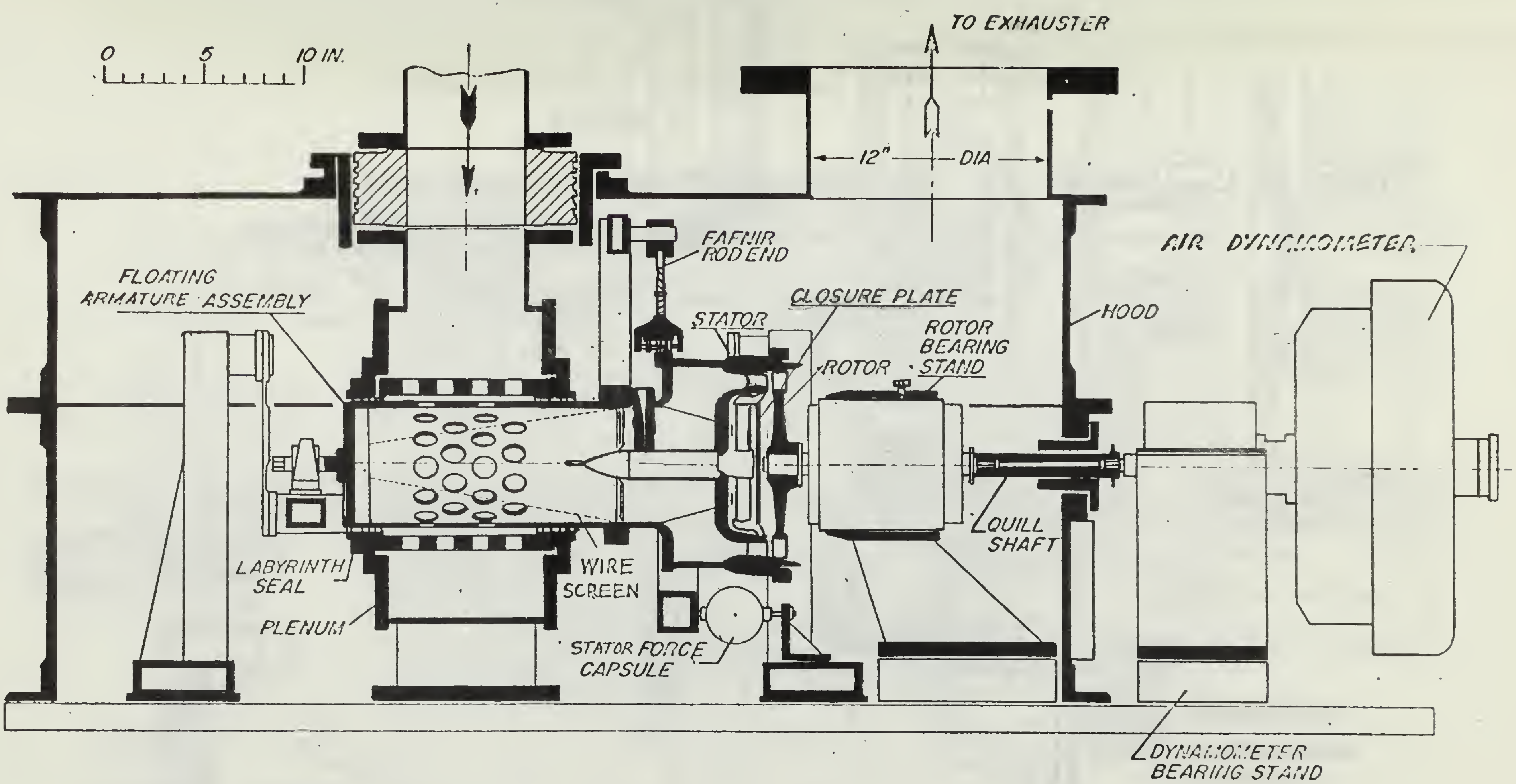

FIGURE 2

TRANSONIC TURBINE TEST RIG

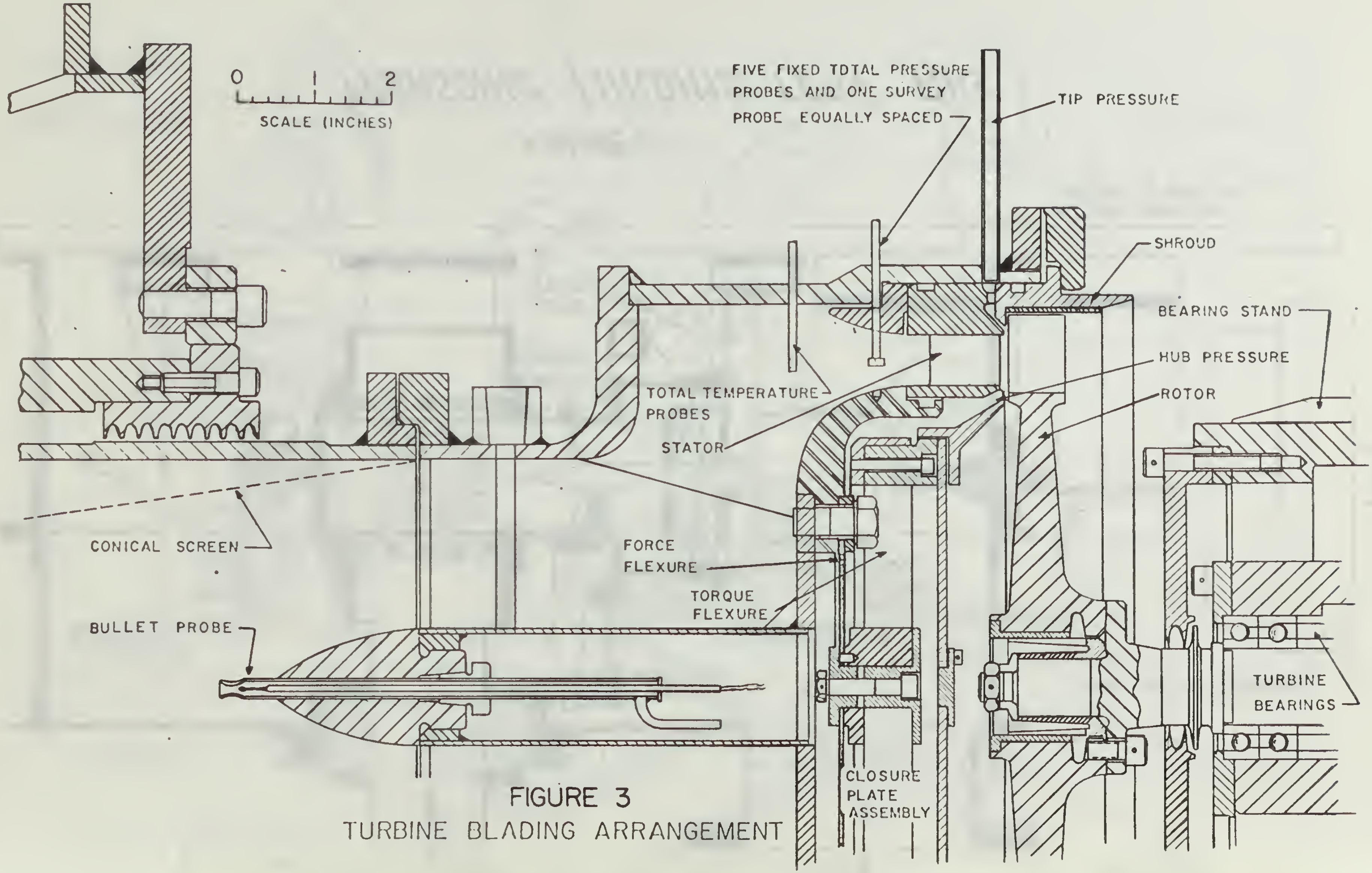

FIGURE 3
TURBINE BLADING ARRANGEMENT

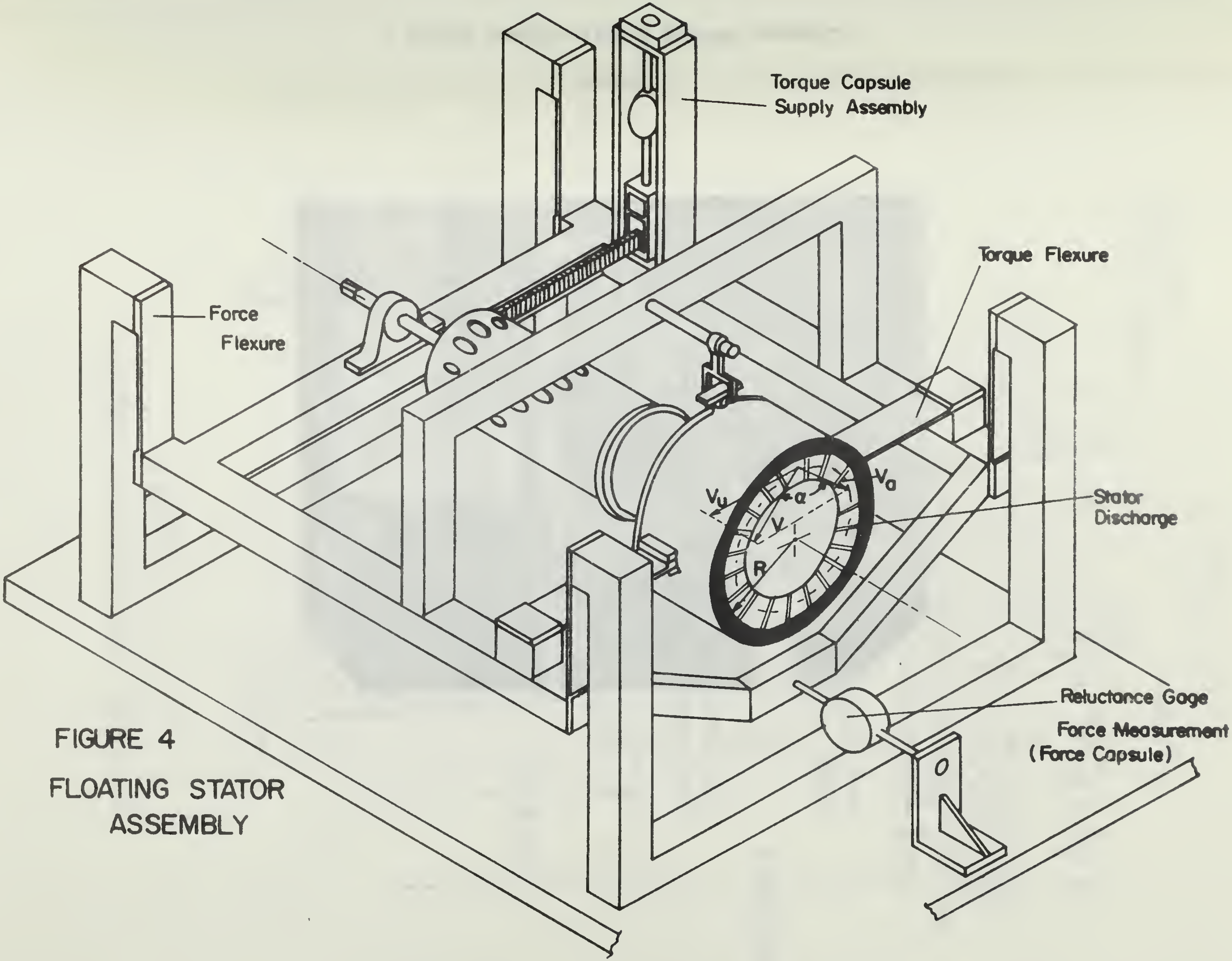

FIGURE 4

FLOATING STATOR
ASSEMBLY

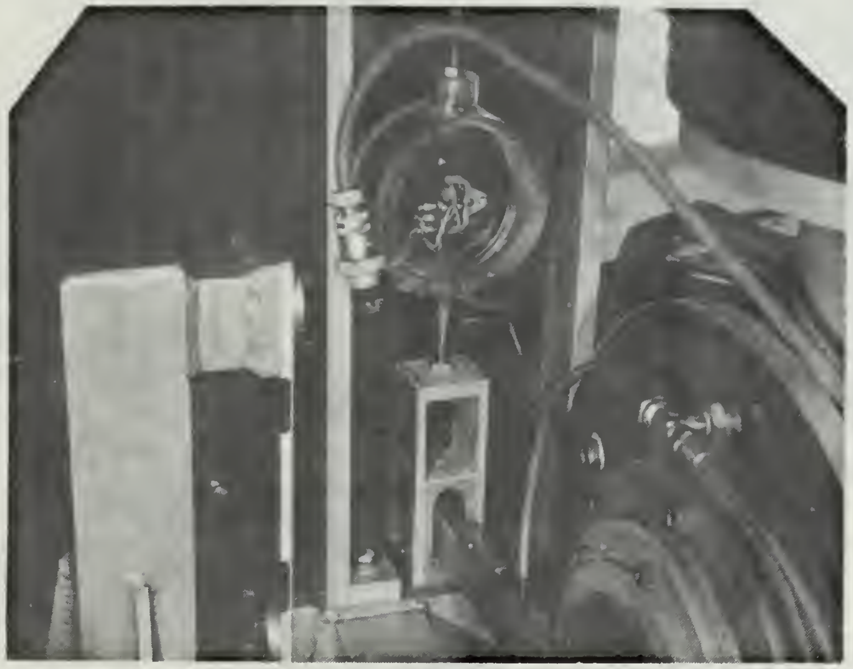

FIGURE 5

STATOR TORQUE CAPSULE SUPPORT ASSEMBLY

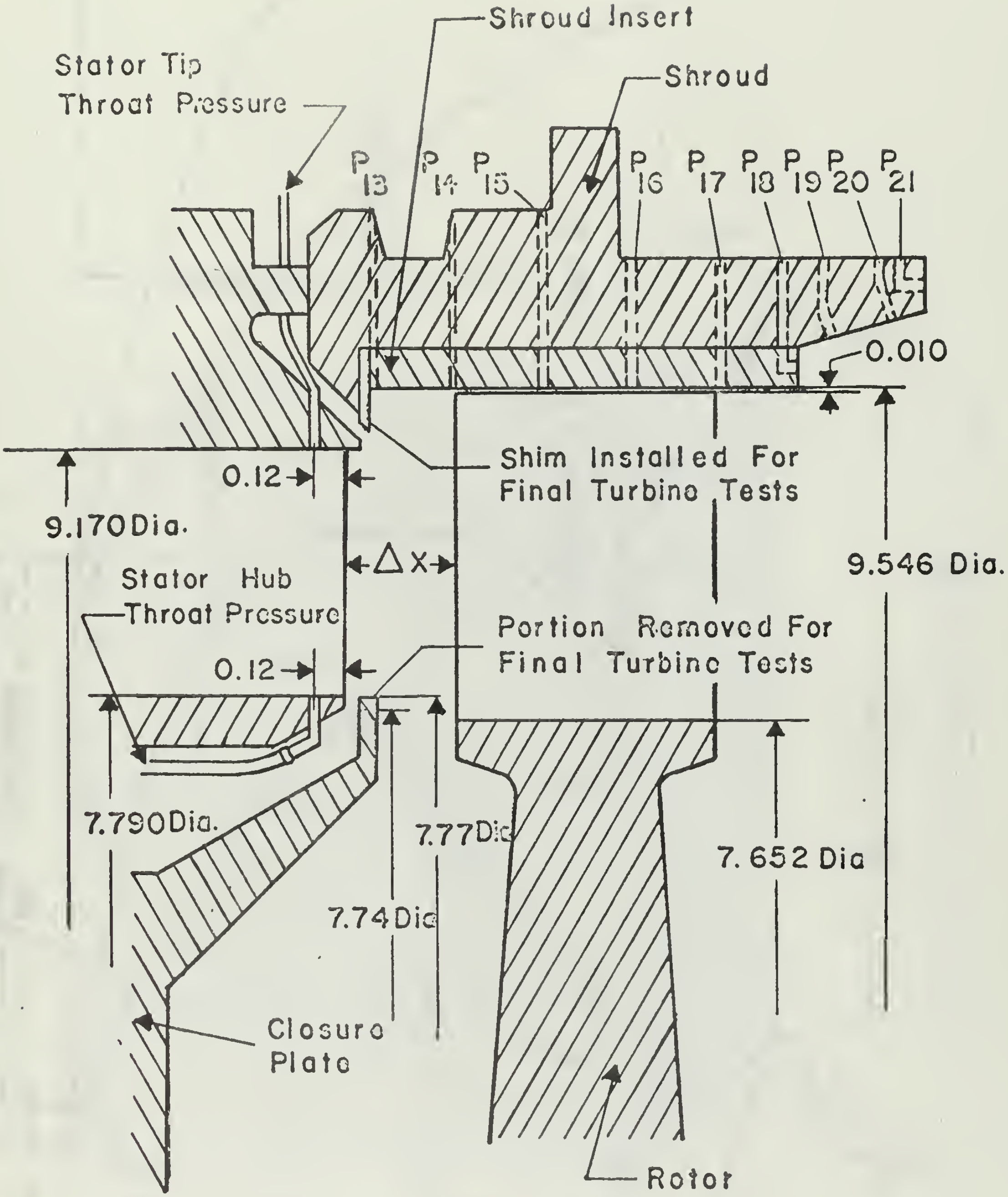

FIGURE 6
TURBINE AND SHROUD DETAILS

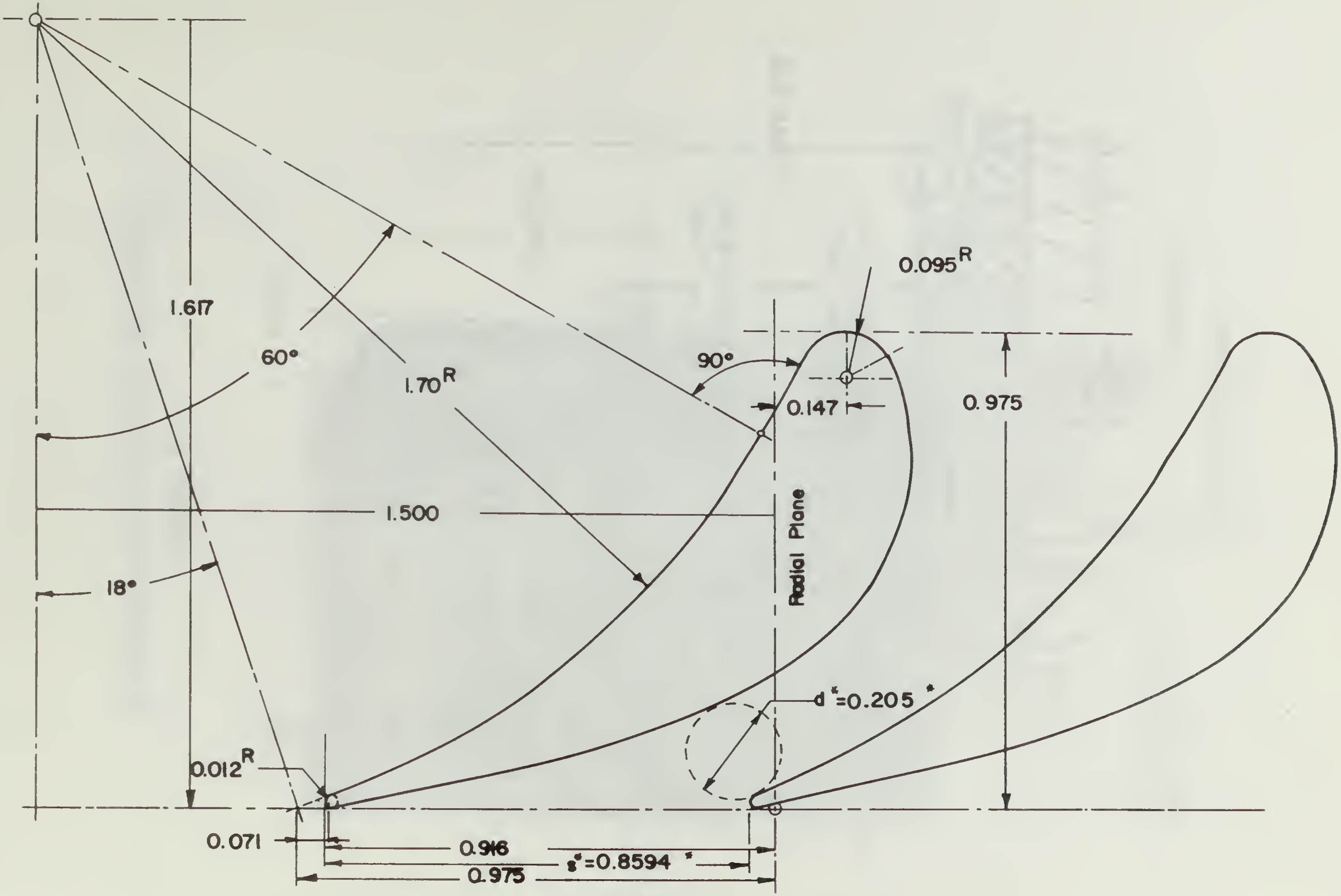

FIGURE 7
MEAN RADIUS BLADE PROFILE CONVERGING NOZZLES

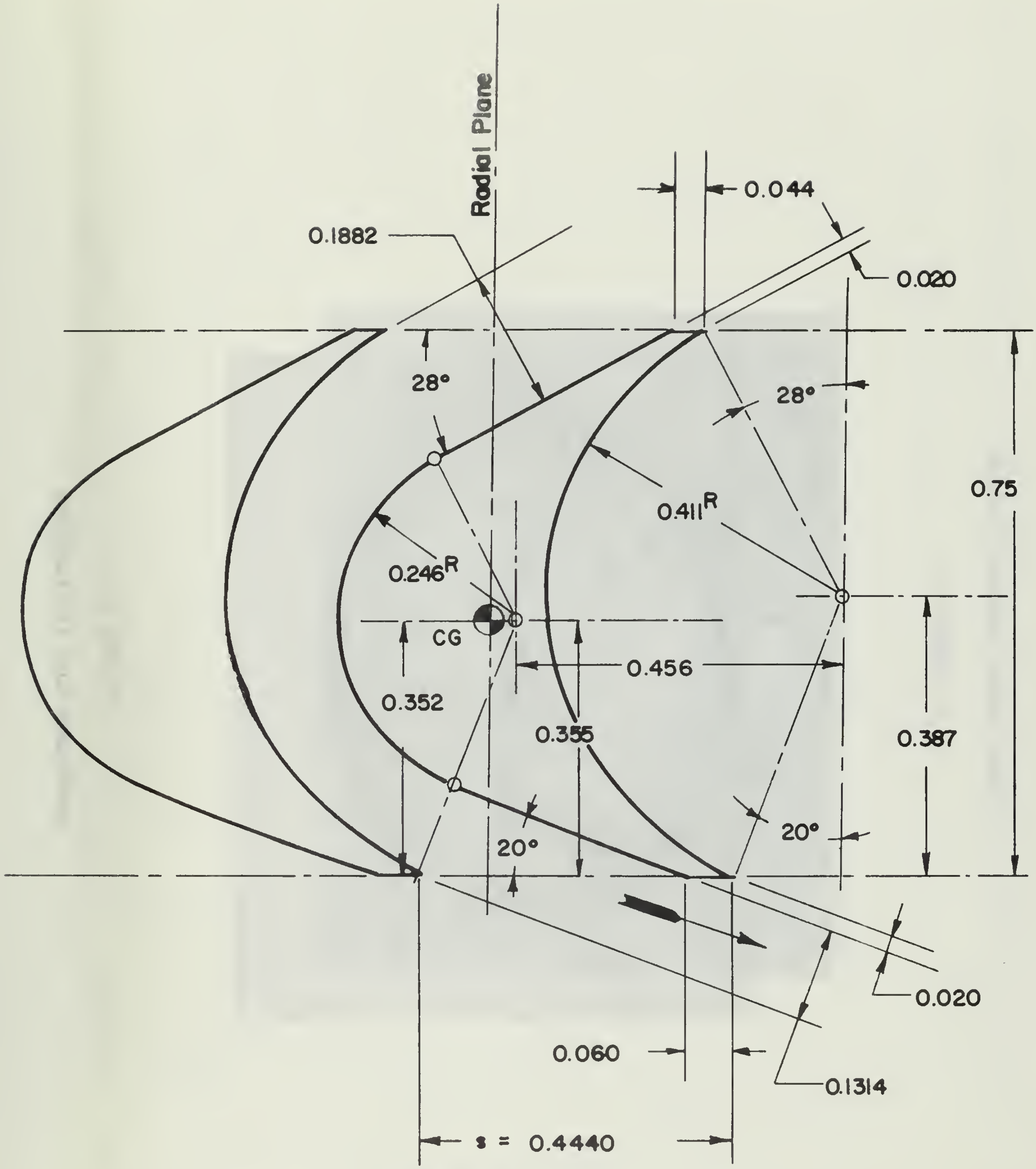

FIGURE 8

MEAN RADIUS BLADE PROFILE
CIRCULAR ARC
SHARP LEADING EDGE ROTOR

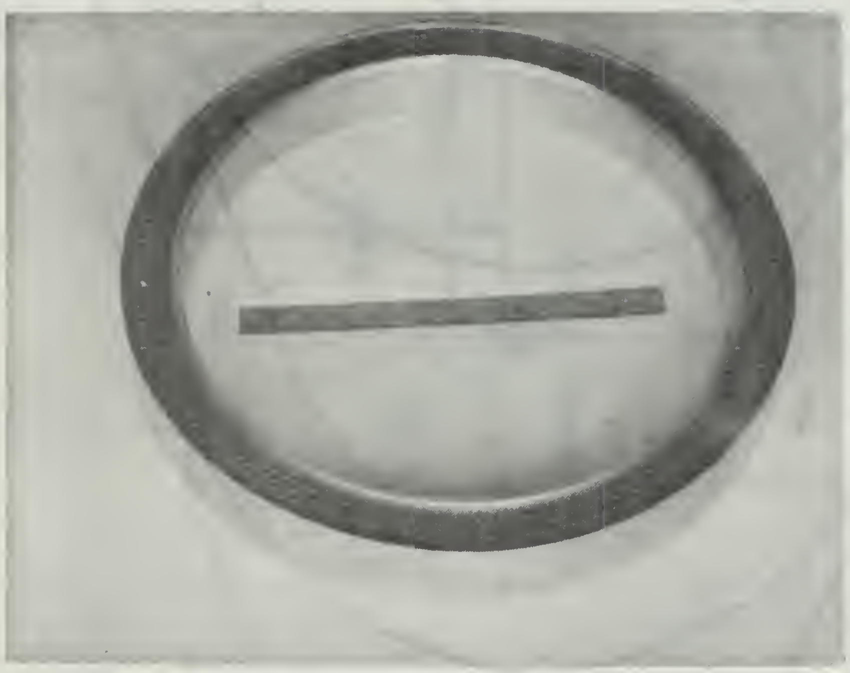

FIGURE 9

HONEYCOMB FLOW STRAIGHTENER

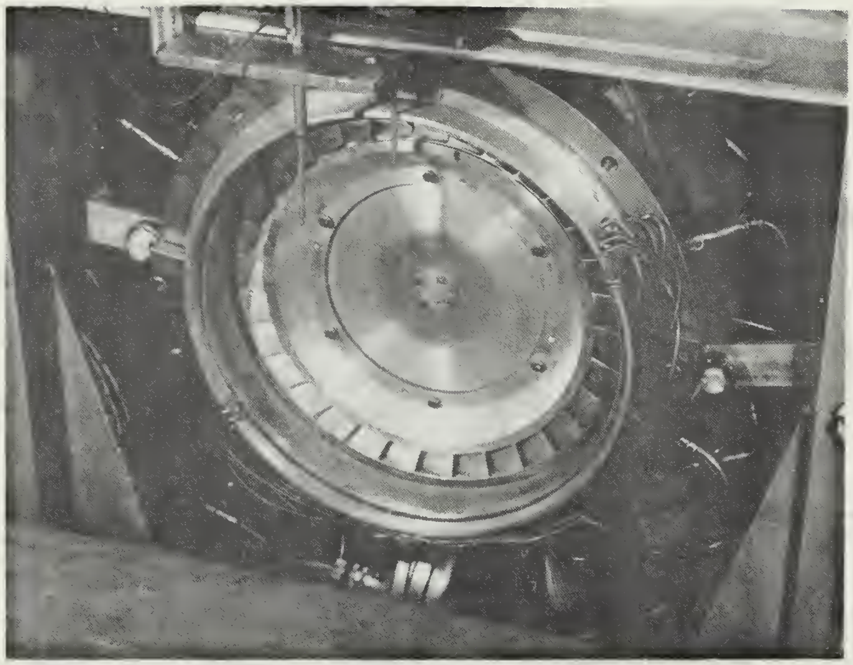

FIGURE 10

STATOR ROLLER BEARING SUPPORTS

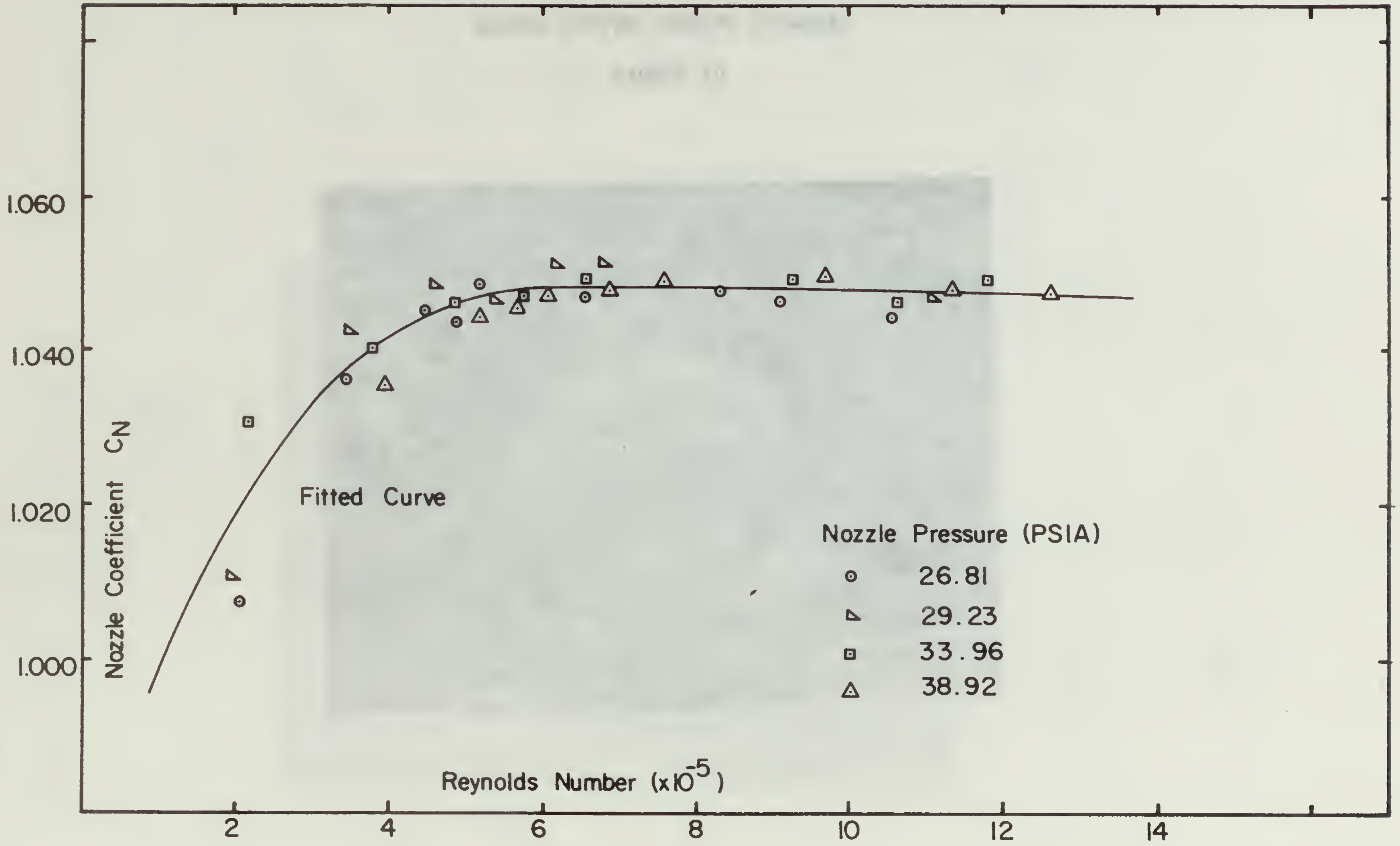

FIGURE 11

NOZZLE COEFFICIENT VS. NOZZLE REYNOLDS NUMBER

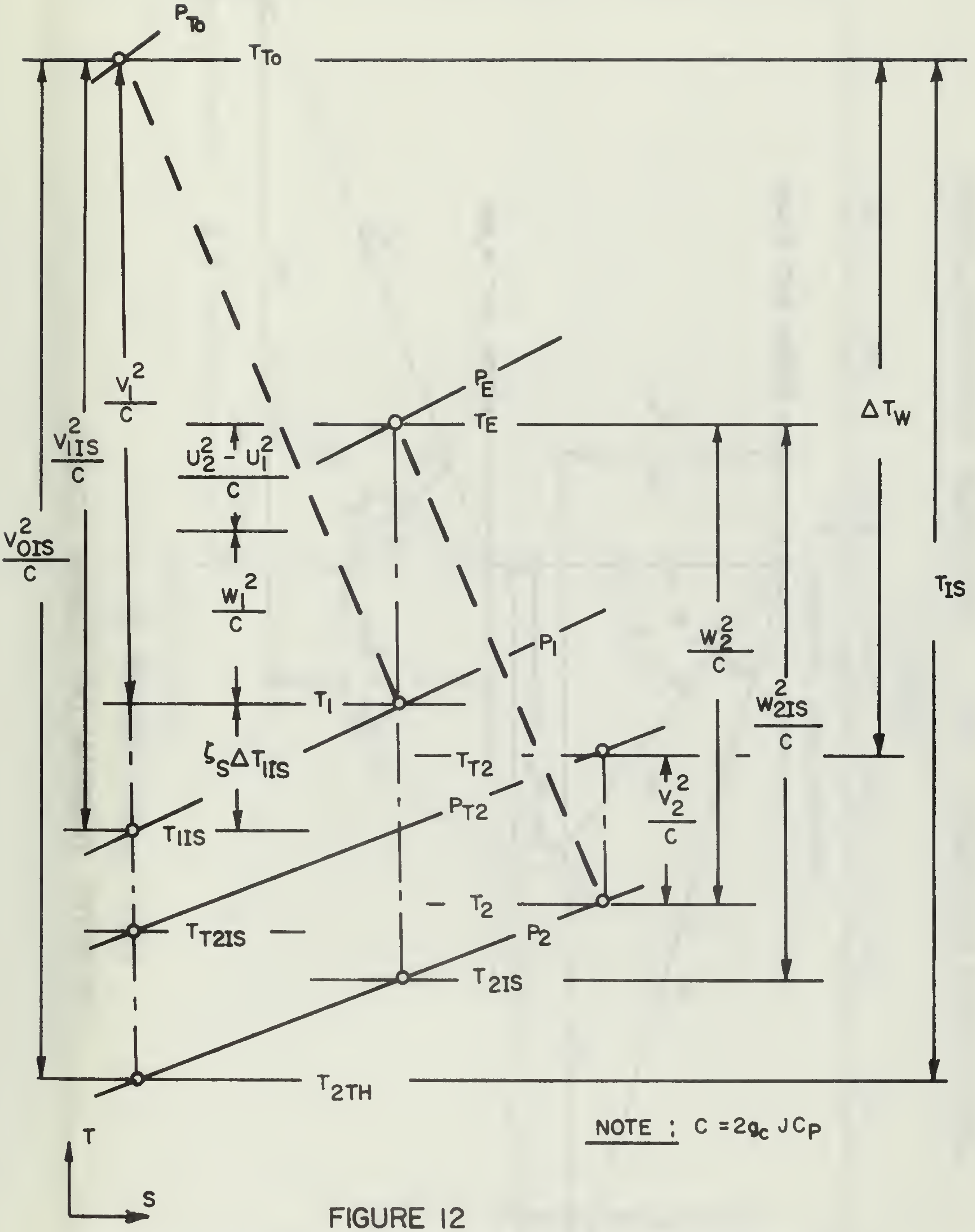

NOTE : $C = 2g_c JC_P$

FIGURE 12

THERMODYNAMIC PROCESS FOR AN AXIAL TURBOMACHINE

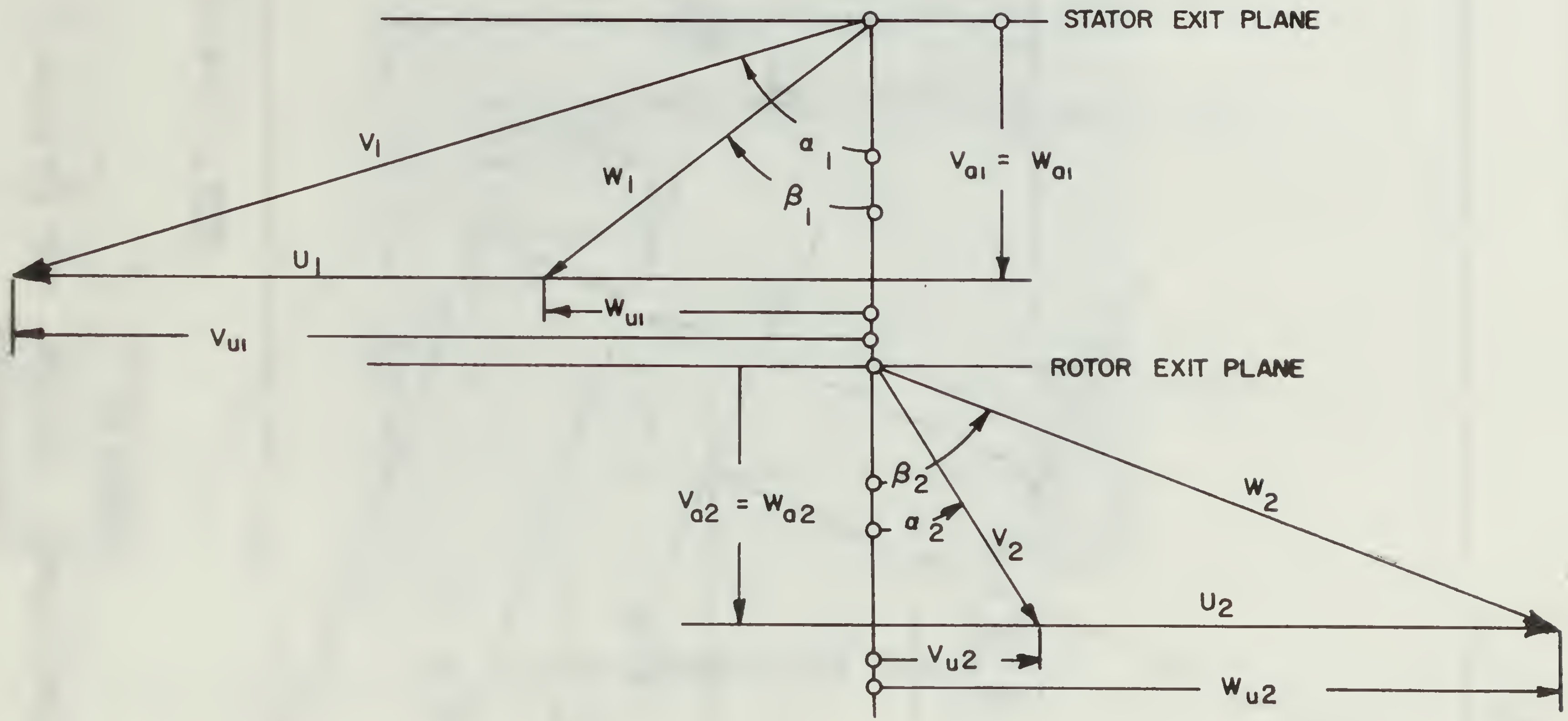

FIGURE 13

VELOCITY DIAGRAM OF TURBINE STAGE

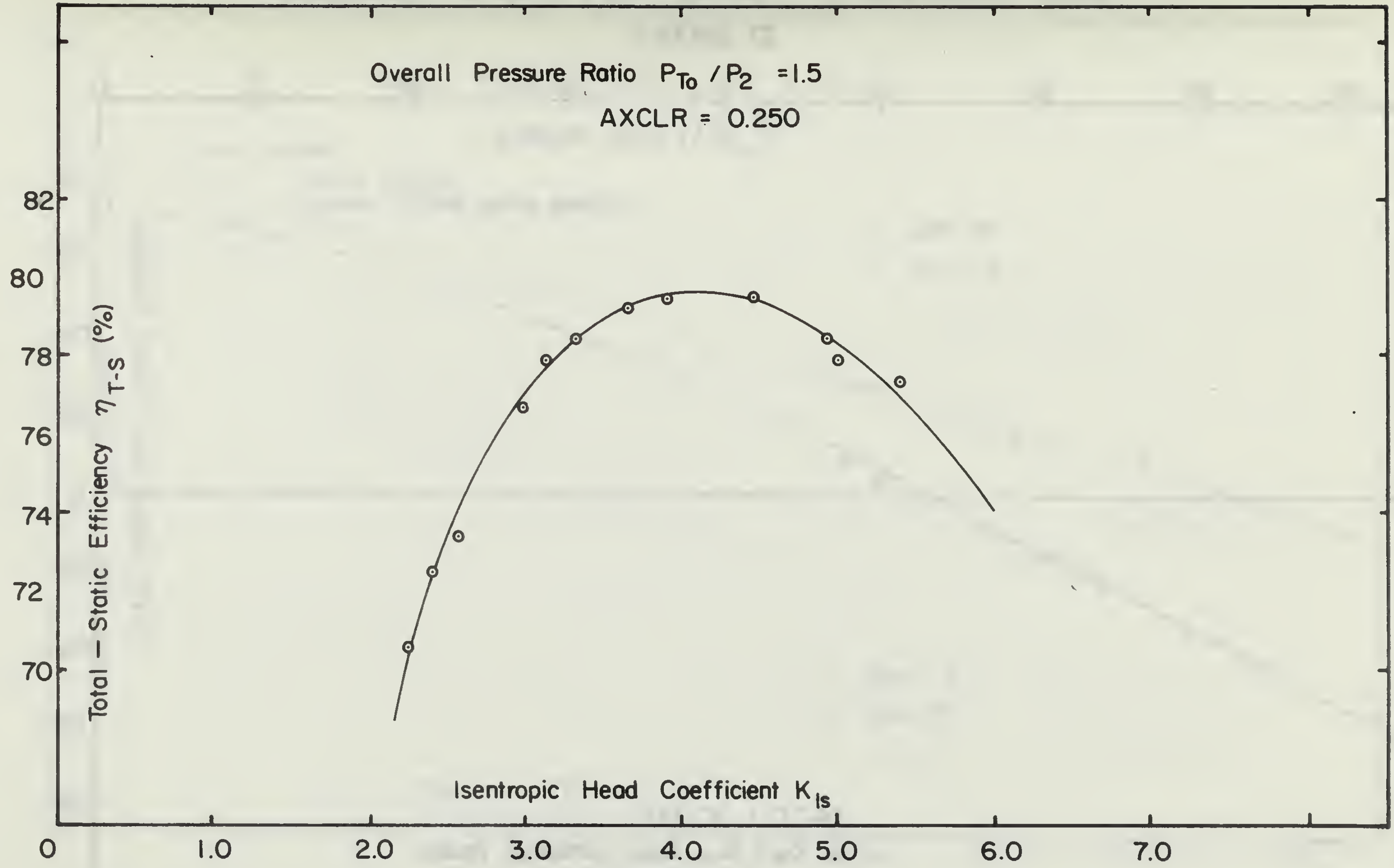

FIGURE 14

TOTAL-STATIC EFFICIENCY VS. ISENTROPIC HEAD COEFFICIENT

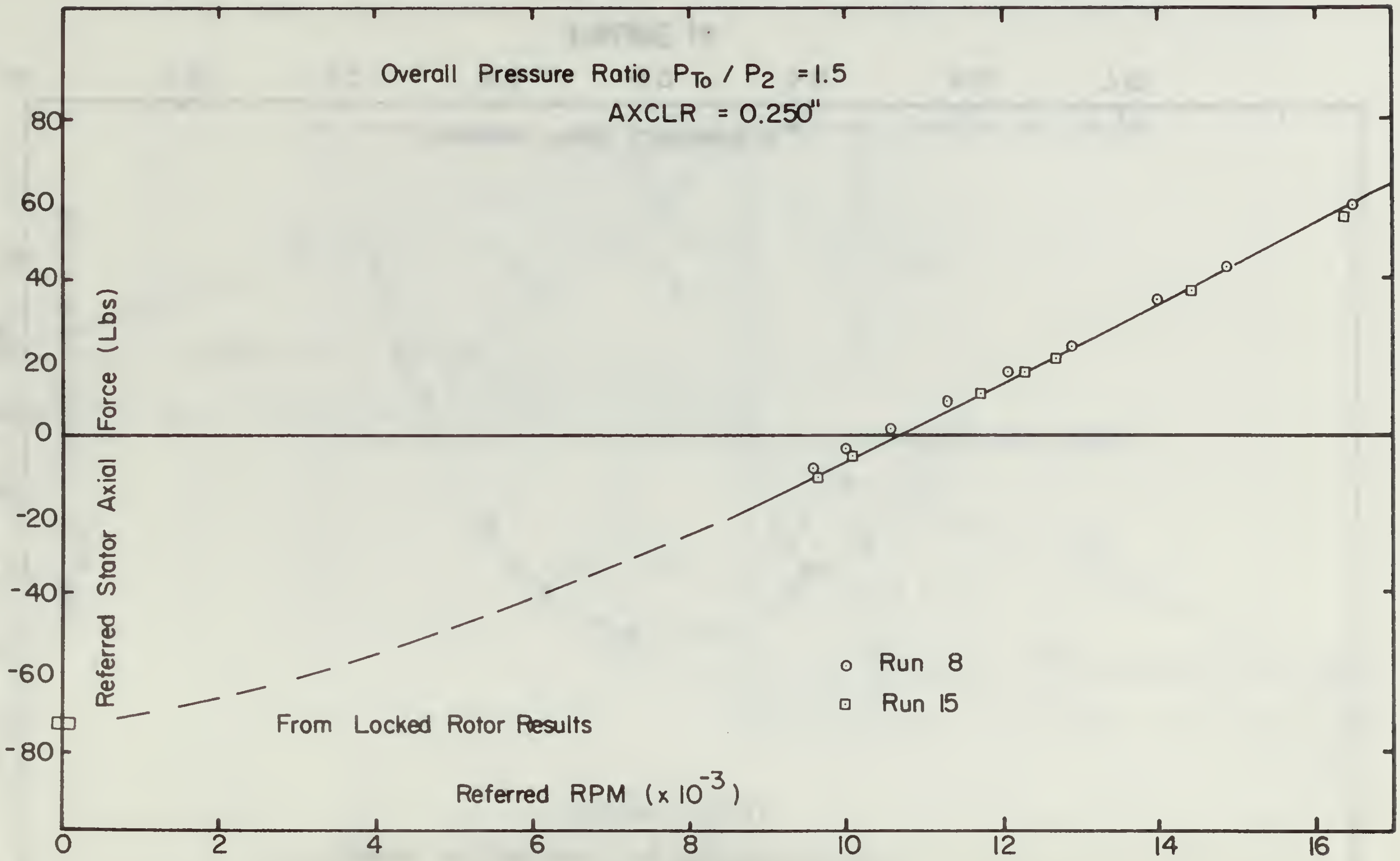

FIGURE 15

REFERRED STATOR AXIAL FORCE VS. REFERRED RPM

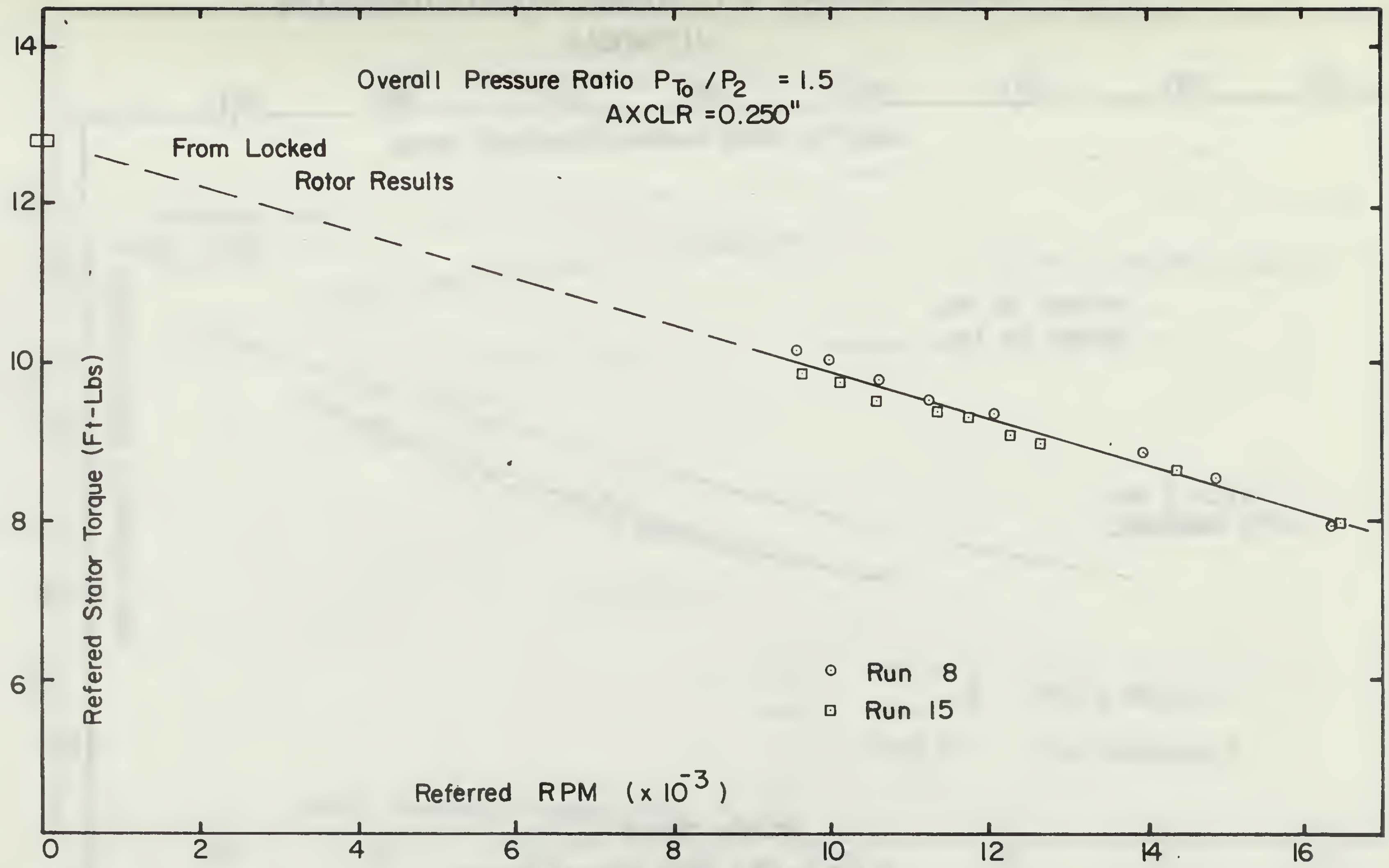

FIGURE 16

REFERRED STATOR TORQUE VS. REFERRED RPM

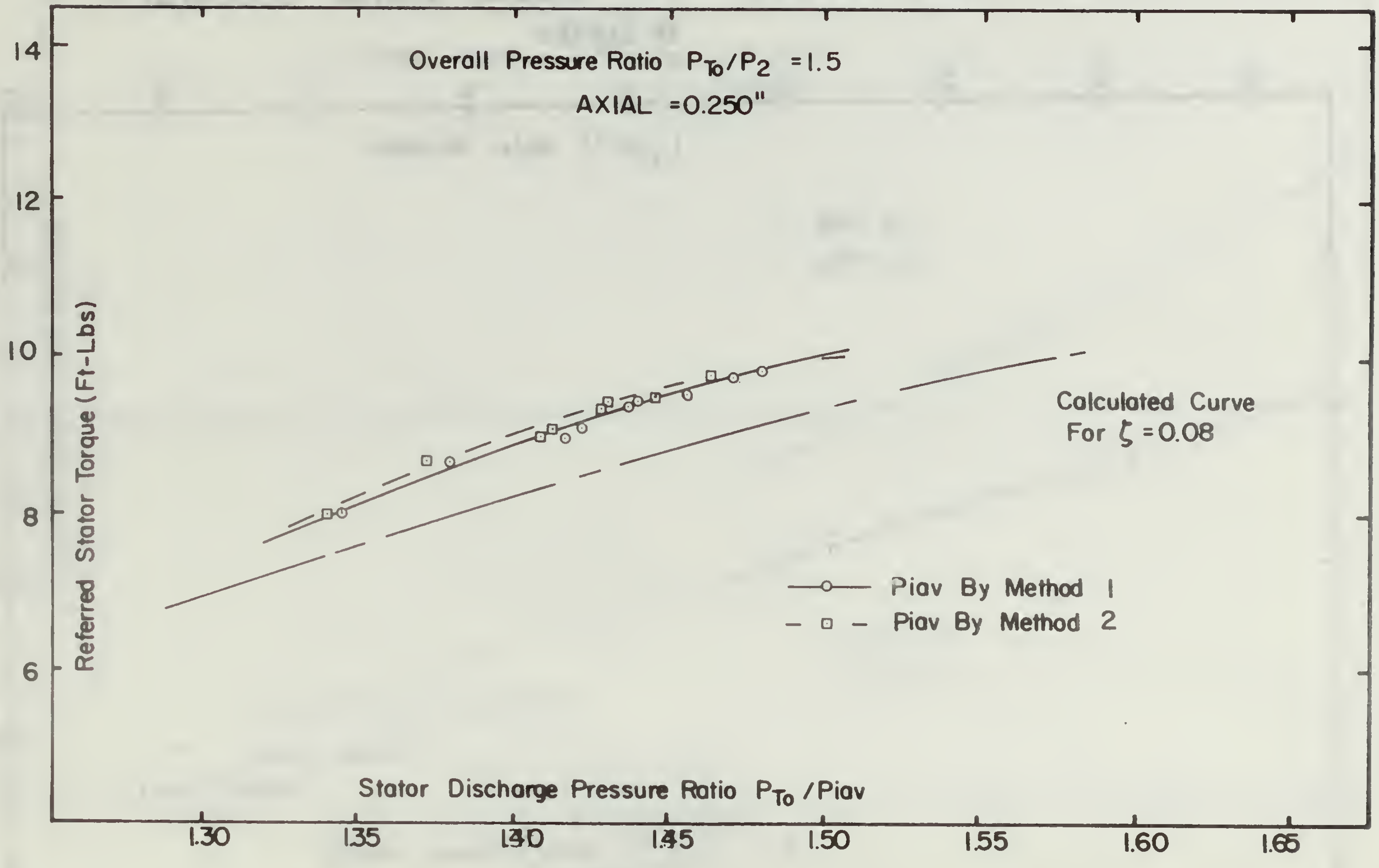

FIGURE 17

REFERRED STATOR TORQUE VS. STATOR PRESSURE RATIO

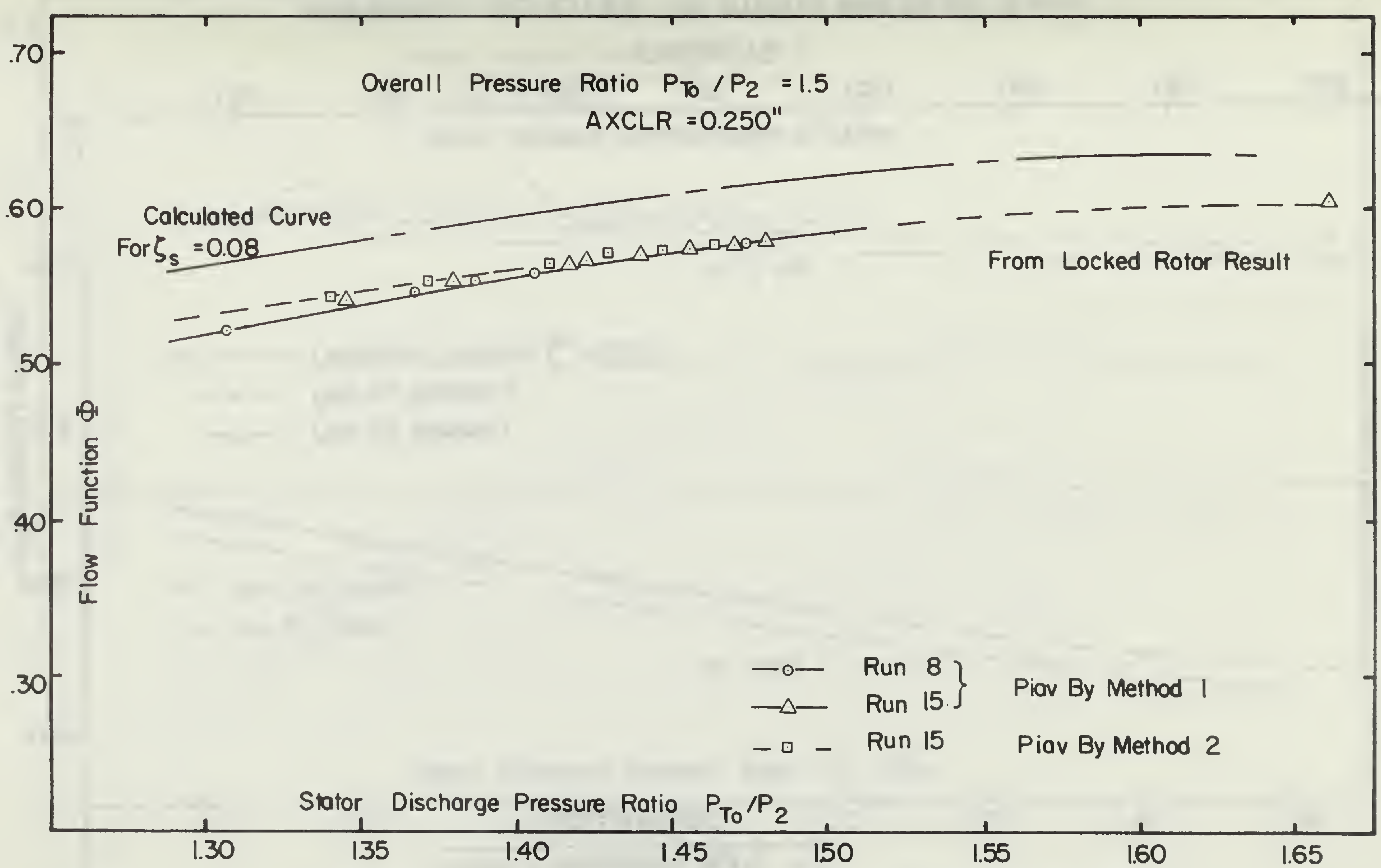

FIGURE 18

FLOW FUNCTION VS. STATOR PRESSURE RATIO

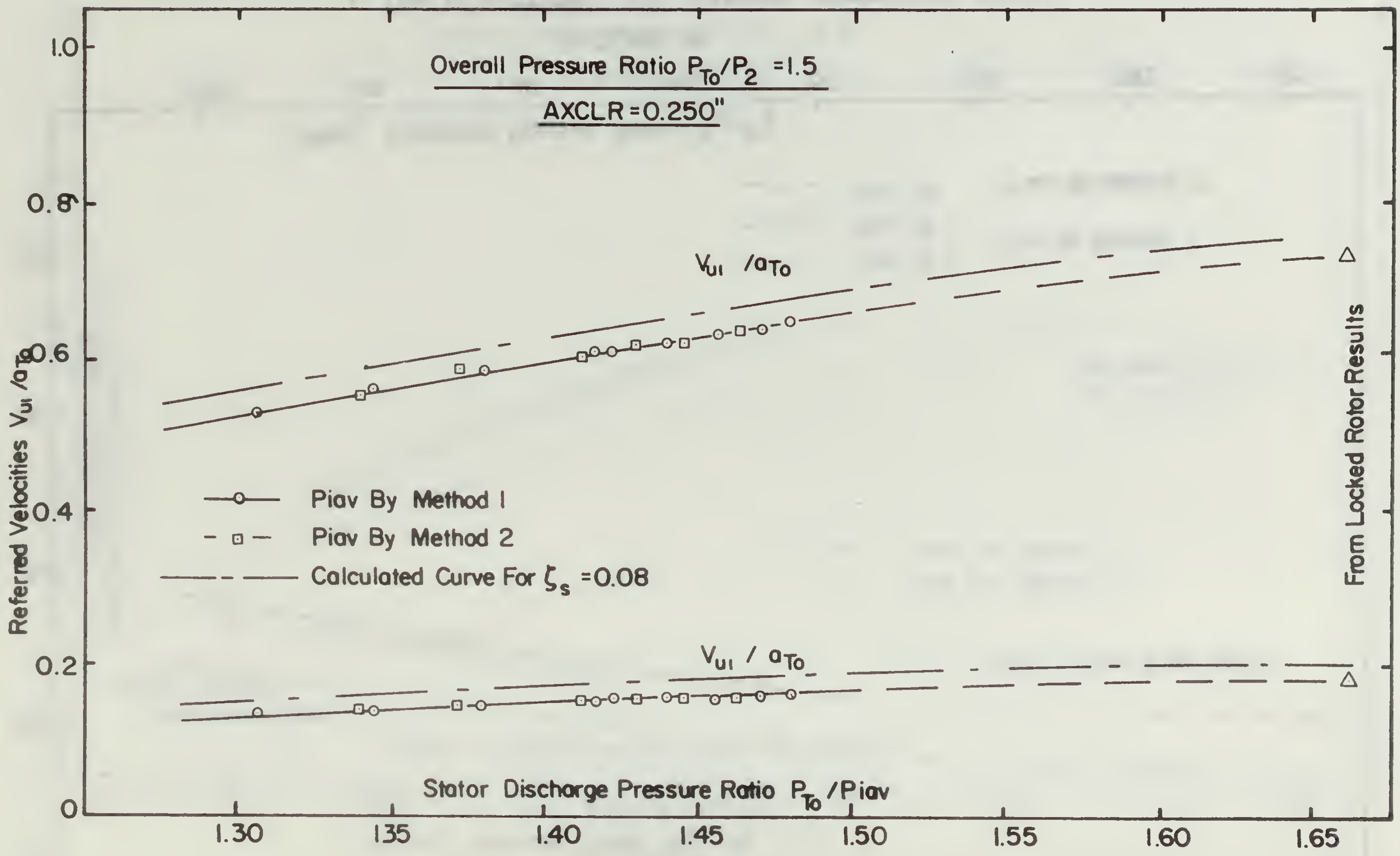

FIGURE 19

REFERRED VELOCITIES VS. STATOR PRESSURE RATIO

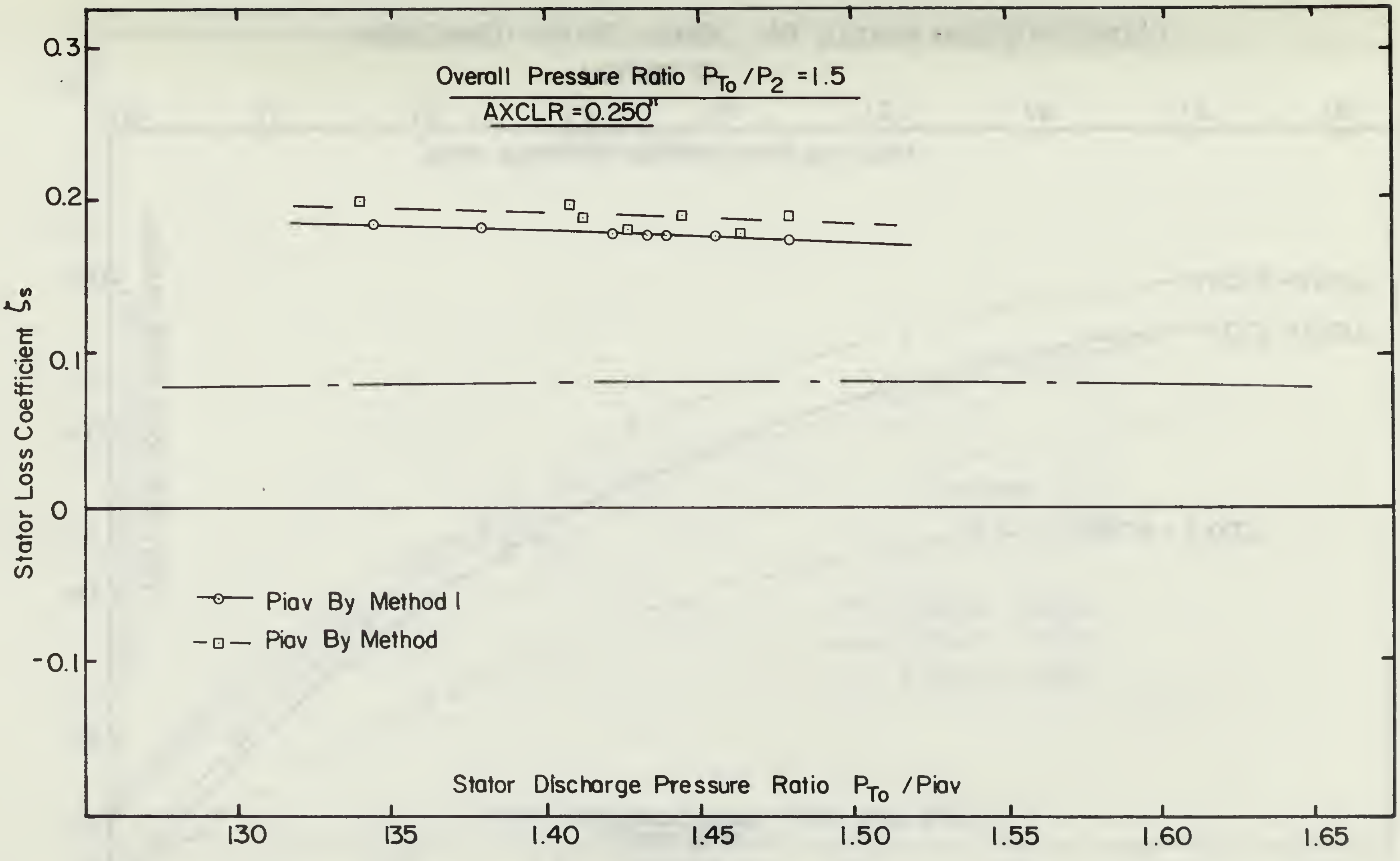

FIGURE 20

STATOR LOSS COEFFICIENT VS. STATOR PRESSURE RATIO

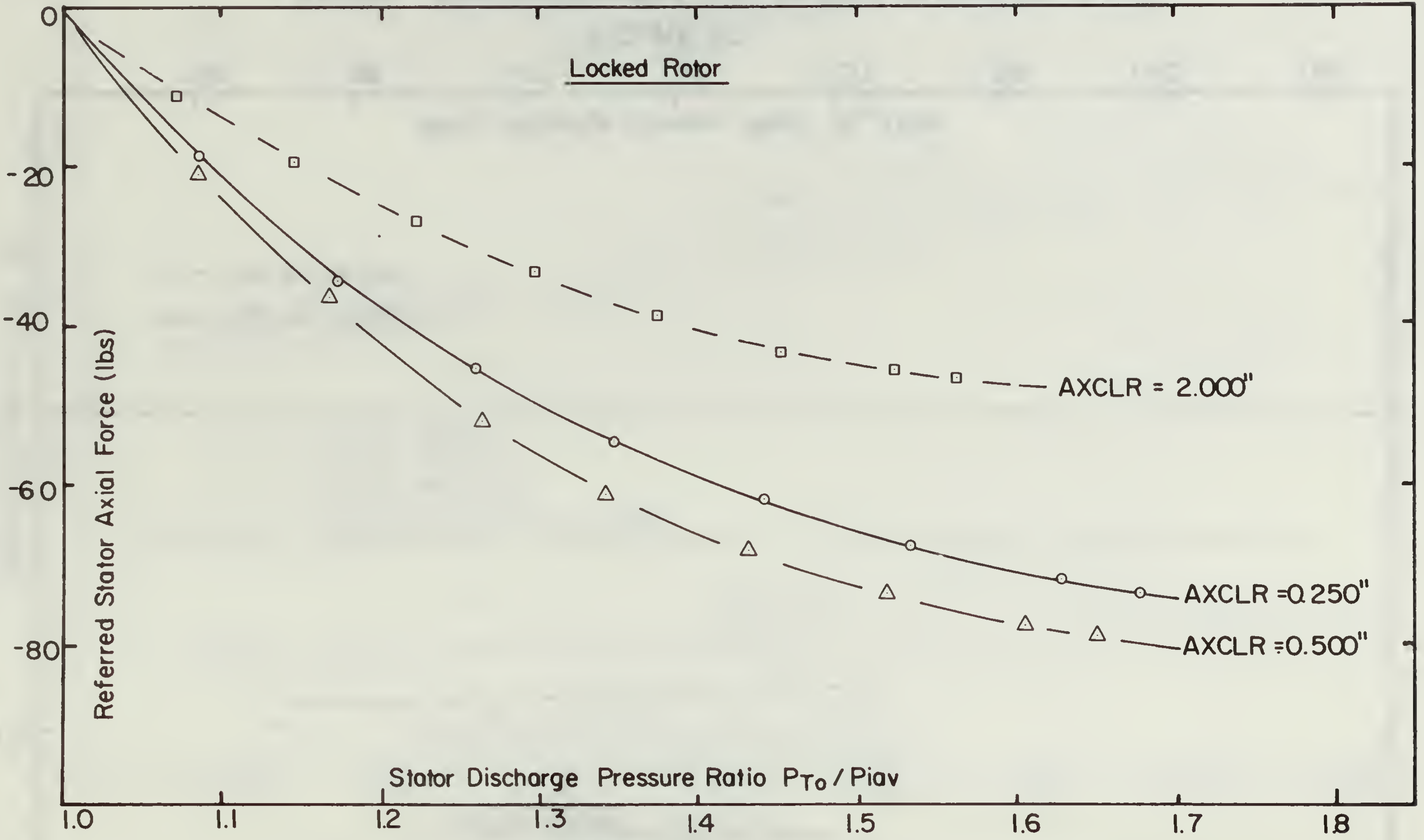

FIGURE 21

REFERRED AXIAL FORCE VS. STATOR PRESSURE RATIO

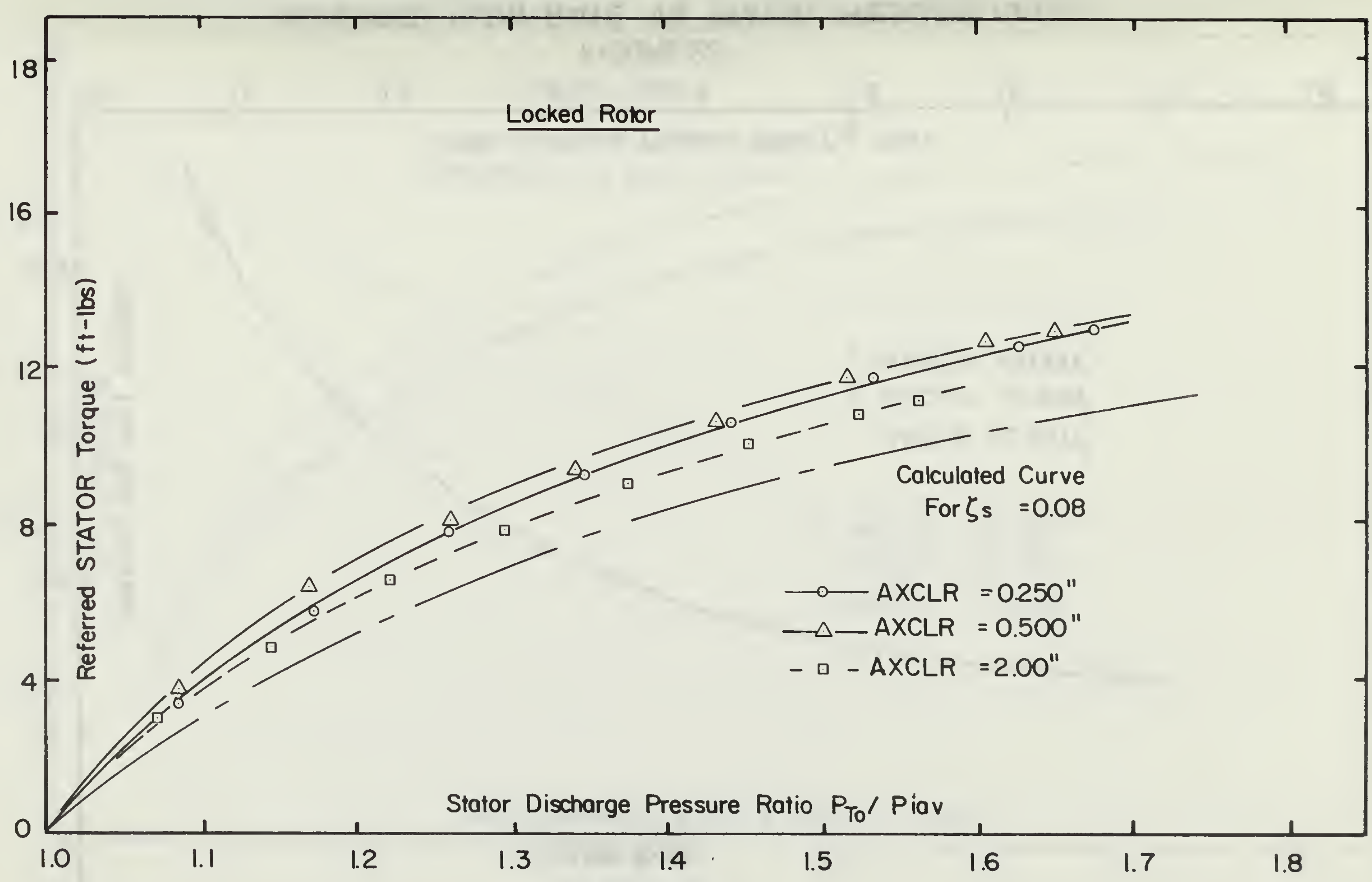

FIGURE 22

REFERRED STATOR TORQUE VS. STATOR PRESSURE RATIO

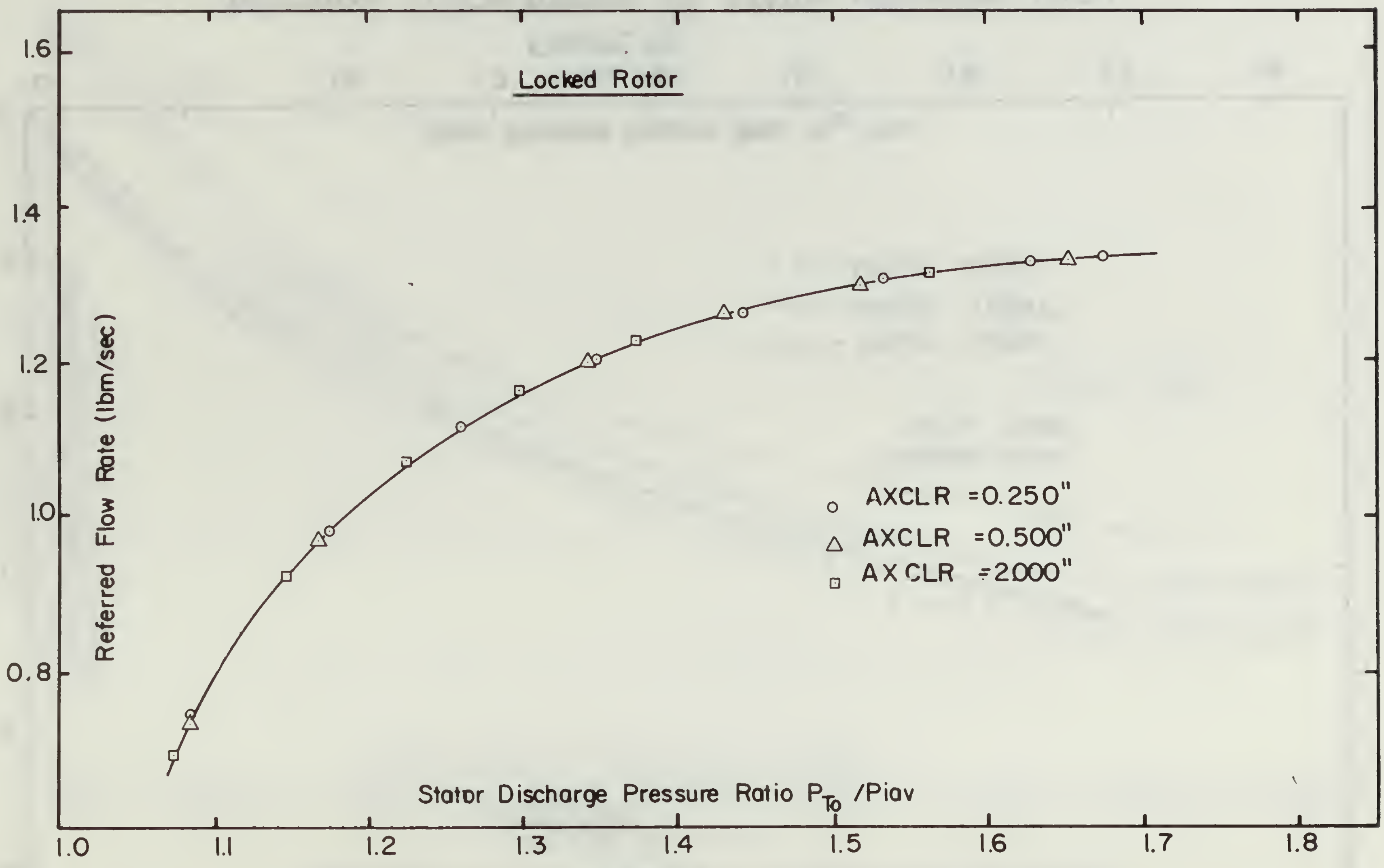

FIGURE 23
REFERRED FLOW RATE VS. STATOR PRESSURE RATIO

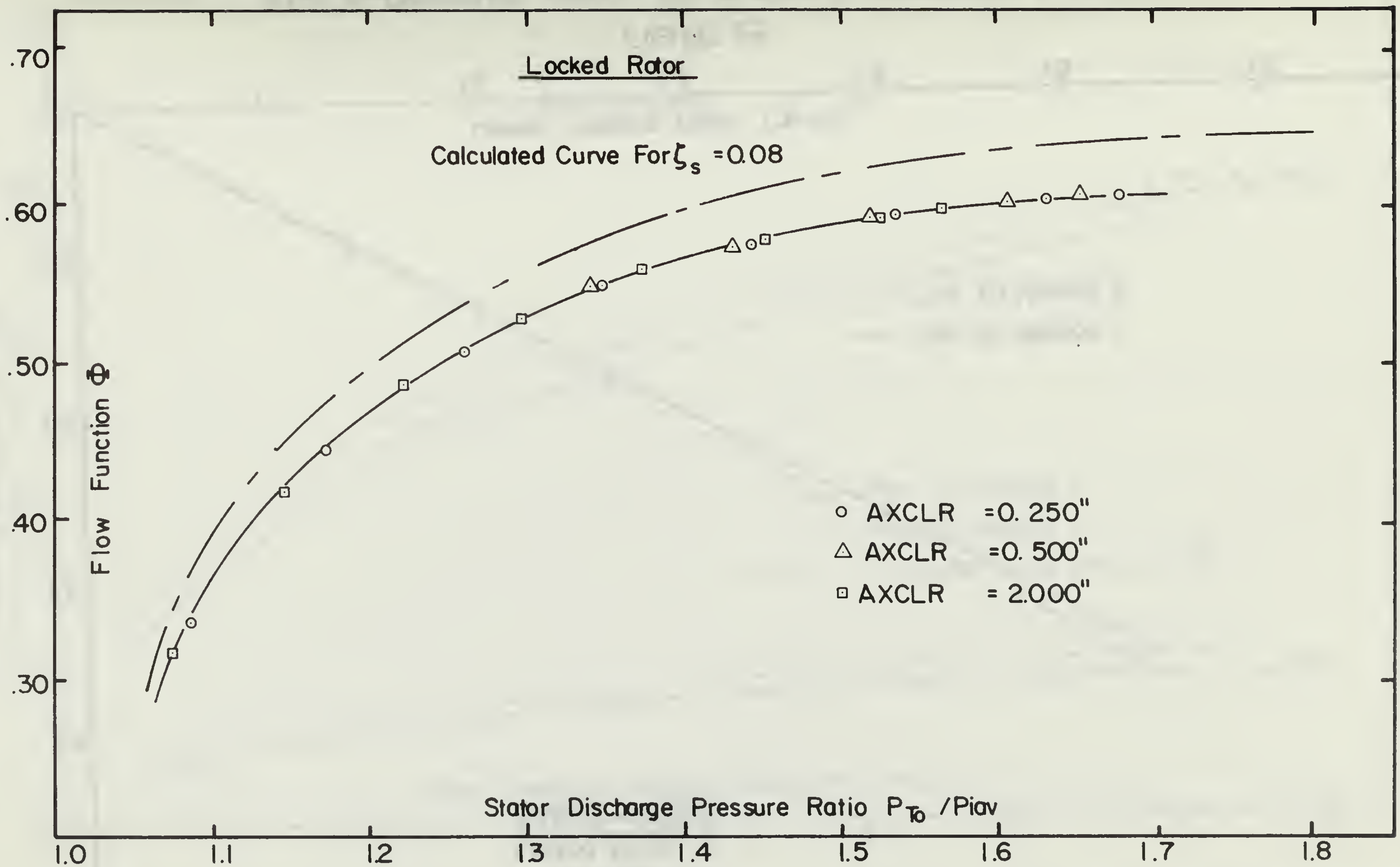

FIGURE 24

FLOW FUNCTION VS. STATOR PRESSURE RATIO

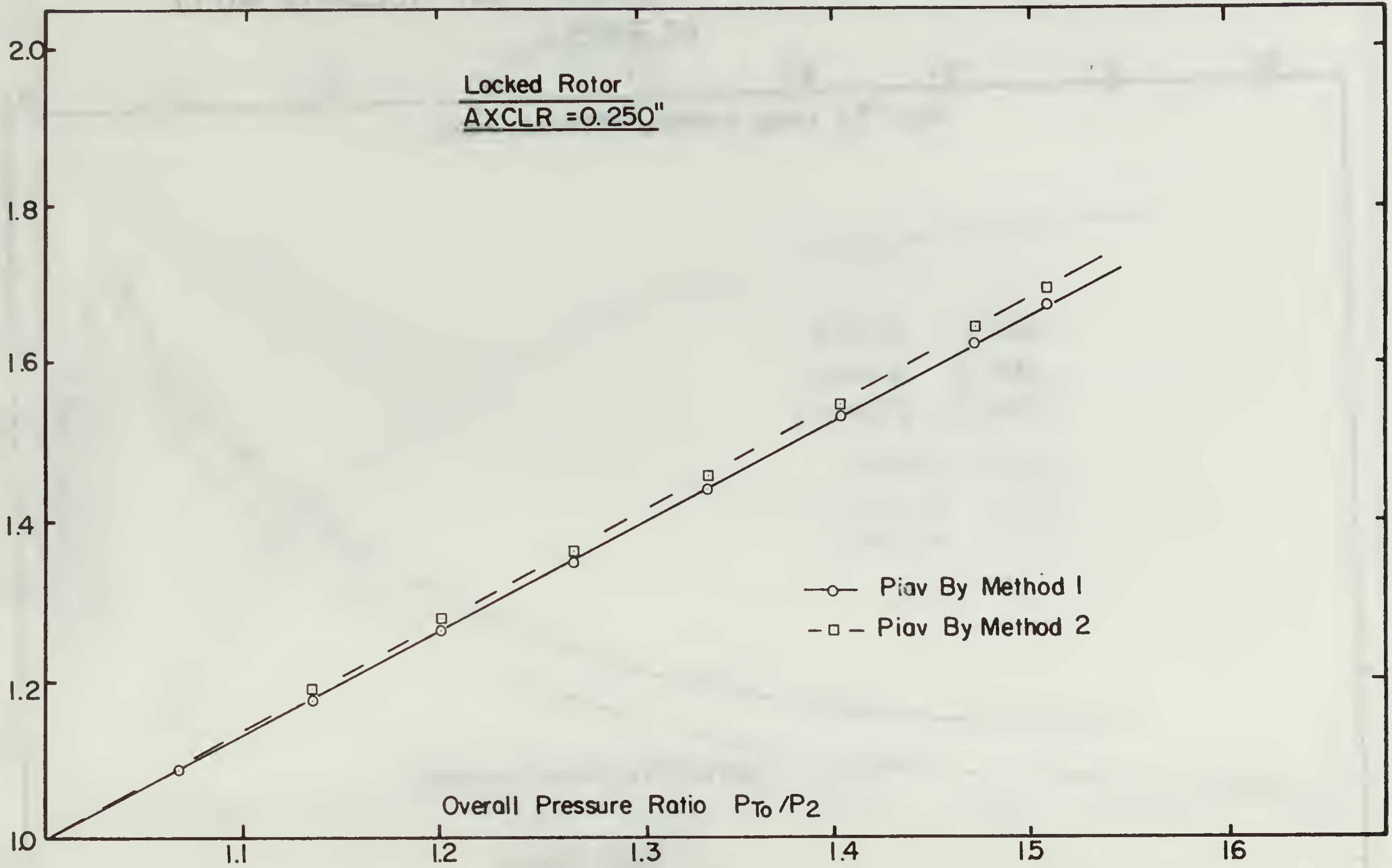

FIGURE 25

STATOR PRESSURE RATIO VS. OVERALL PRESSURE RATIO

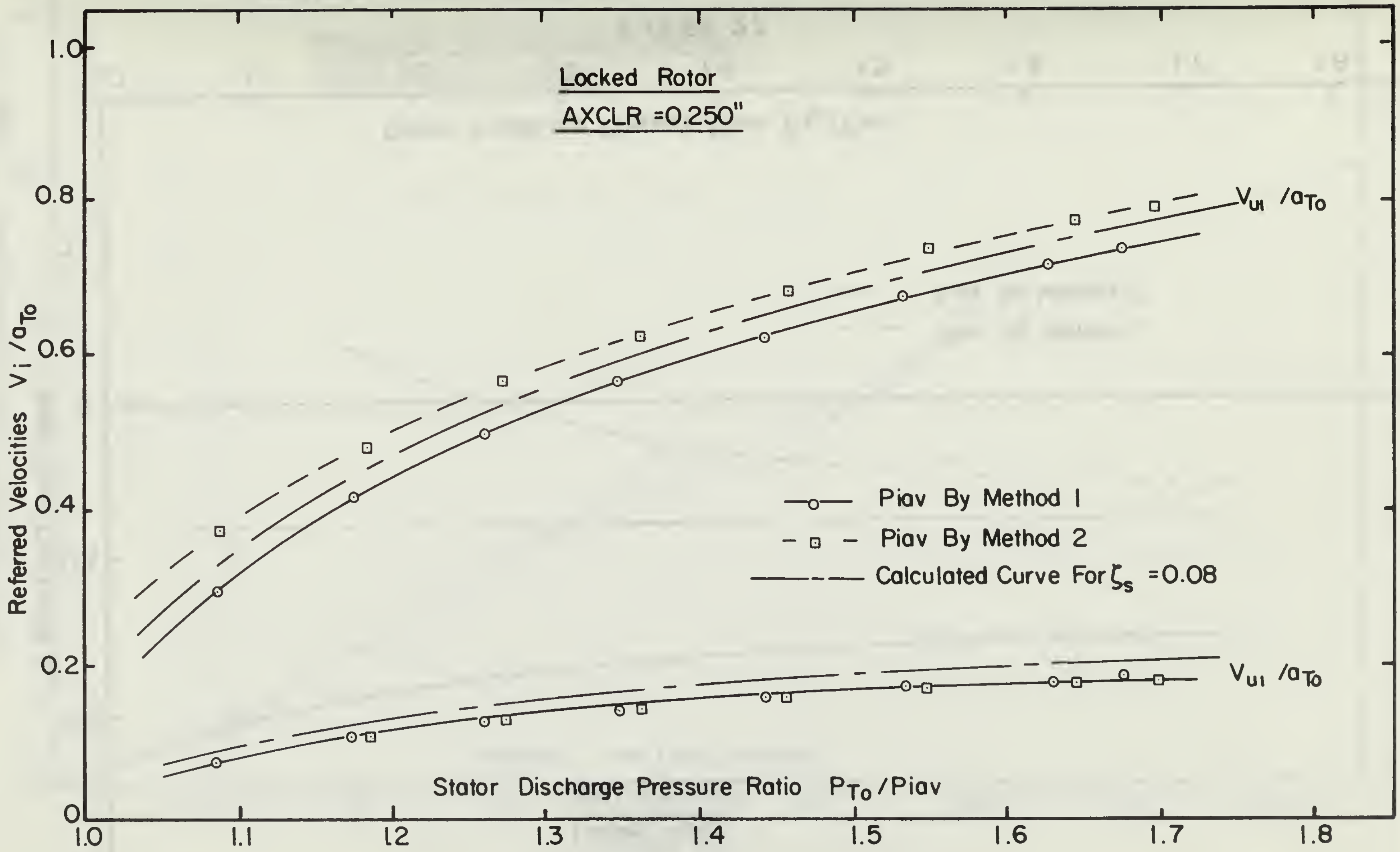

FIGURE 26

REFERRED VELOCITIES VS. STATOR PRESSURE RATIO

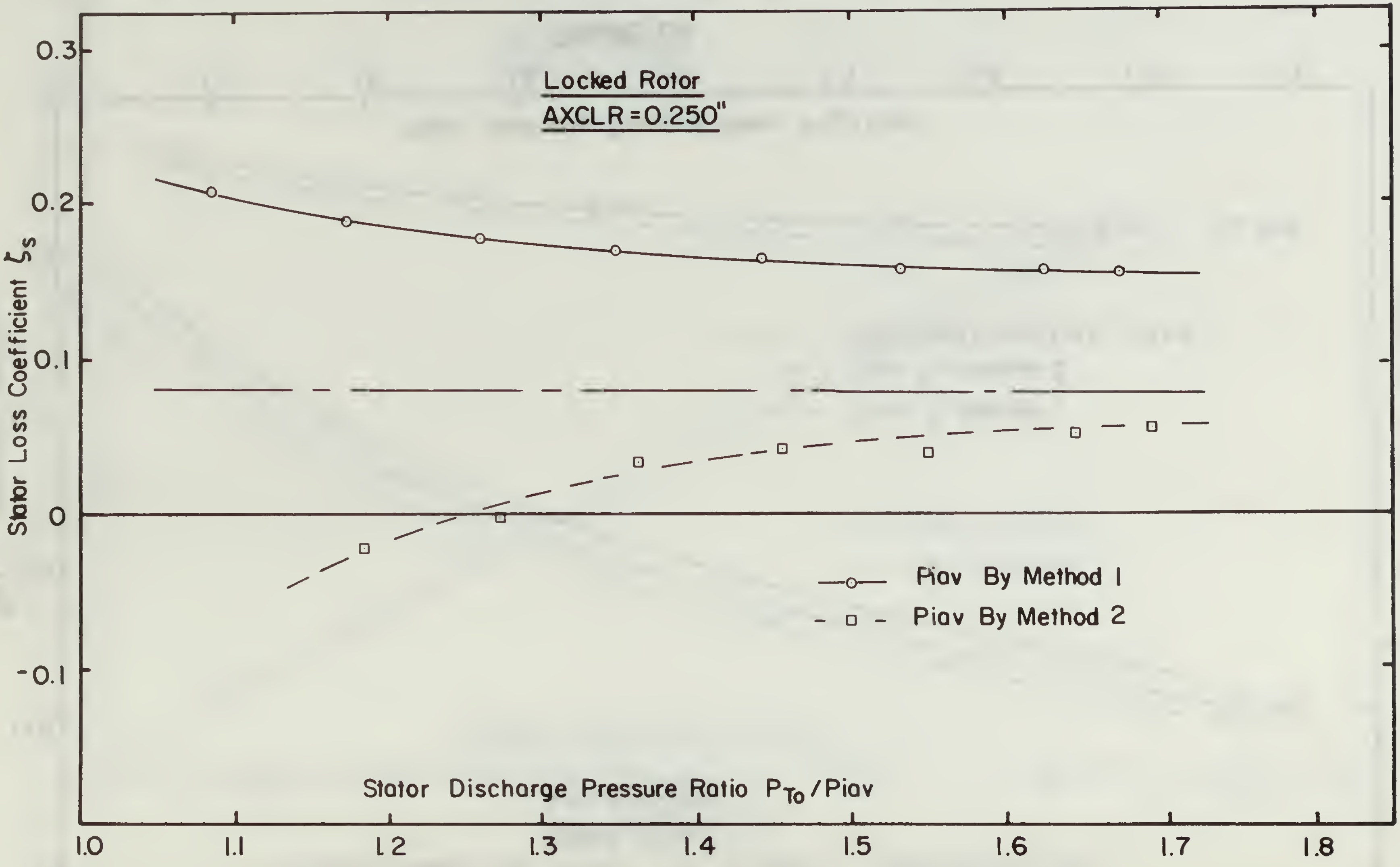

FIGURE 27

STATOR LOSS COEFFICIENT VS. STATOR PRESSURE RATIO

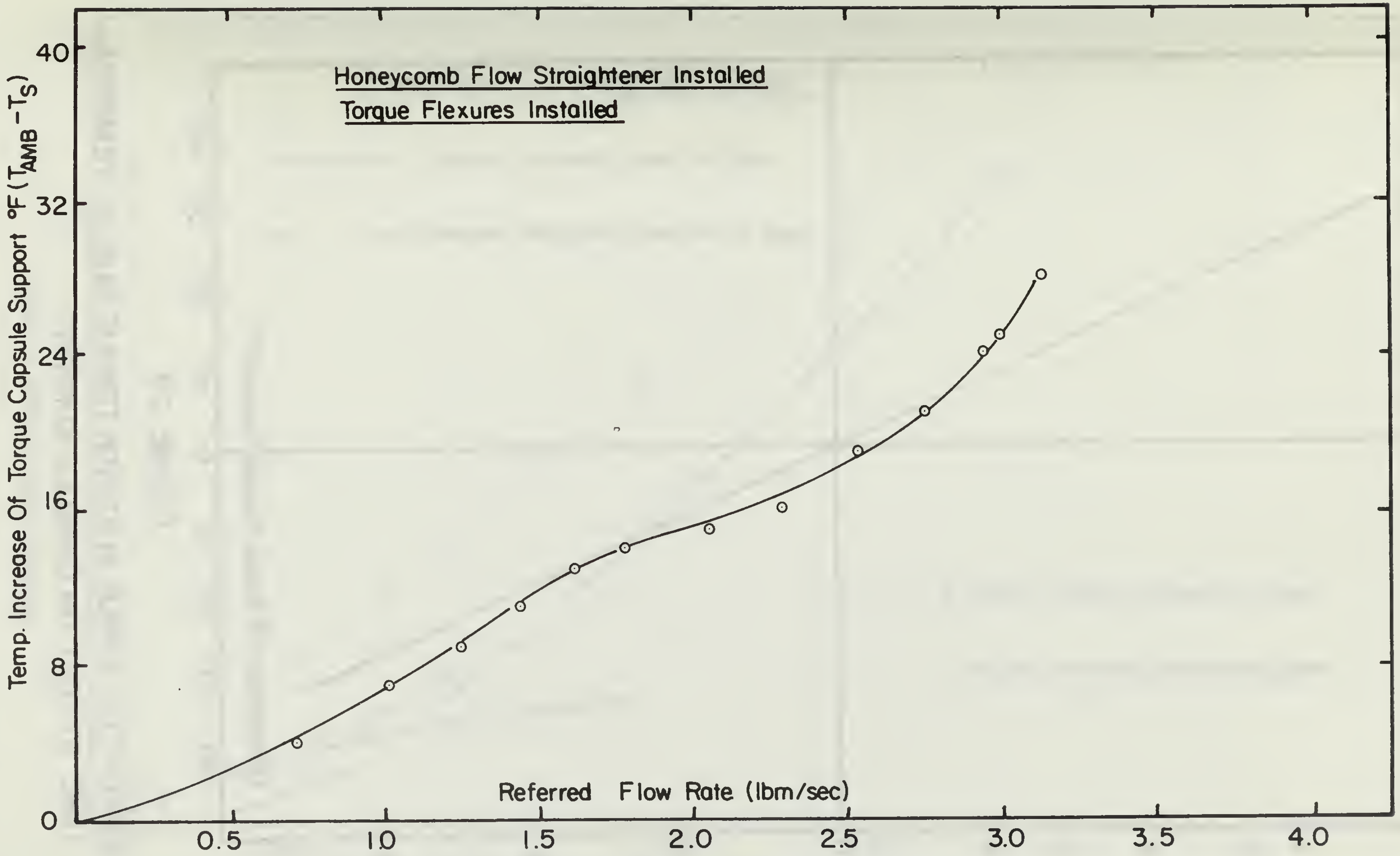

FIGURE 28

TEMPERATURE INCREASE OF CAPSULE SUPPORT VS. REFERRED FLOW RATE

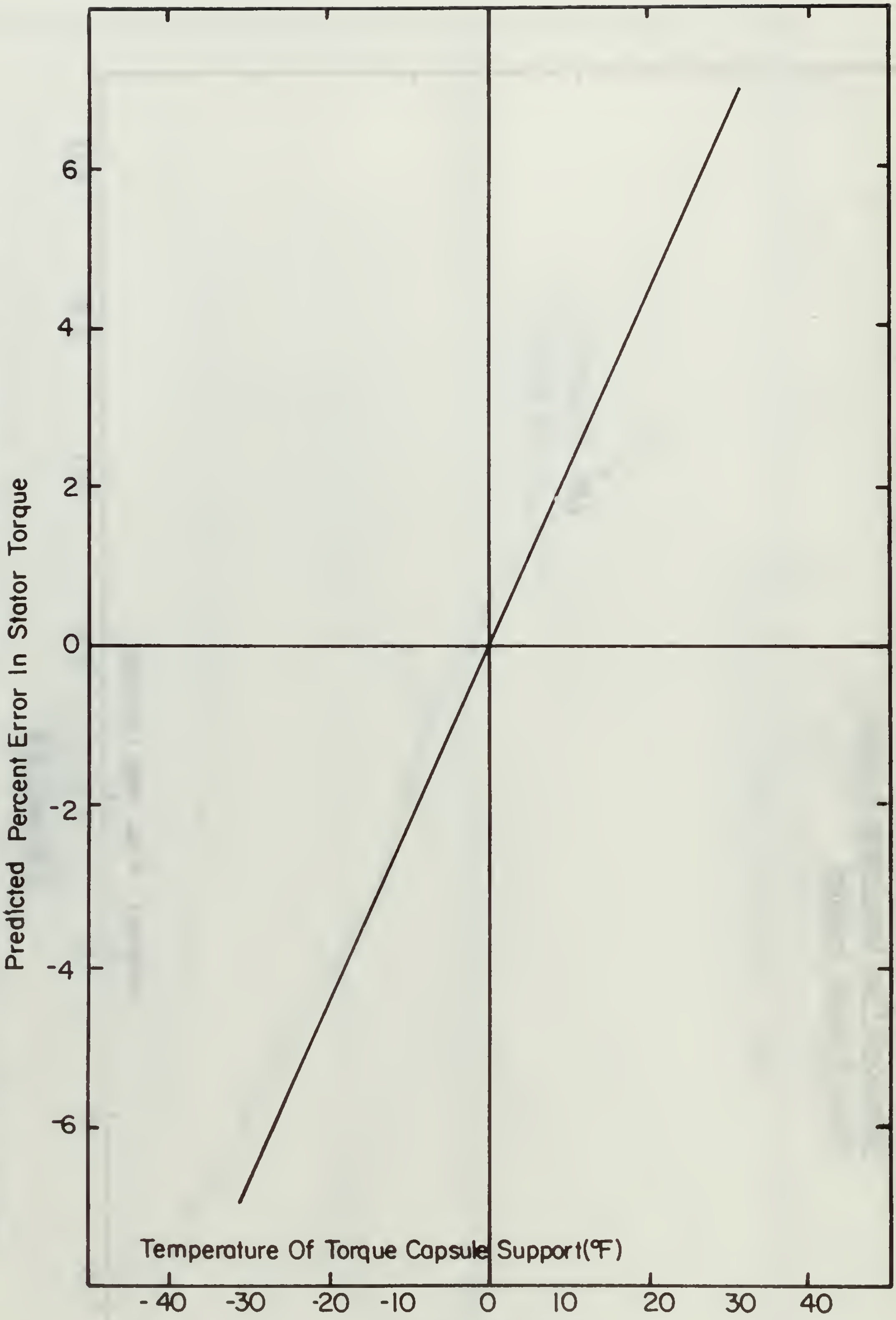

FIGURE 29

PREDICTED ERROR IN STATOR TORQUE DUE TO TEMPERATURE EFFECT ON CAPSULE SUPPORT.

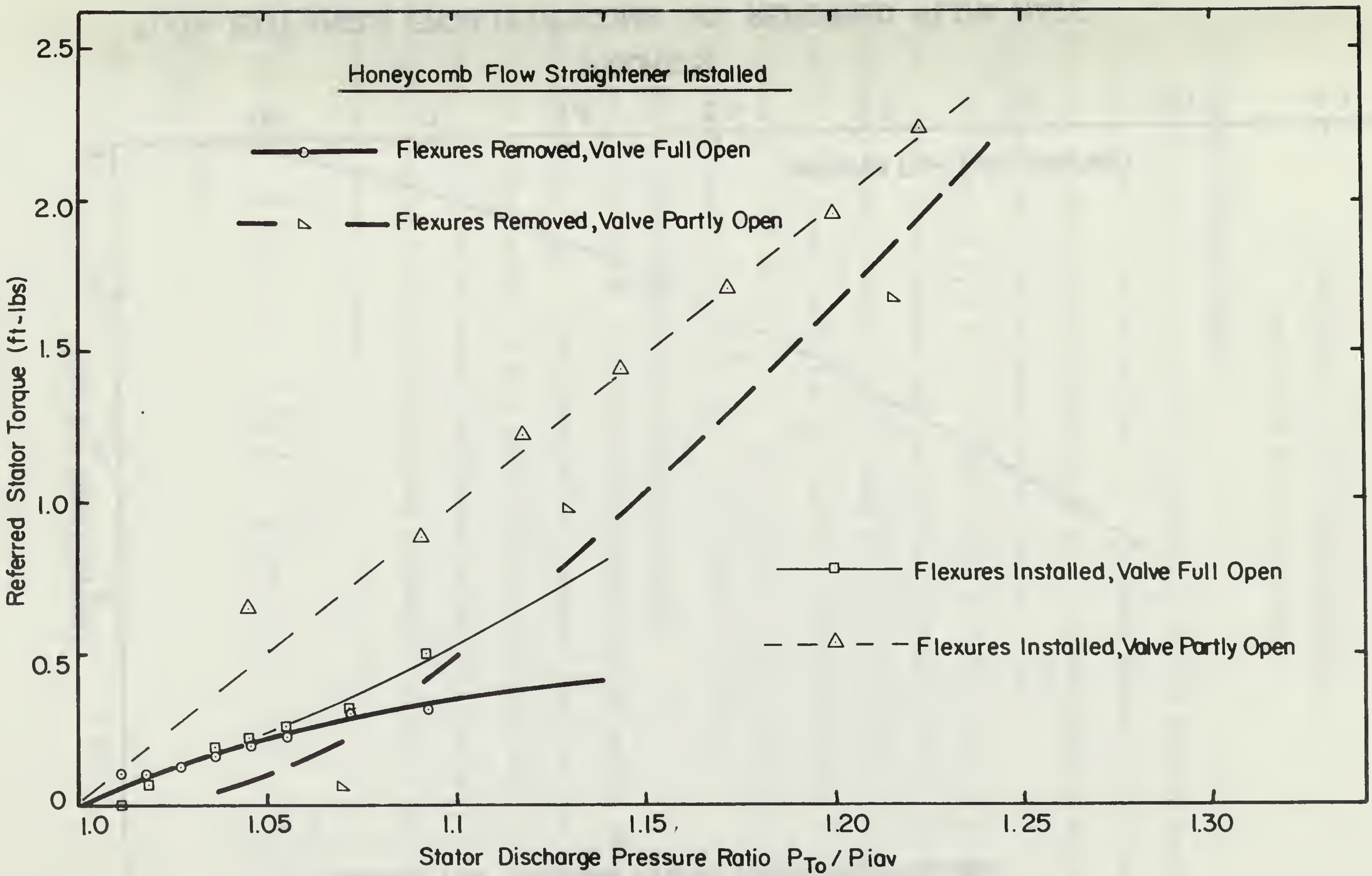

FIGURE 30

REFERRED STATOR TORQUE VS. STATOR PRESSURE RATIO

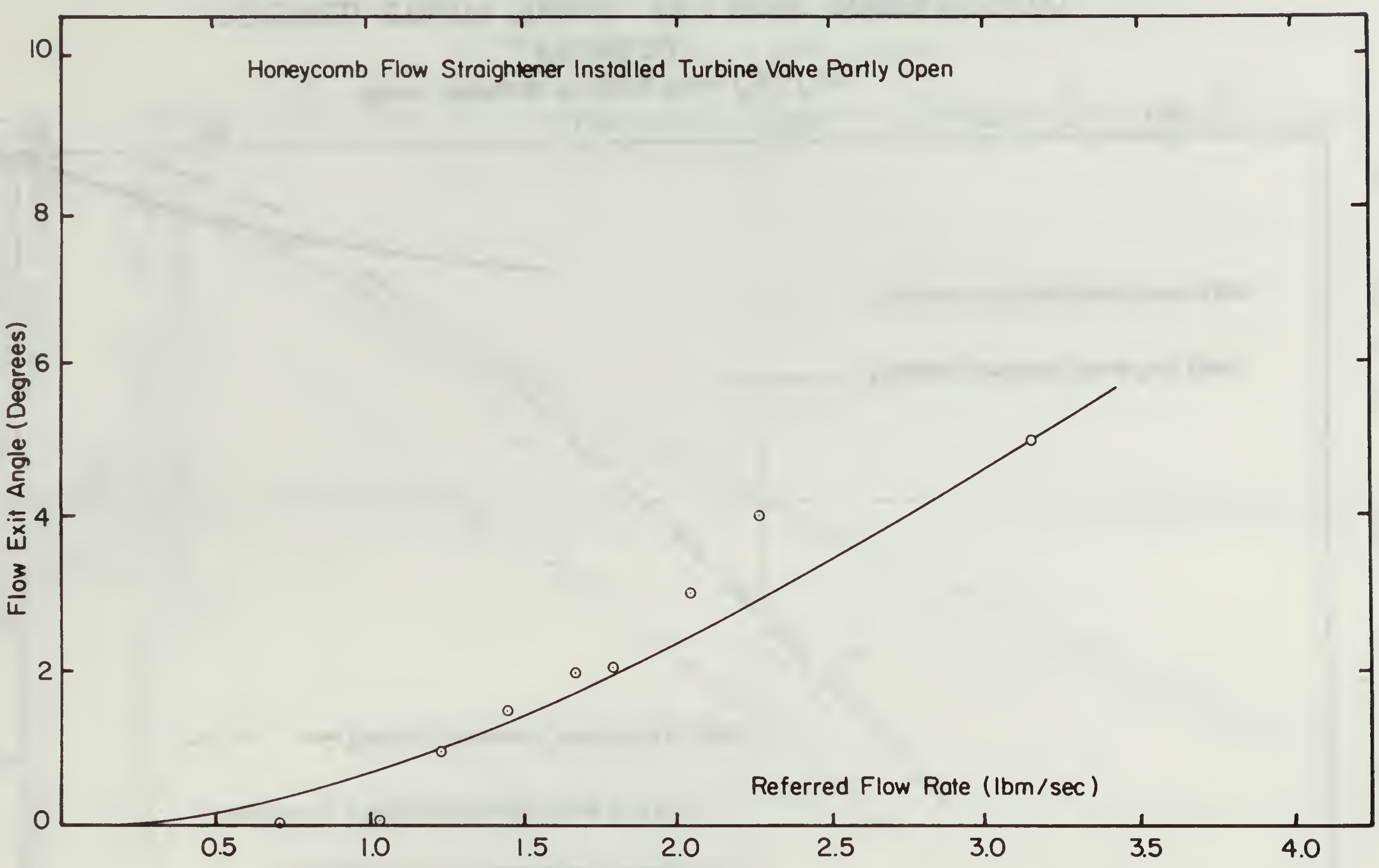

FIGURE 31

FLOW EXIT ANGLE FROM HONEYCOMB VS. REFERRED FLOW RATE

APPENDIX A

PREDICTION OF STATOR DISCHARGE ANGLE AND STATOR LOSS COEFFICIENT

1. Stator Discharge Angle

The prediction of the stator discharge angle uses methods described by Vavra [Ref. 8] and Ainley [Ref. 2]. In these methods, it is assumed that the discharge angle is influenced only by blade geometry and Mach number, and that flow incidence angles have no effect.

For values of $M_1 \leq 0.5$, a formula given by Vavra [Ref. 8] is used for a first approximation, and the effects of blade geometry and Mach number are then accounted for by using the method described by Ainley [Ref. 2]. A linear variation of α is then assumed for values of M_1 between $M_1 = 0.5$ and $M_1 = 1.0$. The results of these calculations for the blade geometry shown in Fig. 7 are listed in Table III.

2. Stator Loss Coefficient By Method of Ainley

The prediction of stator loss coefficient uses the method described by Ainley [Ref. 2]. In this method it is assumed that the loss coefficient is independent of Mach number and is influenced only by blade geometry and flow incidence. The losses are divided into profile losses Y_ρ which include mixing losses, secondary losses Y_s, and tip clearance losses Y_k, where

$$Y_{\rho(i = 0)} = \left\{ Y_{\rho(\alpha 1 = 0)} + \left(\frac{\alpha_1}{\alpha_2}\right)^2 \left[Y_{\rho(\alpha 1 = \alpha 2)} - Y_{\rho(\alpha 1 = 0)} \right] \right\} \times \left(\frac{t/C}{0.2}\right)^{\alpha_1/\alpha_2}$$

and

$$Y_s + Y_K = \left[\lambda + B\left(\frac{K}{h}\right)\right]\left(\frac{C_L}{s/C}\right)^2\left(\frac{\cos^2 \alpha_2}{\cos^3 \alpha_m}\right)$$

Values of $Y_\rho = f(s/C)$ are given in Fig. 4 of Ref. 2 and values for

$$\lambda = f\left[\frac{\left(A_2/A_1\right)^2}{\left(1 + \text{I.D./O.D.}\right)}\right]$$

are given in Fig. 8. A relation given by Vavra [Ref. 9] is then used to relate the stator loss coefficient to the pressure loss coefficient. The results of these calculations are listed in Table IV.

3. Loss Coefficient By Method of Traupel

The method of Traupel[5] is one of the most complete methods used and takes into account a large number of variables considered to have an influence on the loss coefficient.

$$\zeta = \zeta_\rho + \zeta_w + \zeta_r + \zeta_{zus}$$

where ζ = Total loss coefficient

ζ_ρ = Profile loss coefficient

ζ_w = Wall loss coefficient

ζ_r = Secondary loss coefficient

ζ_{zus} = Damping wire loss coefficient

The profile loss coefficient is given by:

$$\zeta_\rho = \zeta_{\rho 0} \cdot \chi_{\rho 0} \cdot \chi_M \cdot \chi_s + \zeta_m + \zeta_F$$

where $\zeta_{\rho 0}$ = Basic loss coefficient

$\chi_{\rho 0}$ = Reynolds number correction

---

[5] Traupel, W., "Thermische Turbomaschinen, Erster Band," Springer Verlag, Berlin/Goettingen, Heidelber, 1958, pg. 269-298.

χ_M = Mach number correction

χ_s = Trailing edge thickness correction

ζ_m = Mixing loss correction

ζ_F = Correction for straight blades

The wall loss coefficient, which is due to the friction loss at the annulus of the hub and tip, is given by:

$$\zeta_w = \zeta_{\rho 0} \cdot \chi_{\rho 0} \frac{s. \sin \alpha_1}{h}$$

The secondary loss coefficient is given by:

$$\zeta_r = \psi_\ell \zeta_{r0} + \zeta_s$$

where ψ_ℓ = Aspect ratio correction

ζ_{r0} = Basic secondary loss

ζ_s = Tip leakage loss

A summary of the calculations is listed in Table V.

4. Loss Coefficient Method By Soderberg

The method of Soderberg is taken from a paper by Horlock.[6] Soderberg bases the loss on blade geometry, aspect ratio, thickness ratio, and Reynolds Number, and then relates the loss coefficient to the gas deflection angle through the aspect ratio only. He ignores such parameters as Mach number and certain non-dimensional gas properties.

The results of a calculation for the converging TTTR nozzles is listed in Table VI.

---

[6] Horlock, J. H., "Losses and Efficiencies in Axial Flow Turbines," Ins. J. Mech. Sci., Vol. 2, 1960, pg. 59-60.

TABLE III

Prediction of Stator Discharge Angle

$s = 0.8594$ in

$a = 0.2050$ in

$t = 0.0240$ in

$a/s = 0.2385$ in

$t/s = 0.0279$ in

For $M_1 \leq 0.5$:

$$\alpha^* = \cos^{-1}\left(\frac{a/s}{K_t}\right) \qquad \text{[Ref. 8]}$$

$$\text{where } K_t = 1 - \frac{27}{10^3}\left(\frac{t}{s}\,100\right)^{3.3}\frac{a}{s}$$

$$= 0.9809$$

Hence $\alpha^* = \cos^{-1}(0.24318) = 75.92^{\circ}$

$$\alpha = \alpha^* + 4\left(\frac{s}{e}\right)$$

$$\text{where } e = \frac{\dot{J}^2}{8Z} \qquad \text{[Ref. 2]}$$

$$= 4.5338$$

$4(s/e) = 0.76^{\circ}$

Hence $\alpha = 76.68^{\circ}$

For $M_1 = 1.0$

$$\alpha\,(M_1 = 1.0) = \cos^{-1}\left(\frac{a}{s - t/\cos\alpha^*}\right) = \cos^{-1}(0.27152) = 74.25^{\circ}$$

For M_1 (average) = 0.65 $\qquad \alpha_1$ (average) = 75.90^{0}

TABLE IV

Loss Coefficient by Method of Ainley

$\alpha_1 = 0^o$

$\alpha_2 = -75.90^o$

$t = 0$

$c = 1.4313$

$s = 0.8594$

$s/c = 0.6004$

$Y_{\rho(\alpha 1 = 0)} = 0.0490$ Fig. 4

$$Y_s + Y_K = \left[\lambda + B\left(\frac{K}{h}\right)\right]\left(\frac{C_L}{s/C}\right)^2 \left(\frac{\cos^2 \alpha_2}{\cos^3 \alpha_m}\right)$$

$$\text{where } \tan \alpha_m = \frac{\tan \alpha_1 + \tan \alpha_2}{2} = -1.9906$$

$\alpha_m = -63.33^o$

$B = 0.5$ For non-shrouded wheels

$$\frac{C_L}{s/C} = 2\ (\tan \alpha_1 - \tan \alpha_2) \cos \alpha_m = 3.5720$$

$$\lambda = f\left[\frac{\left(A_2/A_1\right)^2}{\left(1 + I.D./O.D.\right)}\right]$$

$$\frac{A_2}{A_1} = \frac{A_{02} \cos \alpha_2}{A_{01} \cos \alpha_1} = \frac{\pi D_{m2}\ h_2 \cos \alpha_2}{\pi D_{m1}\ h_1 \cos \alpha_1}$$

$h_1 = h_2$, $D_{m1} = D_{m2}$

$$\text{Hence } \lambda = f\left[\frac{\cos^2 \alpha_2/\cos^2 \alpha_1}{\left(1 + R_{hub1}/R_{tip1}\right)}\right] = f\ (0.0321) = 0.0056$$

Fig. 8

$K = 0$

$$Y_s + Y_K = 0.0056\ (3.5720)^2 \quad \frac{\cos^2\ (-75.90)}{\cos^3\ (-63.33)} = 0.0471$$

Hency $Y = Y_\rho + Y_s + Y_k = 0.0961$

$t/s = 0.0279$

Trailing edge correction factor $F = 1.02$

Hence $Y = 1.02\ (0.0961) = 0.0980$

$$\zeta_s = \frac{\left[\dfrac{1 + Y}{1 + Y\left(P_1/P_{TO}\right)}\right]^{\frac{\gamma - 1}{\gamma}} - 1}{\left(\dfrac{1}{P_1/P_{TO}}\right)^{\frac{\gamma - 1}{\gamma}} - 1}$$

[Ref. 9]
page 99

With M_1 (average) = 0.65, $\left(\dfrac{P_1}{P_{TO}}\right)_{\text{average}} = 0.7055$ (Run 15)

$\zeta_s = 0.0756$

TABLE V

Loss Coefficient By Method of Traupel

$\zeta_{\rho 0} = f(\alpha_0, \alpha_1) = 0.0040$ Fig. B3

$\psi_{\rho 0} = f_1(\mathrm{Re}, \frac{KS}{C})$

$$\mathrm{Re} = \frac{V_1 C}{\nu} = \frac{750 \times 1.4313/12}{1.564 \times 10^{-4}} = 5.72 \times 10^5$$

$K = 0$

Hence $\chi_{\rho 0} = 0.92$ Fig. B5

$\psi_M = f(M_1) = 0.075$ for $M_1 = 0.65$ Fig. B4

$\psi_s = f(1-K)$

$$1 - K = 1 - \left(s - \frac{t}{\cos \alpha_1}\right) = 1 - \left(0.8594 - \frac{0.0240}{\cos 75.9^\circ}\right) = 0.2392$$

Hence $\psi_s = 1.60$ Fig. B6

$\zeta_M = f(1 - K) = 0.0700$ Fig. B6

$\zeta_F = f(h/D_m)$

$$h/D_m = \frac{0.690}{8.48} = 0.0814$$

Hence $\zeta_F = 0.0250$ Fig. B7

Thus $\zeta_\rho = 0.0040 \times 0.92 \times 0.075 \times 1.60 + 0.0700 + 0.0250$

or $\zeta_\rho = 0.0954$

$$\zeta_w = 0.0040 \times 0.92 \times \frac{0.8594 \times \sin 75.9}{0.690} = 0.0044$$

$\psi_\ell/\psi_{\rho 0} = f(c/h)$

$$c/h = \frac{1.4313}{0.690} = 2.078$$

Hence $\psi_{\ell}/\psi_{\rho 0} = 1.70$ Fig. B9

and $\psi_{\ell} = 1.70\ (0.92) = 1.563$

$$\zeta_{r0} = f\left(\frac{V_{u1}}{U_1}\right)$$

$\frac{V_{u1}}{U_1} = \frac{725}{555} = 1.306$ From point 8 Run 15

Hence $\zeta_{r0} = 0.0350$ Fig. B8

$\zeta_s = f(h_s/h) = 0$ Not applicable to stator

Hence $\zeta_r = 1.563 \times 0.0350 = 0.0547$

$\zeta_{zus} = 0$ Not applicable to stator

Hence $\zeta_s = 0.0954 + 0.0044 + 0.0547 = 0.1545$

TABLE VI

Loss Coefficient By Method of Soderberg

$$\xi^1 = (1 + \xi^*) \left[0.975 + 0.075 \frac{b}{h} \right] - 1$$

$\alpha_0 = 0$

$\alpha_1 = 75.90^o$

$b = 0.975$ Blade axial chord

$h = 0.690$ Blade height

$t/c = 0.248$ Thickness/chord

$\xi^* = f(\Delta\alpha) = 0.0700$ Fig. 5

Hence $\xi' = 0.1580$

$$\text{And } \zeta_s = \frac{\left[\dfrac{1 + \xi}{1 + \xi \left(P_1/P_{TO} \right)} \right]^{\frac{\gamma - 1}{\gamma}} - 1}{\left(\dfrac{1}{P_1/P_{TO}} \right)^{\frac{\gamma - 1}{\gamma}} - 1}$$

With M_1 (average) $= 0.65$, $\left(\dfrac{P_1}{P_{TO}} \right)_{\text{average}} = 0.7055$ (Run 15)

$\zeta_s = 0.1022$

APPENDIX B

PREDICTION OF TORQUE ON CLOSURE PLATE AND SHROUD

1. Torque on Closure Plate

Because of the proximity of the rotor and its high speed rotation, a core of rotating fluid will be set up between the rotor and closure plate, and friction will thus transmit some torque to the closure plate.

Schlichting [7] gives a formula for the torque transmitted to a stationary flat plate by a rotating parallel plate, assuming the core of fluid rotates at one-half the speed of the wheel.

For turbulent flow:

$$M = 0.037\ \rho\omega^2 R^5 \left(\frac{\nu}{\omega R^2}\right)^{1/5}$$

Using values of ρ and ν for air at $520^\circ R$ and one atmosphere, with $R = 3.87$ in

$$M = 0.037 \times 0.002378 \left(\frac{\pi N}{60}\right)^2 \left(\frac{3.87}{12}\right)^5 \left[\frac{173 \times 10^{-6} \times 60 \times 144}{\pi N \times 3.87^2}\right]^{1/5}$$

This results in a moment of 0.007 ft-lbs at 10,000 RPM and 0.023 ft-lbs at 20,000 RPM.

2. Torque on Shroud

A torque will be transmitted to the rotor shroud by the tangential component of V_1 and by the scrubbing of rotor at the tip. A formula given by Schlichting[8] for the torque transmitted between two rotating cylinders is:

---

[7] Schlichting, H., "Boundary Layer Theory," pg. 607

$$u(r) = \frac{1}{r_2^2 - r_1^2} \left[r\left(\omega_2 r_2^2 - \omega_1 r_1^2\right) - \frac{r_1^2 r_2^2}{r} \left(\omega_2 - \omega_1\right) \right]$$

$$\frac{du}{dr} = \frac{1}{r_2^2 - r_1^2} \left[\left(\omega_2 r_2^2 - \omega_1 r_1^2\right) + \frac{r_1^2 r_2^2}{r^2} \left(\omega_2 - \omega_1\right) \right]$$

$$T = \mu \frac{du}{dr}$$

With $\omega_2 = 0$ and $r = r_2$,

$$M = T A_2 r_2 = \mu \left(\frac{du}{dr}\right) \left(2\pi r_2 h\right) r_2$$

$$\text{or } M = 4\pi\mu h \frac{r_1^2 r_2^2 \omega_1}{r_2^2 - r_1^2}$$

As before, with the core assumed to ratate at one-half the rotor speed, and the values for air at standard conditions, the moment transmitted is 0.018 ft-lbs at 10,000 RPM and 0.037 ft-lbs at 20,000 RPM.

---

[8] Schlichting, H., "Boundary Layer Theory," pg. 81

APPENDIX C

PREDICTION OF STATOR DISCHARGE PRESSURE DISTRIBUTION

The equation of motion for absolute flow through a stator, as given by Vavra [Ref. 9] is:

$$\frac{\partial \overline{V}}{\partial t} + \nabla H = \overline{V} \times (\nabla \times \overline{V}) + T\,\nabla s + \overline{f}_f \tag{C.1}$$

If steady, frictionless flow is assumed, the equation reduces to:

$$\nabla H = \overline{V} \times (\nabla \times \overline{V}) + T\,\nabla s \tag{C.2}$$

Each variable in the above equation may then be expressed in an axisymmetric coordinate system, where

$$\nabla H = \overline{i}_m \frac{\partial H}{\partial m} + \frac{\overline{i}_\theta}{R} \frac{\partial H}{\partial \theta} + \overline{i}_n \frac{\partial H}{\partial n}$$

$$T\,\nabla s = T \left(\overline{i}_m \frac{\partial s}{\partial m} + \frac{\overline{i}_\theta}{R} \frac{\partial s}{\partial \theta} + \overline{i}_n \frac{\partial s}{\partial n} \right),$$

$$\begin{aligned} \text{and } \overline{V} \times (\nabla \times \overline{V}) = {} & \overline{i}_m \left\{ \frac{V_\theta}{R} \left[\frac{\partial (RV_\theta)}{\partial m} - \frac{\partial V_m}{\partial \theta} \right] - V_n \left[\frac{\partial V_m}{\partial n} + V_m K_m \right] \right. \\ & \left. + V_n \left[\frac{\partial V_n}{\partial m} + V_n K_n \right] \right\} + \frac{\overline{i}_\theta}{R} \left\{ V_m \left[\frac{\partial V_m}{\partial \theta} - \frac{\partial (RV_\theta)}{\partial m} \right] \right. \\ & \left. + V_n \left[\frac{\partial V_n}{\partial \theta} - \frac{\partial (RV_\theta)}{\partial n} \right] \right\} + \overline{i}_n \left\{ \frac{V_\theta}{R} \left[\frac{\partial (RV_\theta)}{\partial n} - \frac{\partial V_n}{\partial \theta} \right] \right. \\ & \left. + V_m \left[\frac{\partial V_m}{\partial n} + V_m K_m \right] - V_m \left[\frac{\partial V_n}{\partial m} + V_n K_n \right] \right\} \end{aligned}$$

Equating components:

$$\overline{i}_m : \quad \frac{\partial H}{\partial m} = \left\{ \frac{V_\theta}{R} \left[\frac{\partial (RV_\theta)}{\partial m} - \frac{\partial V_m}{\partial \theta} \right] - V_n \left[\frac{\partial V_m}{\partial n} + V_m K_m \right] + \right.$$

$$V_n \left[\frac{\partial V_n}{\partial m} + V_n K_n \right] \qquad + \frac{\partial s}{\partial m} \tag{C.3}$$

$$\bar{i}_\theta : \frac{1}{R} \frac{\partial H}{\partial \theta} = \frac{V_m}{R} \left[\frac{\partial V_m}{\partial \theta} - \frac{\partial (RV_\theta)}{\partial m} \right] + \frac{V_n}{R} \left[\frac{\partial V_n}{\partial \theta} - \frac{\partial (RV\ )}{\partial n} \right]$$

$$+ \frac{1}{R} \frac{\partial s}{\partial \theta} \tag{C.4}$$

$$\bar{i}_n : \frac{\partial H}{\partial n} = \left\{ \frac{V_\theta}{R} \left[\frac{\partial (RV_\theta)}{\partial n} - \frac{\partial V_n}{\partial \theta} \right] + V_m \left[\frac{\partial V_m}{\partial n} + V_m K_m \right] \right.$$

$$\left. - V_m \left[\frac{\partial V_n}{\partial m} + V_n K_n \right] \right\} + \frac{\partial s}{\partial n} \tag{C.5}$$

where m = streamline coordinate

n = coordinate normal to streamline

K_m = curvature of streamline

K_n = curvature of normal

If axisymmetric flow is assumed, all terms with $\partial/\partial\theta$ vanish and since the equation is written along a streamline where $V_n = 0$

$$\frac{1}{R} \frac{\partial H}{\partial \theta} = 0 = \frac{V_m}{R} \frac{\partial (RV_\theta)}{\partial m} \tag{C.6}$$

Since V_m is not zero, $\dfrac{\partial (RV_\theta)}{\partial m} = 0$ (C.7)

Then $\dfrac{\partial H}{\partial m} = \dfrac{\partial s}{\partial m}$ and if adiabatic flow is assumed then $\dfrac{\partial H}{\partial m} = 0$ means H is constant along a streamline. In addition, $\dfrac{\partial s}{\partial m} = 0$ means the flow is isentropic along a streamline. A consequence of these last two statements results in isentropic flow or $\bar{V} \times (\nabla \times \bar{V}) = 0$. The remaining equation is then:

$$\frac{\partial H}{\partial n} = \frac{V_\theta}{R} \frac{\partial (RV_\theta)}{\partial n} + V_m \frac{\partial V_m}{\partial n} + V_m{}^2 K_m + \frac{\partial s}{\partial n} \tag{C.8}$$

or

$$\frac{\partial}{\partial n}\left(\frac{V_m{}^2}{2}\right) + V_m{}^2 K_m + \frac{V_\theta}{R} \frac{\partial (RV_\theta)}{n} - \frac{\partial H}{\partial n} + T \frac{\partial s}{\partial n} = 0$$

Employing the relation $H = C_\rho T + \left(\frac{V_\theta{}^2 + V_m{}^2}{2}\right)$ the following important equation results:

$$\frac{\partial}{\partial n}\left(V_m{}^2\right) + V_m{}^2\left(2K_m - \frac{1}{C_\rho} \frac{\partial s}{\partial n}\right) + 2 \frac{V_\theta}{R} \frac{\partial (RV_\theta)}{\partial n} - 2 C_\rho \frac{\partial T_T}{\partial n}$$

$$+ \left(2T_T - \frac{V_\theta{}^2}{C_\rho}\right) \frac{\partial s}{\partial n} = 0 \tag{C.9}$$

Equation (C.9) is known as the Radial Equilibrium Equation and is a linear differential equation with variable coefficients.

If three additional important assumptions are made, namely that there is no temperature or entropy gradient at the stator entrance, and that $\frac{\partial (RV_\theta)}{\partial n} = 0$ or free vortex flow exists ahead of the stator, and finally that the streamlines are cylindrical surfaces with $K_m = 0$, then $\frac{\partial}{\partial n}\left(V_m{}^2\right) = 0$, which means V_m is not a function of radius. If $\frac{\partial}{\partial n}(RV_\theta) = 0$ can be maintained in the stator, the same conclusion can be made for V_m at the stator discharge.

The consequence of the above series of assumptions results in a set of velocity profiles as shown in Fig. 32. Also imposed on the profiles shown in Fig. 32 are the effects of annulus friction and secondary flow.

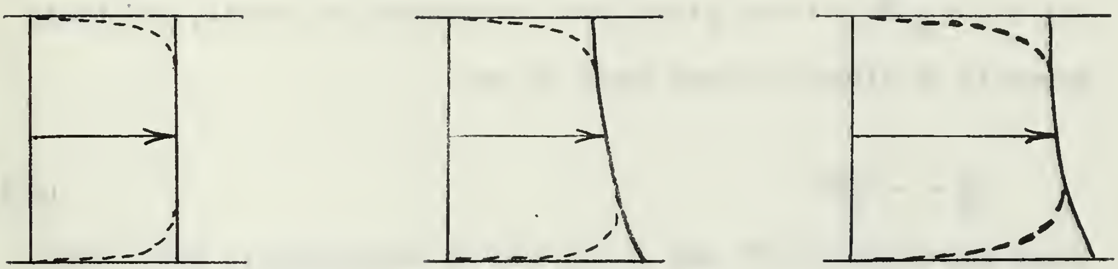

(a) Axial Component V_m (b) Tangential Component V_θ (c) Resultant Velocity V

Figure 32

Predicted Velocity Profiles at Stator Discharge

The unequal pressure between the convex and concave sides of a blade cause trailing vorticies to be formed and are the origin of the secondary flow. The vorticies cause a reduction in the tangential component near the hub and tip radii. It is evident from the above velocity profile in Fig. 32C that the pressure distribution must necessarily be a complicated one and not linear.

When the assumption that $\frac{\partial(RV_\theta)}{\partial n} = 0$ is put in cylindrical coordinates, so that:

$$\frac{\partial(RV_u)}{\partial R} = \frac{\partial(RV_a \tan\alpha)}{\partial R} = 0$$

or

$$V_a R \frac{\partial(\tan\alpha)}{\partial R} + V_a \tan\alpha = 0$$

hence

$$\frac{\partial(\tan\alpha)}{\partial R} = \frac{\partial\alpha}{\partial R} = -\frac{\tan\alpha}{R} \qquad \text{(C.10)}$$

But for $\frac{\partial(RV_u)}{\partial R} = 0$ the blades must themselves be radial, and their geometry is given by Vavra [Ref. 9] as

$$\frac{\partial \alpha}{\partial R} = + \frac{\tan\alpha}{R} \tag{C.11}$$

Since equations (C.10) and (C.11) are in opposition to each other, the blades cannot everywhere be radial, and thus the blades will exert a force on the flow in a radial direction, which will produce curved stream surfaces. As a result, the assumption of axisymmetric stream surfaces is in error, and in addition $\frac{\partial(RV_u)}{\partial R} = 0$ cannot be maintained in the stator, so free vortex flow is not possible. Thus $\frac{\partial V_a^2}{\partial R} = -2\frac{V_u}{R}\frac{\partial(RV_u)}{\partial R}$ and this can be solved if it is assumed there is constant total enthalpy and flow angle ahead of the stator. The solution is given by Vavra [Ref. 8] which is:

$$V_a = V_{am}\left(\frac{R_m}{R}\right)^{\sin^2\alpha_1}$$

where V_{am} = axial velocity at the mean raduis. Thus $V_a = f(R)$ and the resulting velocity or pressure distribution becomes extremely complicated.

APPENDIX D

```
 STATOR RESULTS

CONFIGURATION-   CONVERGING NOZZLES, SHROUD P/N 1050, INSERT P/N 2005-3(STRAIGHT)

RUN NUMBER 15     DATE  1 AUG 69
                                                 METHOD J= 1


                              FORCE AND MOMENT BALANCE(LBS AND FT-LBS)
POINT  FAX(+) CLFAX(+)  FC(+)   F1(-)    F2(-)    F3(-)    F4(-)    F5(-)  F6A(-)     FNET  TORQ(+) CLTORQ(+)  KFAX      RTORQ

  1    -15.60     9.35 1201.90  272.24   56.54    46.18    56.55    86.75  666.72     10.67   14.73     0.03    -10.46      9.88
  2     -7.52    10.07 1201.90  274.22   56.54    46.19    56.55    87.37  671.85     11.74   14.60     0.03     -5.04      9.78
  3      0.80    10.78 1201.90  276.13   56.54    46.19    56.47    87.91  677.91     12.27   14.17     0.04      0.54      9.51
  4     12.08    11.73 1201.90  279.43   56.54    46.19    56.43    88.91  686.30     11.91   14.03     0.04      8.11      9.42
  5     17.36    12.28 1201.90  280.96   56.54    46.19    56.40    89.23  690.49     11.68   13.97     0.04     11.61      9.34
  6     25.44    12.80 1201.90  283.02   56.54    46.19    56.24    89.83  696.55     11.77   13.57     0.04     17.07      9.10
  7     30.00    13.15 1201.90  284.23   56.54    46.19    56.19    90.14  700.28     11.44   13.40     0.04     20.12      8.98
  8     56.40    14.56 1201.90  291.34   56.54    45.80    55.71    92.02  720.78     10.63   12.90     0.04     37.90      8.67
  9     84.40    17.02 1201.90  299.11   56.54    45.75    55.79    94.15  742.22      9.75   11.90     0.04     56.67      7.99


                              FLOW RATES(LBM/SEC), RE(NOZ), FLOW FNC, AND STATOR BLOCKAGE FACTOR
POINT  NOZZLE FLOW  TURBINE FLOW   LABLEAK        RE          PHI        XI

  1      1.8657        1.8322      0.0335      521710.     0.5795    0.8905
  2      1.8532        1.8193      0.0339      516144.     0.5768    0.8893
  3      1.8382        1.8048      0.0334      510943.     0.5746    0.8903
  4      1.8241        1.7904      0.0338      506216.     0.5709    0.8905
  5      1.8275        1.7934      0.0340      507129.     0.5699    0.8898
  6      1.8116        1.7778      0.0339      502897.     0.5663    0.8897
  7      1.8043        1.7711      0.0338      501011.     0.5641    0.8884
  8      1.7685        1.7344      0.0341      490720.     0.5537    0.8889
  9      1.7332        1.6990      0.0343      480832.     0.5420    0.8886


                              PRESSURES(PSIA) AND PRESSURE RATIOS
PAMB=14.57
PCINT  PNOZ   PTPL   PTC    P1AV    PHC   PLENUM PR(PTPL/PHD)  STATOR PR(PTO/P1AV)

  1    36.03  22.12  21.91  14.81  14.57        1.5186                1.4793
  2    36.00  22.13  21.93  14.92  14.57        1.5196                1.4700
  3    35.97  22.07  21.87  15.03  14.57        1.5152                1.4559
  4    36.02  22.08  21.87  15.20  14.57        1.5156                1.4390
  5    36.15  22.17  21.96  15.28  14.57        1.5219                1.4366
  6    36.10  22.08  21.90  15.40  14.57        1.5162                1.4223
  7    36.03  22.09  21.91  15.47  14.57        1.5166                1.4167
  8    36.03  22.07  21.86  15.85  14.57        1.5149                1.3791
  9    36.09  22.07  21.88  16.27  14.57        1.5149                1.3446


                              TEMPRATURES(DEG R)
POINT   TTPL    TTO     T1     T1IS

  1    557.93  556.93  508.15  497.89
  2    561.70  560.64  512.52  502.21
  3    563.52  562.39  515.21  505.16
  4    565.23  564.30  518.39  508.57
  5    565.60  564.65  518.97  509.12
  6    565.26  564.44  520.03  510.39
  7    565.53  564.71  520.88  511.22
  8    565.60  564.95  524.31  515.25
  9    565.77  564.95  527.57  519.12
```

```
                              ABSOLUTE  VELOCITIES(FT/SEC), ANGLES(DEG), VEL COEF, AND MACH NOS
POINT   VA1       VU1       V1        V1S      ALPHA 1  VCOEFS    MV1     MVA1     RVA1     RVU1

  1    185.74    741.86    764.76    841.56    75.91   0.9088  0.6921  0.1684  0.1608  0.6413
  2    184.91    737.55    760.38    837.89    75.91   0.9079  0.6852  0.1666  0.1593  0.6355
  3    183.04    730.26    752.86    824.18    75.92   0.9134  0.6766  0.1646  0.1575  0.6282
  4    180.63    720.44    742.74    814.28    75.92   0.9177  0.6655  0.1614  0.1551  0.6197
  5    180.16    718.57    740.81    810.75    75.93   0.9175  0.6634  0.1613  0.1547  0.6169
  6    177.64    708.53    730.46    805.81    75.93   0.9055  0.6535  0.1591  0.1525  0.6084
  7    176.49    703.49    725.68    801.66    75.92   0.9052  0.6486  0.1577  0.1515  0.6043
  8    169.72    676.54    697.89    771.63    75.93   0.9044  0.6218  0.1512  0.1457  0.5811
  9    162.97    650.31    670.13    742.04    75.92   0.9031  0.5952  0.1447  0.1399  0.5574


                              RELATIVE VELOCITIES(FT/SEC), ANGLES(DEG), AND MACH NOS
POINT   WA1       WU1       W1        U1       BETA 1    MW1

  1    185.74    371.73    415.71    370.01    63.42   0.3762
  2    184.91    349.24    394.99    388.51    62.09   0.3559
  3    183.04    323.25    371.50    407.01    60.47   0.3339
  4    180.63    283.46    336.12    436.98    57.49   0.3012
  5    180.16    265.31    320.69    453.26    55.82   0.2872
  6    177.64    234.13    293.93    474.35    52.82   0.2623
  7    176.48    214.74    277.95    489.15    50.59   0.2484
  8    169.72    121.13    208.55    555.76    35.53   0.1954
  9    162.97     18.40    164.00    631.61     6.44   0.1457


                              EFFICIENCIES
POINT  ZETA STATOR  ETA STAT(=(1.-ZETAS)

  1       0.1741          0.8259
  2       0.1764          0.8236
  3       0.1756          0.8244
  4       0.1761          0.8239
  5       0.1773          0.8227
  6       0.1783          0.8217
  7       0.1806          0.8194
  8       0.1820          0.8180
  9       0.1844          0.8156
```

```
 ROTOR RESULTS

CONFIGURATION-  CIRCULAR ARC, SHARP LE ROTOR, P/N 1034-A, AXIAL CLNC  0.250 IN, RADIAL CLNC 0.009 IN

RUN NUMBER 15    DATE  1 AUG 69
                                          METHOD J= 1


                            PRESSURES(PSIA) AND PRESSURE RATIOS
PAMB=14.57

POINT   PTO    P1AV   PT2   P2=PHO   OVERALL PR(PTO/P2)

  1    21.91  14.81  14.76  14.57       1.5041
  2    21.93  14.92  14.76  14.57       1.5055
  3    21.87  15.03  14.75  14.57       1.5018
  4    21.87  15.20  14.76  14.57       1.5018
  5    21.96  15.28  14.78  14.57       1.5075
  6    21.90  15.40  14.82  14.57       1.5035
  7    21.91  15.47  14.84  14.57       1.5041
  8    21.86  15.85  15.04  14.57       1.5008
  9    21.88  16.27  15.35  14.57       1.5021


                            TEMPERATURES(DEG R)

POINT    TTO      T1      TE      TT2      T2     T2IS    T2TH    TT2IS   DELTA TIS  DELTA TW

  1    556.83  508.15  522.83  509.38  507.44  505.74  495.53  497.43    61.30     47.45
  2    560.64  512.52  525.83  512.08  510.20  509.03  498.79  500.64    61.85     48.56
  3    562.39  515.21  527.06  513.96  512.08  510.66  500.70  502.53    61.69     48.43
  4    564.30  518.39  528.20  515.10  513.10  512.10  502.40  504.35    61.90     49.21
  5    564.65  518.97  527.97  515.10  512.95  511.87  502.16  504.27    62.48     49.55
  6    564.44  520.03  527.70  515.77  513.27  511.85  502.37  504.81    62.08     48.67
  7    564.71  520.88  527.83  516.29  513.52  512.04  502.54  505.25    62.17     48.43
  8    564.85  524.31  528.60  520.00  515.27  511.79  502.99  507.61    61.86     44.85
  9    564.95  527.57  530.67  525.51  517.69  511.14  502.95  510.54    62.00     39.45
```

```
                              ABSOLUTE VELOCITIES(FT/SEC) AND ANGLES(DEG)

POINT   VA2      VU2       V2       V1S    ALPHA 2    MV2     STAGE LOADING FACTOR   STAGE FLOW FACTOR

  1    150.30   -24.19   152.20   863.19   -10.60   .1385           2.05                   .40
  2    150.05   -13.37   150.62   862.31    -4.93   .1369           1.91                   .38
  3    149.41    15.43   150.20   860.91     5.85   0.1354          1.73                   .36
  4    148.52    43.44   154.74   862.37    16.3    0.1394          1.54                   .34
  5    148.73    61.12   160.79   866.41    22.34   0.1444          1.43                   .32
  6    147.51    91.33   173.36   863.55    31.67   0.1561          1.23                  0.31
  7    147.04   107.81   182.32   864.25    36.25   0.1641          1.20                  0.30
  8    144.48   183.73   238.48   862.12    52.71   0.2143          0.97                  0.26
  9    142.20   271.35   306.75   863.05    62.34   0.2747          0.59                  0.22


                              RELATIVE VELOCITIES(FT/SEC), ANGLES(DEG), AND REL VEL COEFS

POINT   WA2      WU2       W2       U2       W2IS    BETA 2    DBETA   WCOEFS    MW2

  1    150.30  -402.56   430.08   374.77   453.12   -69.54   132.97   0.9491   0.3835
  2    150.05  -406.53   433.38   393.50   449.21   -69.74   131.83   0.9648   0.3914
  3    149.41  -395.94   424.13   412.24   443.84   -69.37   129.85   0.9556   0.3924
  4    148.52  -393.16   425.89   442.60   439.33   -69.59   127.08   0.9681   0.3836
  5    148.73  -397.37   424.86   454.39   439.74   -69.51   125.33   0.9662   0.3827
  6    147.51  -389.45   416.45   481.45   436.45   -69.25   122.77   0.9542   0.3750
  7    147.04  -387.63   414.58   495.44   435.53   -69.23   119.81   0.9519   0.3732
  8    144.48  -373.16   400.16   562.90   449.34   -68.84   104.36   0.8905   0.3596
  9    142.20  -368.37   394.87   639.73   484.44   -68.89    75.34   0.8151   0.3540


                              EFFICIENCIES, RPM, WORK OUTPUT(HP), AND ENTHALPY DROP(BTU/LBM)

POINT  ZETA ROTOR  ETA RLTER(1.-ZETAR)  RPM       HP    DELTA HIS  DELTA HW  REHEAT FACTOR  EFF DEGREE OF REACTION

  1     0.0991          0.9009         10000.   29.51    14.71      11.38       1.0206              0.0145
  2     0.0692          0.9308         10500.   29.40    14.84      11.65       1.0205              0.0460
  3     0.0868          0.9132         11000.   29.67    14.80      11.62       1.0199              0.0622
  4     0.0624          0.9376         11810.   29.91    14.85      11.81       1.0193              0.1032
  5     0.0665          0.9335         12250.   30.17    14.99      11.89       1.0193              0.1165
  6     0.0896          0.9104         12820.   29.37    14.83      11.69       1.0189              0.1321
  7     0.0939          0.9061         13220.   29.11    14.92      11.62       1.0189              0.1438
  8     0.2069          0.7931         15020.   26.41    14.84      10.76       1.0175              0.1824
  9     0.3356          0.6644         17070.   22.75    14.89       9.46       1.0163              0.2091
```

```
GENERAL RESULTS

RUN NUMBER 15     DATE  1 AUG 69

POINT  PRESSURE  REFERRED  ISENTROPIC  EFFICIENCY  EFFICIENCY  REFERRED   REFERRED  REFERRED  DEGREE OF  DEGREE OF  DEGREE OF
         RATIO     SPEED   HEAD COEFF  TOT-STATIC   TOT-TOT    FLOW RATE   MOMENT     POWER    REACTION   REACTION   REACTION
                    RPM                 PERCENT     PERCENT    LBM/SEC     FT-LB       HP       (HUB)      (MEAN)     (TIP)

  1     1.5041     9651.     5.3795      77.40       79.89      1.2728     10.393    19.098    -0.0928     0.0385     0.1648
  2     1.5055    10100.     4.9229      78.51       80.93      1.2671     10.049    19.323    -0.0751     0.0552     0.1805
  3     1.5018    10564.     4.4740      78.50       80.92      1.2620      9.514    19.136    -0.0549     0.0724     0.1949
  4     1.5018    11323.     3.8946      79.50       82.09      1.2541      8.932    19.255    -0.0266     0.0996     0.2212
  5     1.5075    11741.     3.6538      79.30       82.07      1.2519      8.653    19.343    -0.0124     0.1114     0.2305
  6     1.5035    12289.     3.3145      78.41       81.63      1.2440      8.072    18.888     0.0077     0.1293     0.2466
  7     1.5041    12670.     3.1216      77.89       81.45      1.2391      7.755    18.709     0.0201     0.1396     0.2549
  8     1.5008    14393.     2.4064      72.50       78.39      1.2163      6.205    17.004     0.0877     0.1989     0.3065
  9     1.5021    16356.     1.8673      63.62       72.62      1.1905      4.700    14.636     0.1564     0.2608     0.3621
```

```
 STATOR RESULTS

CONFIGURATION-   CONVERGING NOZZLES, SHROUD P/N 1050, INSERT P/N 2605-3(STRAIGHT)

RUN NUMBER 15    DATE  1 AUG 69
                                        METHOD J= 2


                          FORCE AND MOMENT BALANCE(LBS AND FT-LBS)
POINT  FAX(+) CLFAX(+)  FC(+)    F1(-)    F2(-)    F3(-)    F4(-)    F5(-)   F6A(-)     FNET  TORQ(+) CLTORQ(+)  RFAX      RTORQ

  1    -15.60    9.35 1201.90   272.32   56.54    46.19    56.55    86.75   666.72     10.59   14.73     0.03    -10.46      9.98
  2     -7.52   10.07 1201.90   275.52   56.54    46.19    56.55    87.37   671.85     10.43   14.65     0.03     -5.04      9.78
  3      0.80   10.79 1201.90   276.22   56.54    46.19    56.47    87.91   677.91     10.24   14.17     0.04      0.54      9.51
  4     12.08   11.72 1201.90   281.33   56.54    46.19    56.43    88.91   686.30     10.01   14.03     0.04      8.11      9.42
  5     17.36   12.28 1201.90   282.62   56.54    46.19    56.40    89.29   690.49     10.02   13.97     0.04     11.61      9.34
  6     25.44   12.80 1201.90   285.00   56.54    46.19    56.24    89.83   696.55      9.79   13.57     0.04     17.07      9.10
  7     30.00   13.15 1201.90   286.02   56.54    46.19    56.19    90.14   700.28      9.70   13.40     0.04     20.12      8.98
  8     56.40   14.56 1201.90   292.90   56.54    45.80    55.71    92.02   720.78      9.11   12.90     0.04     37.90      8.67
  9     84.40   17.02 1201.90   300.25   56.54    45.76    55.79    94.15   742.22      8.61   11.90     0.04     56.67      7.99


                          FLOW RATES(LBM/SEC), RE(NOZ), FLOW FNC, AND STATOR BLOCKAGE FACTOR
POINT  NOZZLE FLOW  TURBINE FLOW   LABLEAK        RE         PHI       XI

  1      1.8657        1.8322      0.0335      521710.    0.5795    0.8906
  2      1.8532        1.8193      0.0339      516144.    0.5768    0.8915
  3      1.8382        1.8048      0.0334      510943.    0.5746    0.8939
  4      1.8241        1.7904      0.0338      506216.    0.5709    0.8942
  5      1.8275        1.7934      0.0340      507129.    0.5699    0.8930
  6      1.8116        1.7778      0.0339      502897.    0.5663    0.8937
  7      1.8048        1.7711      0.0338      501011.    0.5641    0.8920
  8      1.7685        1.7344      0.0341      490720.    0.5537    0.8925
  9      1.7332        1.6990      0.0343      480832.    0.5420    0.8917


                          PRESSURES(PSIA) AND PRESSURE RATIOS
PAMB=14.57
POINT  PNOZ   PTPL   PTC    P1AV    PHO    PLENUM PR(PTPL/PHO)  STATOR PR(PTO/P1AV)

  1   36.03  22.12  21.91  14.81  14.57        1.5186                 1.4789
  2   36.00  22.13  21.93  14.99  14.57        1.5196                 1.4630
  3   35.97  22.07  21.87  15.14  14.57        1.5152                 1.4453
  4   36.02  22.08  21.87  15.30  14.57        1.5156                 1.4293
  5   36.15  22.17  21.96  15.37  14.57        1.5219                 1.4282
  6   36.10  22.08  21.90  15.50  14.57        1.5162                 1.4124
  7   36.03  22.09  21.91  15.56  14.57        1.5166                 1.4080
  8   36.03  22.07  21.86  15.93  14.57        1.5149                 1.3719
  9   36.09  22.07  21.88  16.33  14.57        1.5149                 1.3395


                          TEMPERATURES(DEG R)
POINT   TTPL    TTC     T1     T1IS

  1   557.93  556.83  509.13  497.93
  2   561.70  560.64  513.15  502.89
  3   563.52  562.39  516.87  506.22
  4   565.23  564.30  518.98  509.56
  5   565.60  564.65  519.88  509.98
  6   565.26  564.44  521.42  511.41
  7   565.53  564.71  522.40  512.11
  8   565.60  564.85  524.07  516.06
  9   565.77  564.95  528.67  519.69
```

```
                                 ABSOLUTE VELOCITIES(FT/SEC), ANGLES(DEG), VEL COFF, AND MACH NOS
POINT   VA1       VU1       V1       V11S     ALPHA 1  VCOFFS    MV1      MVA1     RVA1     PVU1

  1    185.96    733.87   757.07    841.20    75.78   0.9000   0.6845   0.1681   0.1608   0.6344
  2    184.52    732.50   755.39    832.98    75.86   0.9069   0.6803   0.1662   0.1590   0.6311
  3    182.63    716.57   739.48    821.50    75.70   0.9002   0.6635   0.1639   0.1571   0.6164
  4    179.93    715.61   737.89    811.01    75.89   0.9098   0.6608   0.1611   0.1545   0.6146
  5    179.68    711.02   733.38    810.40    75.82   0.9050   0.6562   0.1608   0.1543   0.6104
  6    177.15    696.81   718.97    798.20    75.74   0.9007   0.6423   0.1583   0.1521   0.5983
  7    176.19    690.88   712.99    794.96    75.69   0.8969   0.6364   0.1573   0.1513   0.5931
  8    169.07    679.21   699.94    765.67    76.02   0.9142   0.6237   0.1507   0.1451   0.5830
  9    163.01    639.85   660.29    737.45    75.71   0.8954   0.5858   0.1446   0.1399   0.5492


                                 RELATIVE VELOCITIES(FT/SEC), ANGLES(DEG), AND MACH NOS
POINT   WA1       WU1       W1       U1       BETA 1   MW1

  1    185.96    363.86   408.63    370.01    62.93   0.3694
  2    184.52    343.99   390.36    388.51    61.79   0.3515
  3    182.63    309.56   359.41    407.01    59.46   0.3225
  4    179.93    278.63   331.68    436.98    57.15   0.2970
  5    179.68    257.76   314.21    453.26    55.12   0.2811
  6    177.15    222.45   284.37    474.35    51.47   0.2541
  7    176.19    201.72   267.84    489.15    48.86   0.2391
  8    169.07    123.46   209.35    555.76    36.14   0.1866
  9    163.01      8.24   163.21    631.61     2.89   0.1448


                                 EFFICIENCIES
POINT   ZETA STATOR   ETA STATOR(1.-ZETAS)

  1       0.1900            0.8100
  2       0.1776            0.8224
  3       0.1897            0.8103
  4       0.1722            0.8278
  5       0.1811            0.8189
  6       0.1887            0.8113
  7       0.1956            0.8044
  8       0.1643            0.8357
  9       0.1983            0.8017
```

```
 ROTOR RESULTS

CONFIGURATION-  CIRCULAR ARC, SHARP LE ROTOR, P/N 1034-A, AXIAL CLNC  0.250 IN, RADIAL CLNC 0.009 IN

RUN NUMBER 15     DATE  1 AUG 69
                                              METHOD J= 2


                                  PRESSURES(PSIA) AND PRESSURE RATIOS
PAMB=14.57
POINT    PTO     P1AV    PT2    P2=PHD   OVERALL PR(PTO/P2)

  1     21.91   14.81   14.77   14.57       1.5041
  2     21.93   14.99   14.76   14.57       1.5055
  3     21.87   15.14   14.75   14.57       1.5018
  4     21.87   15.30   14.76   14.57       1.5018
  5     21.96   15.37   14.77   14.57       1.5075
  6     21.90   15.50   14.80   14.57       1.5035
  7     21.91   15.56   14.82   14.57       1.5041
  8     21.86   15.93   15.05   14.57       1.5008
  9     21.88   16.33   15.30   14.57       1.5021


                                  TEMPERATURES(DEG R)
POINT     TTO       T1       TF       TT2       T2      T2IS     T2TH    TT2IS    DELTA TIS   DELTA TW

  1     556.83   509.13   523.32   509.38   507.39   506.67   495.53   497.47      61.30       47.45
  2     560.64   513.15   526.16   512.08   510.18   508.97   498.79   500.65      61.85       48.56
  3     562.39   516.87   527.98   513.96   512.10   511.24   500.70   502.52      61.69       48.43
  4     564.30   518.98   528.55   515.17   513.14   511.70   502.40   504.32      61.90       49.21
  5     564.65   519.88   528.54   515.10   513.02   511.91   502.16   504.20      62.48       49.55
  6     564.44   521.42   528.63   515.77   513.43   512.19   502.37   504.65      62.08       48.67
  7     564.71   522.40   528.89   516.29   513.74   512.64   502.54   505.04      62.17       48.43
  8     564.85   524.07   528.39   520.00   515.20   510.80   502.99   507.63      61.86       44.85
  9     564.95   528.67   531.74   525.51   518.14   511.64   502.95   510.10      62.00       39.45
```

```
                                      ABSOLUTE VELOCITIES(FT/SEC) AND ANGLES(DEG)
POINT   VA2       VU2        V2       V2IS    ALPHA 2   MV2     STAGE LOADING FACTOR  STAGE FLOW FACTOR

  1    150.29    -36.02    154.55    858.19   -13.48  0.1400          2.05                  0.40
  2    150.05    -18.05    151.14    862.01    -6.86  0.1365          1.91                  0.38
  3    149.42      1.79    149.43    860.91     0.68  0.1347          1.73                  0.36
  4    148.52     38.67    153.47    862.37    14.59  0.1382          1.53                  0.34
  5    148.75     53.67    158.13    866.41    19.84  0.1424          1.43                  0.32
  6    147.56     79.43    167.58    863.59    28.29  0.1509          1.29                  0.31
  7    147.10     94.96    175.09    864.25    32.85  0.1576          1.20                  0.30
  8    144.45    191.98    240.25    862.12    53.04  0.2159          0.87                  0.26
  9    142.32    261.32    297.56    863.09    61.43  0.2667          0.59                  0.22


                                     RELATIVE VELOCITIES(FT/SEC), ANGLES(OEG), AND REL VEL COEFS
POINT   WA2       WU2        W2        U2       W2IS     BETA 2    OBETA  WCOEFS   MW2

  1    150.29   -410.78    437.41    374.77    447.27    -69.90   132.83  0.9780  0.3961
  2    150.05   -411.56    438.06    393.50    454.42    -69.97   131.76  0.9640  0.3956
  3    149.42   -410.46    436.81    412.24    448.50    -70.00   129.46  0.9739  0.3938
  4    148.52   -403.93    430.37    442.60    449.99    -69.81   126.96  0.9564  0.3876
  5    148.75   -405.42    431.85    459.09    446.97    -69.85   124.97  0.9662  0.3890
  6    147.56   -401.02    427.31    480.45    444.39    -69.80   121.27  0.9616  0.3847
  7    147.10   -400.49    426.64    495.44    441.82    -69.83   118.70  0.9656  0.3840
  8    144.45   -370.92    398.06    562.90    459.63    -68.72   104.86  0.8660  0.3578
  9    142.32   -378.41    404.28    639.73    491.45    -69.39    72.28  0.8226  0.3623


                                     EFFICIENCIES, RPM, WORK OUTPUT(HP), AND ENTHALPY OROP(BTU/LBM)
POINT  ZETA ROTOR  ETA ROTOR(1.-ZETAR)  RPM       HP   OELTA HIS  DELTA HW  REHEAT FACTOR  EFF OEGREE OF REACTION

  1      0.0436         0.9564        10000.   29.51   14.71      11.38      1.0225             0.0350
  2      0.0707         0.9293        10500.   29.99   14.84      11.65      1.0204             0.0587
  3      0.0515         0.9485        11000.   29.67   14.80      11.62      1.0211             0.0949
  4      0.0853         0.9147        11810.   29.91   14.85      11.81      1.0185             0.1143
  5      0.0665         0.9335        12250.   30.17   14.99      11.89      1.0194             0.1329
  6      0.0754         0.9246        12820.   29.37   14.89      11.68      1.0196             0.1565
  7      0.0675         0.9325        13220.   29.11   14.92      11.62      1.0201             0.1700
  8      0.2500         0.7500        15020.   26.41   14.84      10.76      1.0155             0.1787
  9      0.3233         0.6767        17070.   22.75   14.88       9.46      1.0173             0.2249
```

```
GENERAL RESULTS

RUN NUMBER 15     DATE  1 AUG 69

POINT  PRESSURE  REFERRED  ISENTROPIC  EFFICIENCY  EFFICIENCY  REFERRED   REFERRED  REFERRED  DEGREE OF  DEGREE OF  DEGREE OF
         RATIO     SPEED   HEAD COEFF  TOT-STATIC   TOT-TOT    FLOW RATE   MOMENT    POWER    REACTION   REACTION   REACTION
                    RPM                  PERCENT    PERCENT    LBM/SEC     FT-LB      HP        (HUB)     (MEAN)      (TIP)

  1     1.5041     9651.     5.3795      77.40       79.94      1.2729     10.393    19.098    -0.0928    0.0392     0.1648
  2     1.5055    10190.     4.9229      78.51       80.95      1.2671     10.049    19.323    -0.0751    0.0662     0.1805
  3     1.5018    10554.     4.4740      79.50       80.89      1.2620      9.514    19.136    -0.0549    0.0894     0.1949
  4     1.5018    11323.     3.8946      79.50       82.05      1.2541      8.932    19.255    -0.0266    0.1156     0.2212
  5     1.5075    11741.     3.6538      79.30       81.98      1.2519      8.653    19.343    -0.0124    0.1251     0.2305
  6     1.5035    12249.     3.3145      78.41       81.41      1.2440      8.072    18.888     0.0077    0.1457     0.2466
  7     1.5041    12675.     3.1216      77.89       81.16      1.2391      7.755    18.709     0.0201    0.1539     0.2549
  8     1.5008    14393.     2.4064      72.50       78.50      1.2163      6.205    17.004     0.0877    0.2112     0.3065
  9     1.5021    16356.     1.8673      63.62       72.04      1.1905      4.700    14.636     0.1564    0.2699     0.3621
```

Printout of Programs FLOCAL and TTTR for use of IBM 360/67 computor.

```
C PROGRAM FLOCAL.THIS PROGRAM CALCULATES THE NOZZLE DISCHARGE COEFFICIENT(KN)
C OF THE TTTR BY MATCHING THE FLOW THROUGH THE NOZZLE WITH THAT OF THE FLOW
C THROUGH A STANDARD SHARP-EDGED ORIFICE.INPUT DATA-PBAR(IN HG),TBAR(DEG F),
C TCR(DEG F),DH(IN H2O),PREF1,PNOZ(IN HG),TNOZ(MV),DPFL(CM H2O),PREF,POR(IN
C HG),TOR(MV),L(NO OF DATA SETS),N(NO OF DATA POINTS IN EACH SET)
C
      DIMENSION DH(100),PREF1(100),PNOZ(100),TNOZ(100),TNOZR(100),DPFL(
     1 100),PREF(100),POR(100),TOR(100),TORR(100),WFL(100),QKN(100),
     2 RE(100)
C
C READ INPUT DATA
      WRITE(6,14)
      READ(5,15)L
      DO 13 M=1,L
      READ(5,15)N
      READ(5,16)PBAR,TBAR,TCR
      READ(5,16) (DH(I),I=1,N)
      READ(5,16) (PREF1(I),I=1,N)
      READ(5,16) (PNOZ(I),I=1,N)
      READ(5,16) (TNOZ(I),I=1,N)
      READ(5,16) (DPFL(I),I=1,N)
      READ(5,16) (PREF(I),I=1,N)
      READ(5,16) (POR(I),I=1,N)
      READ(5,16) (TOR(I),I=1,N)
C
C INPUT CONSTANTS
      D1O=6.065
      D2O=4.2425
      D1N=7.975
      D2N=4.25
      BETAO=D2O/D1O
      BETAN=D2N/D1N
      GAM=1.4
      EX1=GAM/(GAM-1.)
      EX2=(GAM-1.)/GAM
      EX3=2./GAM
      A=D2O*(830.-5000.*BETAO+9000.*BETAO**2-4200.*BETAO**3+530./SQRT(
     1 D1O))
      B=0.5993+0.007/D1O
      C=0.3640+0.076/SQRT(D1O)
      QKE=B+C*BETAO**4
      QKINF=QKE/(1.+A*(0.15E-04/D2O))
C
C COMPUTE CORRECTED PRESS AND TEMPS
      GHGBR=13.63905-0.00136303*TBAR
      GHGCR=13.63905-0.00136303*TCR
      CHGBR=0.4891585*GHGBR/13.54
      CHGCR=0.4891585*GHGCR/13.54
      GW68=0.9983763+68.*0.106058E-03-(68.**2)*0.159319E-05
      GWCR=0.9983763+TCR*0.106058E-03-(TCR**2)*0.159319E-05
      PAMB=PBAR*CHGBR
C
C CALCULATIONS FOR ORIFICE FLOW RATE
      DO 12 I=1,N
      QDPFL=DPFL(I)
      DPFL(I)=QDPFL/2.54*GWCR*62.42732/1728.
      POR(I)=CHGCR*(PREF(I)-POR(I))+PAMB
      TOR(I)=33.252+34.86*TOR(I)-0.1855*TOR(I)**2
      TORR(I)=TOR(I)+459.69
      ALPHAO=1.+1.93*(TOR(I)-68.)*0.1E-04
      YO=1.0-(0.41+0.35*BETAO**4)*DPFL(I)/(GAM*POR(I))
      ZO=1.9+2.4*(TOR(I)-100.)*0.1E-02
      HW680=QDPFL/2.54*GWCR/GW68
      FR=1.0
      WFL(I)=0.1638427*D20**2*ALPHAO*QKINF*FR*YO*SQRT(POR(I)*HW680/
     1 TORR(I))
   10 XO=2.27376*WFL(I)/(D20*ZO)
      FR=1.+(A/XO)*0.1E-05
      WFLC=0.1638427*D20**2*ALPHAO*QKINF*FR*YO*SQRT(POR(I)*HW680/
     1 TORR(I))
      IF(ABS(WFLC-WFL(I)).LE.0.0001) GO TO 11
      WFL(I)=WFLC
      GO TO 10
   11 WFL(I)=WFLC
C
C CALCULATIONS FOR NOZZLE DISCHARGE COEFFICIENT
      QDH=DH(I)
      DH(I)=QDH*GWCR*62.42732/1728.
      PNOZ(I)=CHGCR*(PREF1(I)-PNOZ(I))+PAMB
      TNOZ(I)=33.252+34.86*TNOZ(I)-0.1855*TNOZ(I)**2
      TNOZR(I)=TNOZ(I)+459.69
      ALPHAN=1.+2.52*(TNOZ(I)-68.)*0.1E-04
      R=1.-(DH(I)/PNOZ(I))
      YN=SQRT(R**EX3*EX1*((1.-R**EX2)/(1.-R))*((1.-BETAN**4)/(1.-R**EX3*
     1 BETAN**4)))
      ZN=1.9+2.4*(TNOZ(I)-100.)*0.1E-02
      HW68N=QDH*GWCR/GW68
      QKN(I)=6.10342*WFL(I)*SQRT(TNOZR(I)/(HW68N*PNOZ(I)))/(D2N**2*YN*
     1 ALPHAN)
      RE(I)=2.27376*WFL(I)/(D2N*ZN)*0.1E+07
   12 CONTINUE
C
C WRITE OUTPUT DATA
      WRITE(6,17)
      WRITE(6,18)M,PNOZ(1)
      WRITE(6,19)
      WRITE(6,20)PAMB,N,GAM
      WRITE(6,21)
      DO 13 I=1,N
      WRITE(6,22)I,WFL(I),QKN(I),RE(I)
   13 CONTINUE
C
   14 FORMAT(1H1,32X,'FLOW NOZZLE CALIBRATION FOR THE TRANSONIC TURBINE
     1 TEST RIG')
   15 FORMAT(I3)
   16 FORMAT(8F10.0)
   17 FORMAT(////32X,'TEST SERIES',25X,'NOZZLE SUPPLY PRESSURE')
   18 FORMAT(/35X,I3,38X,F5.2)
   19 FORMAT(/32X,'ATMOS. PRESS.',11X,'DATA POINTS',11X,'GAMMA')
   20 FORMAT(/35X,F6.2,19X,I2,17X,F3.1)
   21 FORMAT(//34X,'POINT',8X,'FLOW RATE',8X,'DISCHARGE',8X,'REYNOLDS',/
     1 47X,'(LBM/SEC)',7X,'COEFFICIENT',8X,'NUMBER',//)
   22 FORMAT(36X,I2,9X,F8.4,8X,F9.5,7X,F11.2)
      STOP
      END
```

```
C CHARACTERISTICS OF THE TRANSONIC TURBINE TEST RIG, USING ONE-DIMENSIONAL
C ANALYSIS, AT THE MEAN RADIUS.
C
C INPUT DATA AXCLR, RADCLR(IN), PBAR(IN HG), TBAR, TCR(DEG R), DH(IN H2O), PREF1
C PNOZ,PTPL,PTO,PREF2,PHUB,PTIP,P13-P21,PHD,PCL1-PCL3(IN HG), TNOZ,TTPL,TTO,
C THD(MV), AXIL,TORQR,DYNAR(COUNTS-10,000), RPM, CLAXIL,CLTRQR(COUNTS),
C MM(NO OF RUNS), NRUN(RUN NO), N(NO OF DATA POINTS IN EACH RUN)
C
      REAL*4 MVA1M,MVA1,MV1M,MV1C,MV1,MW1,MV2,MW2
C
      DIMENSION DH(50),PREF1(50),PNOZ(50),PTPL(50),PTO(50),PREF2(50),
     1PHUB(50),PTIP(50),P13(50),P14(50),P15(50),P16(50),P17(50),P18(50),
     2P19(50),P20(50),P21(50),PHD(50),PCL1(50),PCL2(50),PCL3(50),
     3TNOZ(50),TTPL(50),TTO(50),THD(50),AXIL(50),TORQR(50),DYNAR(50),
     4RPM(50),CLAXIL(50),CLTRQR(50)
C
      DIMENSION FAX(50),CLFAX(50),F0(50),F1(50),F2(50),F3(50),F4(50),
     1 F5(50),F6A(50),FNET(50),TORQ(50),CLTORQ(50),FLOWN(50),FLOWT(50),
     2 FLOWL(50),RE(50),PHI(50),XI(50),P1AV(50),PRPL(50),PRS(50),T1(50),
     3 T1IS(50),VA1(50),VU1(50),V1(50),V1IS(50),ALPH1(50),VCOFS(50),
     4 MV1(50),MVA1(50),WA1(50),WU1(50),W1(50),U1(50),BETA1(50),MW1(50),
     5 ZETAS(50),ETAS(50),PT2(50),PR(50),TE(50),TT2(50),T2(50),T2IS(50),
     6 T2TH(50),TT2IS(50),DELTW(50),DELTIS(50),DELHW(50),DELHIS(50),
     7 VA2(50),VU2(50),V2(50),VOIS(50),ALPH2(50),WA2(50),WU2(50),W2(50),
     8 U2(50),W2IS(50),BETA2(50),DBETA(50),WCOFS(50),ZETAR(50),ETAR(50),
     9 REFRPM(50),XKIS(50),ETATS(50),ETATT(50),REFLOW(50),REFMOM(50),
     * HP(50),REFHP(50),REACHB(50),REACMN(50),REACTP(50),F(50),MV2(50),
     * MW2(50),REACEF(50),QNOZ(50),QTPL(50),PTQ(50),QHD(50),TTPQ(50),
     * TTO(50),SLF(50),SFF(50),RFAX(50),RTORQ(50),RVA1(50),RVU1(50)
C
      READ(5,10) MM
   10 FORMAT(I3)
      CALL CANCEL (2)
C
      DO 13 M=1,MM
      CALL        INPUT(NRUN,N,AXCLR,RADCLR,PBAR,TBAR,TCR,DH,PREF1,PNOZ,
     1 PTPL,PTO,PREF2,PHUB,PTIP,P13,P14,P15,P16,P17,P18,P19,P20,P21,PHD,
     2 PCL1,PCL2,PCL3,TNOZ,TTPL,TTO,THD,AXIL,TORQR,DYNAR,RPM,CLAXIL,
     3 CLTRQR,DA,T,E)
C
      CALL        SETCON(D1N,D2N,BETAN,RG,GAM,GC,CP,CJ,C,EX1,EX2,EX3,PI,
     1 ZNS,TETS,RTIP1,RHUB1,RTIP2,RHUB2,AAXS,AAXR,ATHS,RM1,RM2,SKT,RKT,
     2 RADCLR,B1,B2,B3,B4,B5,D1,D2,D3,D4,D5,D6,CL1,CL2,CL3)
      DO 12 J=1,2
      DO 11 I=1,N
      QDH=DH(I)                                                         0028
      QPREF1=PREF1(I)
      QPNOZ=PNOZ(I)                                                     0029
      QPTPL=PTPL(I)                                                     0031
      QPTO=PTO(I)
      QPREF2=PREF2(I)
      QPHUB=PHUB(I)                                                     0032
      QPTIP=PTIP(I)                                                     0033
      QP13=P13(I)
      QP14=P14(I)
      QP15=P15(I)                                                       0049
      QP16=P16(I)                                                       0050
      QP17=P17(I)                                                       0051
      QP18=P18(I)
      QP19=P19(I)
      QP20=P20(I)
      QP21=P21(I)
      QPHD=PHD(I)                                                       0041
      QTNOZ=TNOZ(I)                                                     0030
      QTTPL=TTPL(I)                                                     0035
      QTTO=TTO(I)
      QTHD=THD(I)
      QAXIL=AXIL(I)                                                     0039
      QTORQR=TORQR(I)                                                   0038
      QDYNAR=DYNAR(I)                                                   0040
      QRPM=RPM(I)                                                       0037
      QLAXIL=CLAXIL(I)
      QLTRQR=CLTRQR(I)                                                  0045
C
      CALL CNVERT(PBAR,TBAR,TCR,PAMB,HW68,QDH,QPREF1,QPNOZ,QPTPL,QPTO,
     1 QPREF2,QPHUB,QPTIP,QP13,QP14,QP15,QP16,QP17,QP18,QP19,QP20,QP21,
     2 QPHD,QPCL1,QPCL2,QPCL3,QTNOZ,TNOZR,QTTPL,TTPLR,QTTO,TTOR,QTHD,
     3 QAXIL,QFAX,QTCRQR,QTORQ,QDYNAR,DYNA,QLAXIL,QLFAX,QLTRQR,QLTORQ,
     4 CL1,CL2,CL3)
C
      CALL FLORAT(D2N,RG,GC,EX1,EX2,EX3,HW68,QDH,QPNCZ,QPTPL,QPHD,PRP,
     1 QTNOZ,TNOZR,QTTPL,TTPLR,QTHD,B1,B2,B3,B4,B5,D1,D2,D3,D4,D5,D6,
     2 NRUN,I,QRE,QFLCWN,QFLOWL,QFLOWT,BETAN)
C
      CALL STATOR(RG,GAM,GC,C,PI,EX1,EX2,EX3,EPS,RTIP1,RHUB1,RM1,QPHUB,
     1 QPTIP,QP1AV,QPTO,QP13,QP18,QP19,QP20,QP21,QPHD,QPRS,QFLOWT,AAXS,
     2 ATHS,SKT,    J,TTOR,T1RM,T1ISR,QZETAS,QETAS,QPHI,QXI,QRPM,VA1M,
     3 QVU1,V1M,QV1IS,VCOEFS,ALPH1M,MV1M,MVA1M,QU1,QWA1,QWU1,QW1,QBETA1,
     4 QMW1,QTORQ,QLTORQ,QFAX,QLFAX,QF0,QF1,QF2,QF3,QF4,QF5,QF6A,QFNET,
     5 QRFAX,QRTORQ,QRVA1,QRVU1)
C
      CALL       ROTOR(RG,GC,CJ,CP,C,PI,EX1,EX2,RM1,RM2,AAXR,RKT,QPTO,
     1 QP1AV,QPHD,QPT2,PRM,DYNA,QFLOWT,TTOR,T1RM,T2R,TT2R,QDELTW,T2ISR,
     2 TER,QVU1,QU1,QW1,QBETA1,QVU2,QVA2,QV2,QALPH2,QU2,QWU2,QWA2,QW2,
     3 QW2IS,QBETA2,QDBETA,WCOEFS,QZETAR,QETAR,QMV2,QMW2,GAM,QRPM,QSLF,
     4 QSFF)
```

```
C
      CALL        PERFRM(C,PI,EX2,QPTO,QPHUB,QPTIP,QPHD,QPT2,DYNA,QRPM,
     1 QFLOWT,TTOR,TT2R,T2THR,TT2ISR,QDLHIS,QDELHW,QDLTIS,QDELTW,QVOIS,
     2 QV1IS,QU1,QV2,QETATS,QETATT,QEACMN,QEACHB,QEACTP,QXKIS,QEFLOW,
     3 QEFRPM,QEFMOM,QHP,QEFHP,T2ISR,QF,V1M,QW1,QU2,QW2,QEACEF,CP)
      FAX(I)=QFAX
      CLFAX(I)=QLFAX
      FO(I)=QFO
      F1(I)=QF1
      F2(I)=QF2
      F3(I)=QF3
      F4(I)=QF4
      F5(I)=QF5
      F6A(I)=QF6A
      FNET(I)=QFNET
      TORQ(I)=QTORQ
      CLTORQ(I)=QLTORQ
      FLOWN(I)=QFLOWN
      FLOWT(I)=QFLOWT
      FLOWL(I)=QFLOWL
      RE(I)=QRE
      PHI(I)=QPHI
      XI(I)=QXI
      QNOZ(I)=QPNOZ
      QTPL(I)=QPTPL
      PTO(I)=QPTO
      P1AV(I)=QP1AV
      QHD(I)=QPHD
      PRPL(I)=PRP
      PRS(I)=QPRS
      TTPQ(I)=TTPLR
      TTO(I)=TTOR
      T1(I)=T1RM
      T1IS(I)=T1ISR
      VA1(I)=VA1M
      VU1(I)=QVU1
      V1(I)=V1M
      V1IS(I)=QV1IS
      ALPH1(I)=ALPH1M
      VCOFS(I)=VCOEFS
      MV1(I)=MV1M
      MVA1(I)=MVA1M
      WA1(I)=QWA1
      WU1(I)=QWU1
      W1(I)=QW1
      U1(I)=QU1
      BETA1(I)=QBETA1
      MW1(I)=QMW1
```

```
ZETAS(I)=QZETAS
ETAS(I)=QETAS
PT2(I)=QPT2
PR(I)=PRM
TE(I)=TER
TT2(I)=TT2R
T2(I)=T2R
T2IS(I)=T2ISR
T2TH(I)=T2THR
TT2IS(I)=TT2ISR
DELTW(I)=QDELTW
DELTIS(I)=QDLTIS
DELHW(I)=QDELHW
DELHIS(I)=QDLHIS
VA2(I)=QVA2
VU2(I)=QVU2
V2(I)=QV2
VOIS(I)=QVOIS
ALPH2(I)=QALPH2
MV2(I)=QMV2
WA2(I)=QWA2
WU2(I)=QWU2
W2(I)=QW2
MW2(I)=QMW2
U2(I)=QU2
W2IS(I)=QW2IS
BETA2(I)=QBETA2
DBETA(I)=QDBETA
WCOFS(I)=WCOEFS
ZETAR(I)=QZETAR
ETAR(I)=QETAR
REFRPM(I)=QEFRPM
XKIS(I)=QXKIS
ETATS(I)=QETATS
F(I)=QF
ETATT(I)=QETATT
REFLOW(I)=QEFLOW
REFMOM(I)=QEFMOM
HP(I)=QHP
REFHP(I)=QEFHP
REACEF(I)=QEACEF
REACHB(I)=QEACHB
REACMN(I)=QEACMN
REACTP(I)=QEACTP
SLF(I)=QSLF
SFF(I)=QSFF
RFAX(I)=QRFAX
RTORQ(I)=QRTORQ
```

```
      RVA1(I)=QRVA1
      RVU1(I)=QRVU1
   11 CONTINUE
C
      CALL      OUTPTS(NRUN,N,FAX,CLFAX,F0,F1,F2,F3,F4,F5,F6A,FNET,J,
     1 TORQ,CLTORQ,FLOWN,FLOWT,FLOWL,RE,PHI,XI,QNOZ,QTPL,PTO,P1AV,QHD,
     2 PRPL,PRS,TTPQ,TTO,T1,T1IS,VA1,VU1,V1,V1IS,ALPH1,VCOFS,MV1,MVA1,
     3 WA1,WU1,W1,U1,BETA1,MW1,ZETAS,ETAS,PAMB,DA,T,E,RFAX,RTORQ,RVA1,
     4 RVU1)
C
      CALL      OUTPTR(NRUN,N,AXCLR,RADCLR,PAMB,PTO,P1AV,PT2,QHD,PR,
     1 TTO,T1,TE,TT2,T2,T2IS,T2TH,TT2IS,DELTIS,DELTW,VA2,VU2,V2,VOIS,
     2 ALPH2,WA2,WU2,W2,U2,W2IS,BETA2,DBETA,WCOFS,ZETAR,ETAR,RPM,HP,
     3 DELHIS,DELHW,REFRPM,XKIS,ETATS,ETATT,REFLOW,REFMOM,REFHP,J,
     4 REACHB,REACMN,REACTP,DA,T,E,F,REACEF,MV2,MW2,SLF,SFF)
   12 CONTINUE
   13 CONTINUE
C
      STOP
      END


      SUBROUTINE INPUT(NRUN,N,AXCLR,RADCLR,PBAR,TBAR,TCR,DH,PREF1,PNOZ,
     1 PTPL,PTO,PREF2,PHUB,PTIP,P13,P14,P15,P16,P17,P18,P19,P20,P21,PHD,
     2 PCL1,PCL2,PCL3,TNOZ,TTPL,TTO,THD,AXIL,TORQR,DYNAR,RPM,CLAXIL,
     3 CLTRQR,DA,T,E)
      DIMENSION DH(50),PREF1(50),PNOZ(50),PTPL(50),PTO(50),PREF2(50),
     1PHUB(50),PTIP(50),P13(50),P14(50),P15(50),P16(50),P17(50),P18(50),
     2P19(50),P20(50),P21(50),PHD(50),PCL1(50),PCL2(50),PCL3(50),
     3TNOZ(50),TTPL(50),TTO(50),THD(50),AXIL(50),TORQR(50),DYNAR(50),
     4RPM(50),CLAXIL(50),CLTRQR(50)
      READ (5,101)NRUN,N,DA,T,E
      READ (5,102)AXCLR,RADCLR                                          0123
      READ (5,102)PBAR,TBAR,TCR                                         0124
      READ (5,102)(DH(I),I=1,N)                                         0126
      READ (5,102)(PREF1(I),I=1,N)
      READ (5,102)(PNOZ(I),I=1,N)                                       0136
      READ (5,102)(PTPL(I),I=1,N)                                       0134
      READ (5,102)(PTO(I),I=1,N)
      READ (5,102)(PREF2(I),I=1,N)
      READ (5,102)(PHUB(I),I=1,N)                                       0138
      READ (5,102)(PTIP(I),I=1,N)                                       0128
      READ (5,102)(P13(I),I=1,N)
      READ (5,102)(P14(I),I=1,N)
      READ (5,102)(P15 (I),I=1,N)                                       0130
      READ (5,102)(P16 (I),I=1,N)                                       0131
      READ (5,102)(P17 (I),I=1,N)                                       0132
      READ (5,102)(P18 (I),I=1,N)                                       0129
      READ (5,102)(P19 (I),I=1,N)
      READ (5,102)(P20 (I),I=1,N)
      READ (5,102)(P21(I),I=1,N)
      READ (5,102)(PHD (I),I=1,N)                                           0139
      READ (5,102)(TNOZ(I),I=1,N)                                           0140
      READ (5,102)(TTPL(I),I=1,N)
      READ (5,102)(TTO(I),I=1,N)
      READ (5,102)(THD(I),I=1,N)
      READ (5,102)(AXIL(I),I=1,N)                                           0142
      READ (5,102)(TORQR(I),I=1,N)                                          0143
      READ (5,102)(DYNAR(I),I=1,N)                                          0144
      READ (5,102)(RPM(I),I=1,N)                                            0145
      READ (5,102)(CLAXIL(I),I=1,N)                                         0146
      READ (5,102)(CLTRQR(I),I=1,N)                                         0147
  101 FORMAT(2I3,4X,3A3)
  102 FORMAT(8F10.0)
      RETURN                                                                0178
      END                                                                   0179

      SUBROUTINE SETCON(D1N,D2N,BETAN,RG,GAM,GC,CP,CJ,C,EX1,EX2,EX3,PI,
     1 ZNS,TETS,RTIP1,RHUB1,RTIP2,RHUB2,AAXS,AAXR,ATHS,RM1,RM2,SKT,RKT,
     2 RADCLR,B1,B2,B3,B4,B5,D1,D2,D3,D4,D5,D6,CL1,CL2,CL3)
C
      D1N=7.975
      D2N=4.250
      BETAN=D2N/D1N
      RG=53.3448
      GAM=1.4                                                               0212
      GC=32.174                                                             0213
      CJ=778.16                                                             0215
      EX1=GAM/(GAM-1.)                                                      0218
      EX2=(GAM-1.)/GAM                                                      0219
      EX3=2./GAM                                                            0220
      CP=EX1*RG/CJ
      C=2.*GC*CJ*CP
      PI=3.1416                                                             0221
      ZNS=31.                                                               0224
      DTHS=0.205                                                            0225
      SS=0.8594                                                             0226
      TETS=0.024                                                            0227
      DTHR=0.1314                                                           0237
      SR=0.4495                                                             0238
      TETR=0.020                                                            0239
      RTIP1=4.585                                                           0228
      RHUB1=3.895                                                           0229
      RTIP2=4.763                                                           0240
      RHUB2=3.826                                                           0241
      AAXS=PI*((RTIP1)**2-(RHUB1)**2)                                   0231
      AAXR=PI*((RTIP2)**2-(RHUB2)**2)                                   0243
      ATHS=DTHS*(RTIP1-RHUB1)*ZNS                                       0232
      RM1=(RTIP1+RHUB1)/2.                                              0230
      RM2=(RTIP2+RHUB2)/2.                                              0242
      SKT=1.-(2.7/1000.)*((TETS/SS*100.)**3.3)*DTHS/SS
      RKT=(1.-(2.7/1000.)*((TETR/SR*100.)**3.3)*DTHR/SR)*((AAXR+PI*
     1 RADCLR*(RTIP2+RADCLR/2.))/AAXR)
      SKT=0.95
      ATHS=ATHS/1.06
      WRITE(6,200) BETAN,AAXS,AAXR,ATHS,RM1,RM2
      WRITE(6,201) SKT,RKT
  200 FORMAT(1H1,10F12.7)
  201 FORMAT(///,10F12.7)
      B1=9.5208828E-01
      B2=4.4891640E-07
      B3=-7.5810743E-13
      B4=5.5023778E-19
      B5=-1.4571314E-25
      D1=-1.004586E-01
      D2=2.122579E-01
      D3=-1.081851E-01
      D4=2.767576E-02
      D5=-3.489933E-03
      D6=1.726733E-04
      CL1=-2.7923457E-03
      CL2=5.1056171E-04
      CL3=9.1106005E-08
      RETURN                                                            0212A
      END                                                               0212B

      SUBROUTINE CNVERT(PBAR,TBAR,TCR,PAMB,HW68,DH,PREF1,PNOZ,PTPL,PTO,
     1 PREF2,PHUB,PTIP,P13,P14,P15,P16,P17,P18,P19,P20,P21,PHD,PCL1,
     2 PCL2,PCL3,TNOZ,TNOZR,TTPL,TTPLR,TTO,TTOR,THD,AXIL,FAX,TORQR,TORQ,
     3 DYNAR,DYNA,CLAXIL,CLFAX,CLTRQR,CLTORQ,CL1,CL2,CL3)
C
      TEMP(X)=32.+35.98*X-.435*X**2
      GHGBR=13.63905-0.00136303*TBAR
      GHGCR=13.63905-0.00136303*TCR
      CHGBR=0.4891585*GHGBR/13.54
      CHGCR=0.4891585*GHGCR/13.54
      GW68=0.9983763+68.*0.106058E-03-(68.**2)*0.159319E-05
      GWCR=0.9983763+TCR*0.106058E-03-(TCR**2)*0.159319E-05
      PAMB=PBAR*CHGBR
      HW68=CH*GWCR/GW68
      DH=DH*GWCR*62.42732/1728.
      PNOZ=CHGCR*(PREF1-PNOZ)+PAMB
      PTPL=CHGCR*(PREF1-PTPL)+PAMB
      PTO=CHGCR*(PREF1-PTO)+PAMB
      PHUB=CHGCR*(PREF2-PHUB)+PAMB
      PTIP=CHGCR*(PREF2-PTIP)+PAMB
      P13=CHGCR*(PREF2-P13)+PAMB
      P14=CHGCR*(PREF2-P14)+PAMB
      P15=CHGCR*(PREF2-P15)+PAMB
      P16=CHGCR*(PREF2-P16)+PAMB
      P17=CHGCR*(PREF2-P17)+PAMB
      P18=CHGCR*(PREF2-P18)+PAMB
      P19=CHGCR*(PREF2-P19)+PAMB
      P20=CHGCR*(PREF2-P20)+PAMB
      P21=CHGCR*(PREF2-P21)+PAMB
      PHD=CHGCR*(PREF2-PHD)+PAMB
      TNOZ=TEMP(TNOZ)
      TNOZR=TNOZ+459.69
      TTPL=TEMP(TTPL)
      TTPLR=TTPL+459.69
      TTO=TEMP(TTO)
      TTOR=TTO+459.69
      THD=TEMP(THD)
      FAX=0.08*AXIL
      TORQ=TORQR/30.
      DYNA=DYNAR/30.
      CLFAX=0.01*CLAXIL
      CLTORQ=(CL1+CL2*CLTRQR+CL3*CLTRQR**2)/12.
      PHUB=PHUB/1.05
      TORQ=TORQ/1.05
      WRITE(6,300) PAMB,HW68,DH,PNOZ,PTPL,PTO,PHUB,PTIP
      WRITE(6,301) P13,P14,P15,P16,P17,P18,P19,P20,P21,PHD
      WRITE(6,301) TNOZ,TNOZR,TTPL,TTPLR,TTO,TTOR,THD
      WRITE(6,301) FAX,TORQ,DYNA,CLFAX,CLTORQ
  300 FORMAT(1H1,10F10.3)
  301 FORMAT(///,10F10.3)
      RETURN
      END


      SUBROUTINE FLORAT(D2N,RG,GC,EX1,EX2,EX3,HW68,DH,PNOZ,PTPL,PHD,PR,
     1 TNOZ,TNOZR,TTPL,TTPLR,THD,B1,B2,B3,B4,B5,D1,D2,D3,D4,D5,D6,NRUN,
     2 I,RE,FLOWN,FLOWL,FLOWT,BETAN)
C
      ALPHAN=1.+2.52*(TNOZ-68.)*0.1E-04
      R=1.-(DH/PNOZ)
      Y1=R**EX3
      Y2=EX1
      Y3=1.-R**EX2
      Y4=1.-R
      Y5=1.-BETAN**4
      Y6=1.-R**EX3*BETAN**4
      ARG=Y1*Y2*(Y3/Y4)*(Y5/Y6)
      YN=SQRT(ARG)
      ZN=1.9+2.4*(TNOZ-100.)*0.1E-02
      WRITE(6,402) ALPHAN,R,YN,ZN
      CN=1.0400
      WN =0.1638427*D2N**2*ALPHAN*YN*CN*SQRT(PNOZ*HW68/TNOZR)
  400 RE=2.27376*WN/(D2N*ZN)*0.1E+07
      CN=B1+RE*(B2+RE*(B3+RE*(B4+B5*RE)))
      WNC=0.1638427*D2N**2*ALPHAN*YN*CN*SQRT(PNOZ*HW68/TNOZR)
      IF(ABS(WNC-WN).LE.0.0001) GO TO 401
      WN=WNC
      GO TO 400
  401 FLOWN=WNC
      RE=2.27376*FLOWN/(D2N*ZN)*0.1E+07
      IF(RE.GT.1.2E+06) GO TO 404
      PR=PTPL/PHD
      WREF=D1+PR*(D2+PR*(D3+PR*(D4+PR*(D5+D6*PR))))
      CORR=(1.+0.32*((TTPL-THD)/TTPL))**1.2
      FLOWL=WREF*PTPL/SQRT(TTPLR*RG/GC)/CORR
      FLOWT=FLOWN-FLOWL
      WRITE(6,403) FLOWN,FLOWL,FLOWT,CN,RE
  402 FORMAT(///,10F10.7)
  403 FORMAT(///,4F10.4,F20.2)
      GO TO 406
  404 WRITE(6,405) NRUN,I
  405 FORMAT(/33X,I4,7X,36HFLOW RATE TOO HIGH, CHECK INPUT DATA/)
  406 RETURN
      END


      SUBROUTINE STATOR(RG,GAM,GC,C,PI,EX1,EX2,EX3,EPS,RTIP1,RHUB1,RM1,
     1 PHUB,PTIP,P1AV,PTO,P13,P18,P19,P20,P21,PHD,PRS,FLOWT,AAXS,ATHS,
     2 SKT,    J,TTOR,T1RM,T1ISR,ZETAS,ETAS,PHI,XI,RPM,VA1M,VU1,V1M,V1IS,
     3 VCOEFS,ALPH1M,MV1M,MVA1M,U1,WA1,WU1,W1,BETA1,MW1,TORQ,CLTORQ,FAX,
     4 CLFAX,F0,F1,F2,F3,F4,F5,F6A,FNET,RFAX,RTORQ,RVA1,RVU1)
      REAL*4 MVA1M,MVA1,MV1M,MV1C,MV1,MW1,MV2,MW2
      IF(J.GE.2) GO TO 500
      P1AV=(PHUB+PTIP)/2.
C IN THIS SECTION, M SUBSCRIPT REPRESENTS VALUES COMPUTED BY CONTINUITY BELOW
      C2=(C*P1AV*ATHS)/(RG*FLOWT)
      V1M=SQRT(C*TTOR+(C2/2.)**2)-C2/2.
      T1RM=TTOR-V1M**2/C
      VA1M=(FLOWT*RG*T1RM)/(P1AV*AAXS*SKT)
      VR=VA1M/V1M
      IF(ABS(VR).GE.1.0) VR=1.0
      AN=ARCOS(VR)
      VU1=V1M*SIN(AN)
      ALPH1M=AN*180./PI
      MV1M=V1M/SQRT(GAM*GC*RG*T1RM)
      MVA1M=VA1M/SQRT(GAM*GC*RG*T1RM)
      CALL       FORCE(PI,RTIP1,RHUB1,AAXS,PHUB,P1AV,PTIP,P13,P18,P19,
     1 P20,P21,PHD,FAX,CLFAX,F0,F1,F2,F3,F4,F5,F6A,FNET)
      GO TO 506
  500 WRITE(6,501)
  501 FORMAT(///,9X,3HEPS8X,4HP1AV9X,3HT1M10X,3HT1C9X,4HVA1M9X,4HVA1C9X,
     14HMV1M9X,4HMV1C7X,8HALPHA 1M5X,8HALPHA 1C/)
      EPS=0.0
  502 P1AV=PHUB/3.*(((1.+EPS)*(RTIP1)**2+(RHUB1)*(RTIP1)-(2.+EPS)*
     1 (RHUB1)**2)/((RTIP1)**2-(RHUB1)**2))+PTIP/3.*(((2.+EPS)*(RTIP1)
     2 **2-(RHUB1)*(RTIP1)-(1.+EPS)*(RHUB1)**2)/((RTIP1)**2-(RHUB1)**2))
      CALL       MOMENT(RG,GAM,GC,C,RM1,AAXS,TORQ,CLTORQ,FLOWT,PI,RTIP1,
     1 RHUB1,FAX,CLFAX,PHUB,PTIP,P1AV,P13,P18,P19,P20,P21,PHD,TTOR,T1RM,
     2 VU1,VA1M,V1M,ALPH1M,MV1M,MVA1M,F0,F1,F2,F3,F4,F5,F6A,FNET)
      C1=FLOWT*RG/(P1AV*AAXS*SKT)
      VA1C=SQRT(C*TTOR-VU1**2+(C/(2.*C1))**2)-C/(2.*C1)
      ALPH1C=ATAN(VU1/VA1C)
      ALPH1C=ALPH1C*180./PI
      V1C=SQRT(VA1C**2+VU1**2)
      T1RC=TTOR-(V1C**2)/C
      MV1C=V1C/SQRT(GAM*GC*RG*T1RC)
      WRITE(6,503)EPS,P1AV,T1RM,T1RC,VA1M,VA1C,MV1M,MV1C,ALPH1M,ALPH1C
  503 FORMAT(10F13.5)
      DIFF=ABS(T1RM-T1RC)
      IF(DIFF-0.01) 506,506,504
  504 IF(T1RC.LT.T1RM) GO TO 505
      EPS=EPS+DIFF/500.
      GO TO 502
  505 EPS=EPS-DIFF/500.
      GO TO 502
  506 PRS=P1AV/PTO
      IF(PRS.GE.1.0) PRS=0.9990
      T1ISR=TTOR*PRS**EX2
      ZETAS=(T1RM-T1ISR)/(TTOR-T1ISR)
      ETAS=1.0-ZETAS
      V1IS=SQRT(C*(TTOR-T1ISR))
      VCOEFS=V1M/V1IS
      PHI=FLOWT/(PTO*ATHS)*SQRT(TTOR*RG/GC)
      PRTHS=PRS
      IF(PRTHS.LT.0.52828) PRTHS=0.52828
      XI=PHI/SQRT(2.*EX1*(PRTHS**EX3-PRTHS**((GAM+1.)/GAM)))
      PRS=1./PRS
      U1=PI*RPM*RM1/360.
      WU1=VU1-U1
      WA1=VA1M
      BETA1=ATAN(WU1/WA1)
      W1=WA1/COS(BETA1)
      BETA1=BETA1*180./PI
      MW1=W1/SQRT(GAM*RG*GC*T1RM)
      RFAX=FAX/(PTO/14.69)
      RTORQ=TORQ/(PTO/14.69)
      RVA1=VA1M/SQRT(GAM*GC*RG*TTOR)
      RVU1=VU1/SQRT(GAM*GC*RG*TTOR)
      RETURN
      END


      SUBROUTINE MOMENT(RG,GAM,GC,C,RM1,AAXS,TORQ,CLTORQ,FLOWT,PI,RTIP1,
     1 RHUB1,FAX,CLFAX,PHUB,PTIP,P1AV,P13,P18,P19,P20,P21,PHD,TTOR,T1RM,
     2 VU1,VA1M,V1M,ALPH1M,MV1M,MVA1M,F0,F1,F2,F3,F4,F5,F6A,FNET)
C
      REAL*4 MVA1M,MVA1,MV1M,MV1C,MV1,MW1,MV2,MW2
      VU1=(TORQ+CLTORQ)*12.*GC/(FLOWT*RM1)
      A0=PI*5.125**2
      A2=PI*(5.125**2-5.003**2)
      A3=PI*(5.003**2-4.901**2)
      A4=PI*(4.901**2-4.773**2)
      A5=PI*(4.773**2-RTIP1**2)
      A6A=PI*RHUB1**2
      F0=A0*PHD
      F1=AAXS*P1AV
      F2=A2*P21
      F3=A3*((P20+P19)/2.)
      F4=A4*P18
      F5=A5*((PTIP+P13)/2.)
      F6A=A6A*PHUB
      FNET=FAX+CLFAX+F0-F1-F2-F3-F4-F5-F6A
      VA1M=FNET*GC/FLOWT
      ALPH1M=ATAN(VU1/VA1M)
      ALPH1M=ALPH1M*180./PI
      V1M=SQRT(VA1M**2+VU1**2)
      T1RM=TTOR-(V1M**2)/C
      MV1M=V1M/SQRT(GAM*GC*RG*T1RM)
      MVA1M=VA1M/SQRT(GAM*GC*RG*T1RM)
      RETURN
      END


      SUBROUTINE FORCE(PI,RTIP1,RHUB1,AAXS,PHUB,P1AV,PTIP,P13,P18,P19,
     1 P20,P21,PHD,FAX,CLFAX,F0,F1,F2,F3,F4,F5,F6A,FNET)
C
      A0=PI*5.125**2
      A2=PI*(5.125**2-5.003**2)
      A3=PI*(5.003**2-4.901**2)
      A4=PI*(4.901**2-4.773**2)
      A5=PI*(4.773**2-RTIP1**2)
      A6A=PI*RHUB1**2
      F0=A0*PHD
      F1=AAXS*P1AV
      F2=A2*P21
      F3=A3*((P20+P19)/2.)
      F4=A4*P18
      F5=A5*((PTIP+P13)/2.)
      F6A=A6A*PHUB
      FNET=FAX+CLFAX+F0-F1-F2-F3-F4-F5-F6A
      RETURN
      END


      SUBROUTINE ROTOR(RG,GC,CJ,CP,C,PI,EX1,EX2,RM1,RM2,AAXR,RKT,PTO,
     1 P1AV,PHD,PT2,PRM,DYNA,FLOWT,TTOR,T1RM,T2R,TT2R,DELTW,T2ISR,TER,
     2 VU1,U1,W1,BETA1,VU2,VA2,V2,ALPH2,U2,WU2,WA2,W2,W2IS,BETA2,DBETA,
     3 WCOEFS,ZETAR,ETAR,MV2,MW2,GAM,RPM,SLF,SFF)
C
      REAL*4 MVA1M,MVA1,MV1M,MV1C,MV1,MW1,MV2,MW2
      VU2=RM1/RM2*VU1-(12.*DYNA*GC)/(RM2*FLOWT)
      U2=U1*RM2/RM1
      WU2=VU2-U2
      DELTW=(DYNA*PI*RPM)/(30.*FLOWT*CJ*CP)
      TT2R=TTOR-DELTW
      T2ISR=T1RM*(PHD/P1AV)**EX2
      TER=T1RM+(W1**2-U1**2+U2**2)/C
      C3=FLOWT*RG/(PHD*AAXR*RKT)
      VA2=SQRT(C*TT2R-VU2**2+(C/(2.*C3))**2)-C/(2.*C3)
      V2=SQRT(VA2**2+VU2**2)
      T2R=TT2R-(V2**2)/C
      MV2=V2/SQRT(GAM*RG*GC*T2R)
      PT2=PHD*(TT2R/T2R)**EX1
      PRM=PTO/PHD
      WA2=VA2
      W2=SQRT(WA2**2+WU2**2)
      MW2=W2/SQRT(GAM*RG*GC*T2R)
      ALPH2=ATAN(VU2/VA2)
      ALPH2=ALPH2*180./PI
      BETA2=ATAN(WU2/WA2)
      BETA2=BETA2*180./PI
      DBETA=BETA1-BETA2
      ZETAR=(T2R-T2ISR)/(TER-T2ISR)
      ETAR=1.0-ZETAR
      W2IS=SQRT(C*(TER-T2ISR))
      WCOEFS=W2/W2IS
      IF(U2.LE.1.0) U2=0.001
      SLF=(VU1-VU2)/U2
      SFF=VA2/U2
      RETURN
      END

      SUBROUTINE PERFRM(C,PI,EX2,PTO,PHUB,PTIP,PHD,PT2,DYNA,RPM,FLOWT,
     1 TTOR,TT2R,T2THR,TT2ISR,DELHIS,DELHW,DELTIS,DELTW,VOIS,V1IS,U1,V2,
     2 ETATS,ETATT,REACMN,REACHB,REACTP,XKIS,REFLOW,REFRPM,REFMOM,HP,
     3 REFHP,T2ISR,F,V1,W1,U2,W2,REACEF,CP)
C
      DELTIS=TTOR*(1.0-(PHD/PTO)**EX2)
      T2THR=TTOR-DELTIS
      TT2ISR=TTOR*(PT2/PTO)**EX2
      DELHIS=CP*(TTOR-T2THR)
      DELHW=CP*(TTOR-TT2R)
      ETATS=DELTW/DELTIS*100.
      F=T2ISR/T2THR
      ETATT=DELTW/(DELTIS-(V2**2)/(C*F))*100.
      VOIS=SQRT(C*DELTIS)
      REACEF=(W2**2-W1**2+U1**2-U2**2)/(V1**2+W2**2-W1**2+U1**2-U2**2)
      REACMN=1.0-(V1IS/VOIS)**2
      REACHB=((PHUB/PHD)**EX2-1.)/((PTO/PHD)**EX2-1.)
      REACTP=((PTIP/PHD)**EX2-1.)/((PTO/PHD)**EX2-1.)
      IF(U1.LE.1.0) U1=0.001
      XKIS=(VOIS/U1)**2
      DEL=PTO/14.69
      THETA=TTOR/518.69
      REFLOW=FLOWT*SQRT(THETA)/DEL
      REFRPM=RPM/SQRT(THETA)
      REFMOM=DYNA/DEL
      HP=(DYNA*PI*RPM)/(30.*550.)
      REFHP=HP/(DEL*SQRT(THETA))
      RETURN
      END

      SUBROUTINE OUTPTS(NRUN,N,FAX,CLFAX,FO,F1,F2,F3,F4,F5,F6A,FNET,J,
     1 TORQ,CLTORQ,FLOWN,FLOWT,FLOWL,RE,PHI,XI,QNOZ,QTPL,PTO,P1AV,QHD,
     2 PRPL,PRS,TTPQ,TTO,T1,T1IS,VA1,VU1,V1,V1IS,ALPH1,VCOFS,MV1,MVA1,
     3 WA1,WU1,W1,U1,BETA1,MW1,ZETAS,ETAS,PAMB,DA,T,E,RFAX,RTORQ,RVA1,
     4 RVU1)
      REAL*4 MVA1M,MVA1,MV1M,MV1C,MV1,MW1,MV2,MW2
      DIMENSION FAX(50),CLFAX(50),FO(50),F1(50),F2(50),F3(50),F4(50),
     1 F5(50),F6A(50),FNET(50),TORQ(50),CLTORQ(50),FLOWN(50),FLOWT(50),
     2 FLOWL(50),RE(50),PHI(50),XI(50),QNOZ(50),QTPL(50),PTO(50),
     3 P1AV(50),QHD(50),PRPL(50),PRS(50),TTPQ(50),TTO(50),T1(50),
    4 T1IS(50),VA1(50),VU1(50),V1(50),V1IS(50),ALPH1(50),VCOFS(50),
    5 MV1(50),MVA1(50),WA1(50),WU1(50),W1(50),U1(50),BETA1(50),MW1(50),
    6 ZETAS(50),ETAS(50),RFAX(50),RTORQ(50),RVA1(50),RVU1(50)
      WRITE(6,800) NRUN,DA,T,E,J
  800 FORMAT(1H1,1X,'STATOR RESULTS',///,1X,'CONFIGURATION-   CONVERGING
    1 NOZZLES, SHROUD P/N 1050, INSERT P/N 2005-3(STRAIGHT)',///,1X,'RU
    2N NUMBER',I3,4X,'DATE ',3A3,//,44X,'METHOD J=',I2)
      WRITE(6,801)
  801 FORMAT(////,30X,'FORCE AND MOMENT BALANCE(LBS AND FT-LBS)',//,1X,
    1'POINT',2X,'FAX(+)',1X,'CLFAX(+)',2X,'FO(+)',3X,'F1(-)',3X,'F2(-)'
    2,3X,'F3(-)',3X,'F4(-)',3X,'F5(-)',2X,'F6A(-)',4X,'FNET',2X,'TORQ(+
    3)',1X,'CLTORQ(+)',2X,'RFAX',5X,'RTORQ',/)
      DO 802 I=1,N
  802 WRITE(6,803) I,FAX(I),CLFAX(I),FO(I),F1(I),F2(I),F3(I),F4(I),F5(I)
    1,F6A(I),FNET(I),TORQ(I),CLTORQ(I),RFAX(I),RTORQ(I)
  803 FORMAT(I4,2X,9F8.2,F9.2,2F8.2,2F9.2)
      WRITE(6,804)
  804 FORMAT(////,30X,'FLOW RATES(LBM/SEC), RE(NOZ), FLOW FNC, AND STATO
    1R BLOCKAGE FACTOR',//,1X,'POINT',2X,'NOZZLE FLOW',2X,'TURBINE FLOW
    2',3X,'LABLEAK',8X,'RE',9X,'PHI',7X,'XI',/)
      DO 805 I=1,N
  805 WRITE(6,806) I,FLOWN(I),FLOWT(I),FLOWL(I),RE(I),PHI(I),XI(I)
  806 FORMAT(I4,2X,F10.4,4X,F10.4,3X,F10.4,3X,F10.0,2F10.4)
      WRITE(6,807) PAMB
  807 FORMAT(////,30X,'PRESSURES(PSIA) AND PRESSURE RATIOS',//,1X,'PAMB=
    1',F5.2,//,1X,'POINT',2X,'PNOZ',3X,'PTPL',3X,'PTO',3X,'P1AV',4X,
    2 'PHD',3X,'PLENUM PR(PTPL/PHD)',2X,'STATOR PR(PTO/P1AV)',/)
      DO 808 I=1,N
  808 WRITE(6,809)I,QNOZ(I),QTPL(I),PTO(I),P1AV(I),QHD(I),PRPL(I),PRS(I)
  809 FORMAT(I4,1X,5F7.2,6X,F7.4,14X,F7.4)
      WRITF(6,810)
  810 FORMAT(////,30X,'TEMPERATURES(DEG R)',//,1X,'POINT',3X,'TTPL',4X,
    1 'TTO',5X,'T1',5X,'T1IS',/)
      DO 811 I=1,N
  811 WRITE(6,812) I,TTPQ(I),TTO(I),T1(I),T1IS(I)
  812 FORMAT(I4,1X,4F8.2)
      WRITE(6,813)
  813 FORMAT(1H1,30X,'ABSOLUTE VELOCITIES(FT/SEC), ANGLES(DEG), VEL COEF
    1, AND MACH NOS',//,1X,'POINT',3X,'VA1',6X,'VU1',7X,'V1',6X,'V1IS',
    2 3X,'ALPHA 1',2X,'VCOEFS',4X,'MV1',4X,'MVA1',4X,'RVA1',4X,'RVU1'/)
      DC 814 I=1,N
  814 WRITE(6,815) I,VA1(I),VU1(I),V1(I),V1IS(I),ALPH1(I),VCOFS(I),
    1 MV1(I),MVA1(I),RVA1(I),RVU1(I)
  815 FORMAT(I4,1X,5F9.2,5F8.4)
      WRITE(6,816)
  816 FORMAT(////,30X,'RELATIVE VELOCITIES(FT/SEC), ANGLES(DEG), AND MAC
    1H NOS',//,1X,'POINT',3X,'WA1',6X,'WU1',7X,'W1',7X,'U1',5X,'BETA 1'
    2,4X,'MW1',/)
```

```
      DO 817 I=1,N
817   WRITE(6,818)I,WA1(I),WU1(I),W1(I),U1(I),BETA1(I),MW1(I)
818   FORMAT(I4,1X,5F9.2,F8.4)
      WRITE(6,819)
819   FORMAT(////,30X,'EFFICIENCIES',//,1X,'POINT',2X,'ZETA STATOR',2X,
     1 'ETA STATOR(1.-ZETAS)',/)
      DO 820 I=1,N
820   WRITE(6,821) I,ZETAS(I),ETAS(I)
821   FORMAT(I4,3X,F10.4,7X,F10.4)
      RETURN
      END


      SUBROUTINE OUTPTR(NRUN,N,AXCLR,RADCLR,PAMB,PTO,P1AV,PT2,QHD,PR,
     1 TTO,T1,TE,TT2,T2,T2IS,T2TH,TT2IS,DELTIS,DELTW,VA2,VU2,V2,VOIS,
     2 ALPH2,WA2,WU2,W2,U2,W2IS,BETA2,DBETA,WCOFS,ZETAR,ETAR,RPM,HP,
     3 DELHIS,DELHW,REFRPM,XKIS,ETATS,ETATT,REFLOW,REFMOM,REFHP,J,
     4 REACHB,REACMN,REACTP,DA,T,E,F,REACEF,MV2,MW2,SLF,SFF)
      REAL*4 MVA1M,MVA1,MV1M,MV1C,MV1,MW1,MV2,MW2
      DIMENSION PTO(50),P1AV(50),PT2(50),QHD(50),PR(50),TTO(50),T1(50),
     1 TE(50),TT2(50),T2(50),T2IS(50),T2TH(50),TT2IS(50),DELTIS(50),
     2 DELTW(50),VA2(50),VU2(50),V2(50),VOIS(50),ALPH2(50),WA2(50),
     3 WU2(50),W2(50),U2(50),W2IS(50),BETA2(50),DBETA(50),WCOFS(50),
     4 ZETAR(50),ETAR(50),RPM(50),HP(50),DELHIS(50),DELHW(50),REFRPM(50)
     5,XKIS(50),ETATS(50),ETATT(50),REFLOW(50),REFMOM(50),REFHP(50),
     6 REACHB(50),REACMN(50),REACTP(50),F(50),REACEF(50),MV2(50),MW2(50)
     7,SLF(50),SFF(50)
      WRITE(6,900) AXCLR,RADCLR,NRUN,DA,T,E,J
900   FORMAT(1H1,1X,'ROTOR RESULTS',///,1X,'CONFIGURATION-  CIRCULAR ARC
     1, SHARP LE ROTOR, P/N 1034-A, AXIAL CLNC ',F6.3,' IN, RADIAL CLNC'
     2,F6.3,' IN',///,1X,'RUN NUMBER',I3,4X,'DATE ',3A3,//,44X,'METHOD J
     3=',I2)
      WRITE(6,901) PAMB
901   FORMAT(////,30X,'PRESSURES(PSIA) AND PRESSURE RATIOS',//,1X,'PAMB=
     1',F5.2,//,1X,'POINT',3X,'PTO',4X,'P1AV',3X,'PT2',3X,'P2=PHD',3X,
     2 'OVERALL PR(PTO/P2)',/)
      DO 902 I=1,N
902   WRITE(6,903) I,PTO(I),P1AV(I),PT2(I),QHD(I),PR(I)
903   FORMAT(I4,2X,4F7.2,6X,F7.4)
      WRITE(6,904)
904   FORMAT(////,30X,'TEMPERATURES(DEG R)',//,1X,'POINT',4X,'TTO',5X,
     1 'T1',6X,'TE',6X,'TT2',5X,'T2',5X,'T2IS',4X,'T2TH',3X,'TT2IS',3X,
     2 'DELTA TIS',2X,'DELTA TW',/)
      DO 905 I=1,N
905   WRITE(6,906) I,TTO(I),T1(I),TE(I),TT2(I),T2(I),T2IS(I),T2TH(I),TT2
     1IS(I),DELTIS(I),DELTW(I)
906   FORMAT(I4,2X,8F8.2,2F10.2)
      WRITE(6,907)
```

```
907 FORMAT(1H1,30X,'ABSOLUTE VELOCITIES(FT/SEC) AND ANGLES(DEG)',//,
   1 1X,'POINT',3X,'VA2',6X,'VU2',7X,'V2',6X,'VOIS',3X,'ALPHA 2',3X,'M
   2V2',4X,'STAGE LOADING FACTOR',2X,'STAGE FLCW FACTOR',/)
    DO 908 I=1,N
908 WRITE(6,909) I,VA2(I),VU2(I),V2(I),VOIS(I),ALPH2(I),MV2(I),SLF(I),
   1 SFF(I)
909 FORMAT(I4,1X,5F9.2,F8.4,F14.2,F21.2)
    WRITE(6,910)
910 FORMAT(////,30X,'RELATIVE VELOCITIES(FT/SEC), ANGLES(DEG), AND REL
   1 VEL COEFS',//,1X,'POINT',3X,'WA2',6X,'WU2',7X,'W2',7X,'U2',6X,
   2 'W2IS',4X,'BETA 2',4X,'DBETA',2X,'WCOEFS',3X,'MW2',/)
    DO 911 I=1,N
911 WRITE(6,912) I,WA2(I),WU2(I),W2(I),U2(I),W2IS(I),BETA2(I),DBETA(I)
   1,WCOFS(I),MW2(I)
912 FORMAT(I4,1X,7F9.2,2F8.4)
    WRITE(6,913)
913 FORMAT(////,30X,'EFFICIENCIES, RPM, WORK OUTPUT(HP), AND ENTHALPY
   1DROP(BTU/LBM)',//,1X,'POINT',2X,'ZETA ROTOR',2X,'ETA ROTOR(1.-ZETA
   2R)',2X,'RPM',6X,'HP',3X,'DELTA HIS',2X,'DELTA HW',2X,'REHEAT FACTO
   3R',2X,'EFF DEGREE OF REACTION',/)
    DO 914 I=1,N
914 WRITE(6,915) I,ZETAR(I),ETAR(I),RPM(I),HP(I),DELHIS(I),DELHW(I),F(
   1I),REACEF(I)
915 FORMAT(I4,4X,F8.4,8X,F8.4,6X,F8.0,F8.2,F8.2,F11.2,F13.4,F19.4)
    WRITE(6,916) NRUN,DA,T,E
916 FORMAT(1H1,1X,'GENERAL RESULTS',///,1X,'RUN NUMBER',I3,4X,'DATE ',
   13A3,////,1X,'POINT',2X,'PRESSURE',2X,'REFERRED',2X,'ISENTROPIC',2X
   2,'EFFICIENCY',2X,'EFFICIENCY',2X,'REFERRED',3X,'REFERRED',2X,'REFE
   3RRED',2X,'DEGREE OF',2X,'DEGREE OF',2X,'DEGREE OF',/,10X,'RATIO',5
   4X,'SPEED',3X,'HEAD COEFF',2X,'TOT-STATIC',4X,'TOT-TOT',3X,'FLOW RA
   5TE',3X,'MOMENT',5X,'POWER',4X,'REACTION',3X,'REACTION',3X,'REACTIO
   6N',/,21X,'RPM',18X,'PERCENT',5X,'PERCENT',4X,'LBM/SEC',4X,'FT-LB',
   77X,'HP',7X,'(HUB)',6X,'(MEAN)',5X,'(TIP)',/)
    DO 917 I=1,N
917 WRITE(6,918)  I,PR(I),REFRPM(I),XKIS(I),ETATS(I),ETATT(I),REFLOW(I
   1),REFMOM(I),REFHP(I),REACHB(I),REACMN(I),REACTP(I)
918 FORMAT(I4,F11.4,F10.0,F11.4,2F12.2,F11.4,F11.3,F10.3,3F11.4)
    RETURN
    END
```

REFERENCES

1. Ainley, D. G. and Mathieson, G. C. R., An Examination of the Flow and Pressure Losses in Blade Rows of Axial-Flow Turbines, Aeronautical Research Council, R & M No. 2891, 1955

2. Ainley, D. G. and Mathieson, G. C. R., A Method of Performance Estimation for Axial-Flow Turbines, Aeronautical Research Council, R & M No. 2974, 1957

3. Brown, R. L., "An Investigation of the Secondary Flow Phenomena in a Cascade of High Deflection Axial-Flow Impulse Turbine Blades," Naval Postgraduate School Thesis, December 1966

4. Commons, P. M., "Instrumentation of the Transonic Turbine Test Rig to Determine the Performance of Turbine Inlet Guide Vanes through the Application of the Momentum and Moment of Momentum Equations," Naval Postgraduate School Thesis, September 1967

5. Harrison, R. G., "An Analysis of Single Stage Axial Flow Turbine Performance Using Three Dimensional Calculating Methods," Naval Postgraduate School Thesis, September 1967

6. Lenzini, M. J., "Calibration of Turbine Test Rig With Impulse Turbine at High Pressure Ratios," Naval Postgraduate School, June 1968

7. Messegee, J. A., "Influence of Axial and Radial Clearance on the Performance of a Turbine Stage With Blunt-Edge Non-Twisted Blades," Naval Postgraduate School Thesis, September 1967

8. Vavra, M. H., Aerothermodynamics and Flow in Turbomachines, New York, London: John Wiley and Sons, Inc., 1960

9. Vavra, M.H., Problems of Fluid Mechanics in Axial Turbomachines, Pts A, B, C, D and E, Von Karman Institute Course Note 556, Rhode-Saint-Genese, Belguim: Von Karman Institute for Fluid Dynamics, March 1969

INITIAL DISTRIBUTION LIST

No. Copies

1. Defense Documentation Center 20
Cameron Station
Alexandria, Virginia 22314

2. Library, Code 0212 2
Naval Postgraduate School
Monterey, California 93940

3. Commander, Naval Air Systems Command 1
Attn: AIR 03C, 330B, 330
Navy Department
Washington, D.C. 20360

4. Professor M.H. Vavra 1
Department of Aeronautics
Naval Postgraduate School
Monterey, California 93940

5. Chairman, Department of Aeronautics 1
Naval Postgraduate School
Monterey, California 93940

6. Office of Naval Research (Power Branch) 1
Attn: Mr. J.K. Patton, Jr.
Navy Department
Washington, D.C. 20360

7. Captain, Stewart G. Esdaile 5
38 Charkay Street
Ottawa 5, Ontario
Canada

Unclassified

Security Classification

DOCUMENT CONTROL DATA - R & D

(Security classification of title, body of abstract and indexing annotation must be entered when the overall report is classified)

1. ORIGINATING ACTIVITY *(Corporate author)* Naval Postgraduate School Monterey, California 93940	2a. REPORT SECURITY CLASSIFICATION Unclassified 2b. GROUP

3. REPORT TITLE

An Investigation of a Transonic Turbine Test Rig

4. DESCRIPTIVE NOTES *(Type of report and, inclusive dates)*

Master's Thesis; (October 1969)

5. AUTHOR(S) *(First name, middle initial, last name)*

Stewart G. Esdaile

6. REPORT DATE October 1969	7a. TOTAL NO. OF PAGES 125	7b. NO. OF REFS 9

8a. CONTRACT OR GRANT NO.	9a. ORIGINATOR'S REPORT NUMBER(S)
b. PROJECT NO.	
c.	9b. OTHER REPORT NO(S) *(Any other numbers that may be assigned this report)*
d.	

10. DISTRIBUTION STATEMENT

This document has been approved for public release and sale; its distribution is unlimited.

11. SUPPLEMENTARY NOTES	12. SPONSORING MILITARY ACTIVITY Naval Postgraduate School Monterey, California 93940

13. ABSTRACT

The Transonic Turbine Test Rig installed in the Turbo-Propulsion Laboratory at the Naval Postgraduate School was designed such that losses in nozzle and rotor blading and overall performance characteristics can be determined for operation at several combinations of blade configurations, pressure ratios and speeds. This study relates the empiracal data for stator loss coefficients to those determined for the converging-nozzle stator presently installed, and discusses reasons for some of the discrepancies. Also discussed are results of the flow nozzle calibration, locked rotor data, and temperature and inlet swirl effects. A method is proposed to reduce these effects for future work on the Turbine Test Rig.

DD FORM 1 NOV 65 1473 (PAGE 1)

S/N 0101-807-6811

Unclassified

Security Classification

A-31408

14. KEY WORDS	LINK A		LINK B		LINK C	
	ROLE	WT	ROLE	WT	ROLE	WT
Transonic Turbine						
Loss Coefficients						

thesE67
An investigation of a transonic turbine
3 2768 002 06228 3
DUDLEY KNOX LIBRARY